Bioanalysis ZONE

SCIEX
The Power of Precision

Pharmaceutical quantification using mass spectrometry: a new wave of technology

Taylor & Francis

Contents

Technology Digest: Pharmaceutical quantification using mass spectrometry: a new wave of technology

by Ellen Williams
Senior Digital Editor, Bioanalysis Zone

Keywords: Mass Spectrometry; Drug Quantification; Triple Quadrupole Mass Spectrometry; Orbitrap™; Quadrupole Time-of-Flight; Specificity; Sensitivity; Mass-to-Charge Ratio; Pharmacokinetics; Bioanalysis; SCIEX 7500+.

Introduction

Various techniques are available for pharmaceutical drug quantification, spanning chromatographic, spectroscopic and mass spectrometry (MS)-based methods. Among these, MS is considered the gold standard due to its superior sensitivity, selectivity and structural elucidation capabilities [1]. Compared with traditional spectroscopic methods such as fluorescence or infrared spectroscopy, MS provides users with direct molecular weight information via measurement of an analyte's mass-to-charge ratio (m/z) [2]. MS-based methods can detect analytes in the nanomolar to picomolar range [3], providing unmatched sensitivity, particularly beneficial for pharmacokinetic (PK) studies where trace-level detection is needed.

The versatility of MS allows it to quantify small molecules, peptides, biologics and metabolites across diverse and complex matrices where endogenous compounds can interfere with detection. Modern MS systems support high-throughput screening and quantification and, when combined with liquid chromatography (LC–MS/MS), allow simultaneous, multi-compound quantification in a single run. MS is widely accepted by regulatory agencies – such as the FDA, EMA and ICH – for drug quantification, with standardized protocols ensuring adherence to Good Laboratory Practice and Good Clinical Practice guidelines. MS is used throughout pharmaceutical and biomedical research, proteomics and metabolomics studies, as well as in forensic and toxicology applications.

The MS instrument landscape

MS instruments differ based on their mass analyzers, each using different physical principles to achieve separation and detection and produce an m/z. The choice of mass analyzer impacts resolution, sensitivity, speed and quantification capability, making certain MS platforms more suited to specific applications. Modern MS mass analyzers fall into one of the following categories: quadrupole, magnetic sector, ion trap, Quadrupole Time-of-Flight (Q-TOF) or Fourier transform (FT).

Here we compare the capabilities of Q-TOF MS, Orbitrap™ and triple quadrupole (QqQ) systems, and highlight the SCIEX 7500+ QqQ system as a principal platform to support regulated bioanalysis in clinical trials and pharmaceutical development.

Q-TOF MS

Q-TOF MS combines the selectivity of a quadrupole mass filter with the high-resolution, accurate mass capabilities of a TOF analyzer. This hybrid configuration enables precise precursor ion selection in the quadrupole, followed by fragmentation analysis in the TOF analyzer. As a scanning technique, Q-TOF enables versatile hybrid functions such as a TOF-MRM mode, which provides the user with full scan information as well as MRM-like quantitative results.

Q-TOF is high-speed technology with a broad dynamic range, allowing concurrent measurement of trace-level to high-abundance ions, particularly useful for complex matrices. Typically achieving a mass accuracy within 2–5 ppm, Q-TOF provides reproducible and unbiased results, supporting confident compound identification. Its higher speed capabilities make Q-TOF an excellent choice for analyzing highly complex samples at a deep level. Q-TOF does not suffer from saturation issues in the same way that Orbitrap systems do, as modern Q-TOF systems often include hardware and software technologies to manage ion abundance and detector performance. When saturation does occur in Q-TOF systems, it tends to be predictable and linear, and the effects are typically less detrimental to mass accuracy.

While Q-TOF MS provides much higher resolution than QqQ systems, it can fall short of Orbitrap, which can provide very high resolution at the expense of speed, and it is typically less sensitive than QqQ for low-abundance analytes. Its higher data complexity and computational demands also make it less optimal for routine use in clinical trials. Q-TOF offers a strong balance of resolution, speed and structural insight, but has lower sensitivity compared to QqQ, as well as greater data handling requirements, which can limit its suitability for high-throughput quantitative applications.

Orbitrap™

Orbitrap systems use a frequency-based mass measurement whereby ions are injected into the mass analyzer and ‘trapped’ in the electrostatic field created by the inner and outer electrodes [5]. Upon entry, the ions are forced into stable oscillatory orbits and the frequency of these oscillations directly correlates to their m/z. The oscillations generate image currents on the detector plates, which Orbitrap records and converts into a mass spectrum using Fourier transform processing [5].

Orbitrap does not rely on radiofrequency or magnetic fields for ion containment, produces higher resolution than QqQ and TOF MS, and has a very high mass accuracy. Its powerful dynamic range enables detection of both low- and high-abundance ions while maintaining a compact design compared to other high-resolution instruments [6]. However, both QqQ and TOF MS surpass Orbitrap in quantification speed and sensitivity. The Orbitrap also relies heavily on the precision of ion injection, making it less optimal for distinguishing ions in complex mixtures. Whilst excellent for high-resolution MS and unknown target identification, Orbitrap is less suited for high-speed, targeted quantification.

QqQ MS

As the name suggests, QqQ systems use three quadrupoles to filter and fragment ions. The most common way to use this is in multiple reaction monitoring (MRM) mode. This approach involves selecting specific precursor ions in the first quadrupole, fragmenting them in the second quadrupole and monitoring them in the third. By monitoring a small number of preselected ions, MRM facilitates highly sensitive detection at the nanogram-per-milliliter level in biological samples [7].

Unlike Orbitrap and TOF, which can resolve ions to four or more decimal places, quadrupoles do not measure precise mass distribution with ultra-fine accuracy. However, QqQ outperforms both Orbitrap and TOF MS in speed and sensitivity, making it the preferred system for PK and clinical trials, where precise drug or metabolite measurements are essential. QqQ is also the industry standard for regulated bioanalysis, primarily due to its rapid, targeted quantification capabilities.

Redefining bioanalysis on the SCIEX 7500+ system

Launched at the 72nd American Society for Mass Spectrometry meeting in Anaheim, California (June 2–6, 2024), the SCIEX 7500+ system represents the latest advancement in SCIEX's high-performance MS portfolio [8]. Building on the success of the SCIEX 7500 system launched in 2020, the SCIEX 7500+ system delivers enhanced robustness, sensitivity and operational efficiency across a large range of sample types and workflows, making it a powerful tool for regulated bioanalysis in clinical trials and pharmaceutical development [9,10].

The SCIEX 7500+ system achieves femtogram-per-milliliter sensitivity across thousands of sample sets, enabling trace-level detection in complex biological matrices. With a processing speed of 800 MRM transitions per second, it is SCIEX's fastest QqQ system to date [8,10,11]. Increased MRM capability allows users to expand quantitation panels, detecting and quantifying a greater number of analytes in a single run.

Additionally, the redesigned DJet+ assembly enhances front-end user serviceability, maximizing instrument uptime and laboratory productivity [8,10,12,13]. Established workflows from the 7500 system can be seamlessly transferred over to the 7500+ system [13].

> *"Instrument downtime and maintenance can be a killer in a CRO environment that runs on monthly revenue targets and client timelines. If an instrument goes down, it can set us up for failure, so reliability and robustness are critical to enable us to meet our goals. The SCIEX 7500+ system has added 2 main things to our workflow; the first is capacity — we are always pushing to have more instruments so we can service more clients in a timely manner. The second is more robust instruments and longer uptime."*
>
> *Dawn Dufield, Ph.D., Scientific Officer, Mass Spectrometry*
> *KCAS Bio (KS, USA)*

Designed to meet the rigorous compliance standards of regulated bioanalysis, the SCIEX 7500+ includes built-in compliance tools to ensure adherence to 21 CFR Part 11 — recommendations from the FDA outlining electronic recordkeeping and data integrity requirements [10]. The system automatically tracks and logs all activities, ensuring audit-ready documentation. Secure, role-based access prevents unauthorized changes to data or method setting, safeguarding data integrity. The electronic signature feature also ensures records cannot be altered, deleted or lost without authorization, and data is protected through automated backups. Beyond regulatory compliance, the SCIEX 7500+ system has been designed with sustainability in mind, demonstrating reduced gas and solvent consumption, which simultaneously improves environmental impact and lowers operational costs [10].

Mass Guard Technology™: a SCIEX innovation

A major development unique to the SCIEX 7500+ system is Mass Guard Technology, designed to prolong instrument resilience and reduce downtime [8,12,13,14]. By actively filtering out potentially contaminating ions, this technology maintains a cleaner ion beam, preserving the system's sensitivity over extended periods of time and reducing the frequency of contamination-related downtime [12,13,14]. This ultimately improves long-term reproducibility, particularly for high throughput bioanalytical workflows where maintaining consistent performance is critical. As a result, contract research organizations (CROs), pharmaceutical companies and clinical laboratories can operate with greater efficiency and reliability when conducting large-scale, regulated bioanalysis.

> *"Robustness is extremely important in a CRO environment as we are always leveraging our instruments to their max, whether that is for sensitivity or capacity/throughput. If performance changes over time, then we are unable to deliver on our commitments to our clients. Furthermore, it takes additional time to clean and get the instrument back to optimal performance, again impacting our timeline and ability to service our clients. I like the SCIEX 7500+ system and it is the most sensitive QqQ we have in our lab. Generally, these instruments are running non-stop to produce bioanalytical data."*
>
> *Dawn Dufield, Ph.D., Scientific Officer, Mass Spectrometry*
> *KCAS Bio (KS, USA)*

Summary

While the choice of MS system depends on the user's specific analytical requirements, QqQ MS remains the gold standard for drug quantification due to its unmatched precision, sensitivity and high throughput capabilities. The ultra-sensitive SCIEX 7500+ system facilitates detection of ultra-low analyte concentrations across a wide range of complex biological matrices. With the fastest MRM rates in SCIEX history, the 7500+ system enables larger quantification panels, higher productivity and greater efficiency in regulated bioanalysis. The incorporation of patented Mass Guard Technology enhances machine durability and minimizes downtime, offering consistent performance over extended use. The built-in compliance tools help laboratories meet the FDA, EMA and other global regulatory standards, making the SCIEX 7500+ system an optimal choice for clinical trials, pharmaceutical development and high-throughput drug quantification.

Disclaimer

This feature has been brought to you in association with SCIEX. The opinions expressed in this feature are those of the author and do not necessarily reflect the views of Bioanalysis Zone or Taylor & Francis.

References

1. Klont F, Hopfgartner G. Mass spectrometry based approaches and strategies in bioanalysis for qualitative and quantitative analysis of pharmaceutically relevant molecules. *Drug Disc. Today Technol.* 40, 64–68 (2021).
2. Rockwood AL, Kushnir MM, Clarke NJ. Mass spectrometry. In: Principles and applications of clinical mass spectrometry. Rifai N, Horvath AR, Wittwer CT (Eds). *Elsevier*, Amsterdam, Netherlands 33–65 (2018).
3. Gorityala S, Roos D, Dong MW. Bioanalysis of Small-Molecule Drugs and Metabolites in Physiological Samples by LC–MS, Part 1: An Overview. *LCGC N. Am.* 39(6), 263–271 (2021).
4. Pareige C, Lefebvre-Ulrikson W, Vurpillot F, Sauvage X. Time-of-Flight Mass Spectrometry - an overview. In: Atom Probe Tomography. C, Lefebvre-Ulrikson W, Vurpillot F, Sauvage X (Eds). *Elsevier*, Amsterdam, Netherlands 123–154 (2016).
5. Makarov A, Grinfeld D, Ayzikov K. Fundamentals of Orbitrap analyzer. In: Fundamentals and applications of Fourier transform mass spectrometry. Kanawati B, Schmitt-Kopplin P (Eds). *Elsevier*, Amsterdam, Netherlands 33–61 (2019).
6. Zubarev RA, Makarov A. Orbitrap Mass Spectrometry *Anal. Chem.* 85(11), 5288–5296 (2013).
7. Yao X, McShane AJ, Castillo MJ. Multiple Reaction Monitoring - an overview. In: Proteomic and metabolomic approaches to biomarker discovery. Issaq HJ, Veenstra TD (Eds). *Academic Press*, MA, USA 259–278 (2013).
8. The SCIEX 7500+ system launches at ASMS 2024. www.sciex.com/about-us/press-releases/2024/sciex-7500plus-system-launches-at-asms2024 [Accessed 20 March 2025].
9. Our History – 50 years of innovation. www.sciex.com/about-us/our-history [Accessed 10 March 2025].
10. Setting a new standard for instrument resilience. https://sciex.com/products/mass-spectrometers/triple-quad-systems/triple-quad-7500-plus-system [Accessed 20 March 2025].
11. Fast scanning quantitative lipidomics analysis using the SCIEX 7500+ system www.sciex.com/content/dam/SCIEX/pdf/tech-notes/life-science-research/MKT-31849-A_Fast_MRM_targeted_lipidomics_analysis_on_the_SCIEX_7500_%20system_FINAL_with_EDITS.pdf [Accessed 31 March 2025].
12. Redefine bioanalysis with enhanced robustness on the SCIEX 7500+ system www.sciex.com/tech-notes/pharma/bioanalysis-pk/redefine-bioanalysis-with-enhanced-robustness-on-the-sciex-7500-plus-system [Accessed 01 April 2025].
13. Achieving exceptional robustness for PFAS analysis in food with the next-generation SCIEX 7500+ system https://sciex.com/tech-notes/food-beverage/food-and-beverage/achieving-exceptional-robustness-for-pfas-analysis-in-food-with-the-next-generation-sciex-7500-plus-system [Accessed 20 March 2025].
14. Discover unparalleled sensitivity and extended instrument uptime on the highly robust SCIEX 7500+ system https://sciex.com/tech-notes/food-beverage/food-and-beverage/Discover-unparalleled-sensitivity-and-extended-instrument-uptime-on-the-highly-robust-SCIEX-7500--system [Accessed 31 March 2025].

Redefine bioanalysis with enhanced robustness on the SCIEX 7500+ system

Ebru Selen[1], Rahul Baghla[1], Ian Moore[2], Eshani Galermo[1], Zoe Zhang[1] and Elliott Jones[1]
[1]SCIEX, USA; [2]SCIEX, Canada

This technical note demonstrates >2x improvement in robustness for an example small molecule analysis on the SCIEX 7500+ system compared to the SCIEX 7500 system. The measurements were made over 10,000 rat plasma matrix injections with no divert valve (**Figure 1**). Small molecule pharmaceutical compounds such as alprazolam, sulfamethoxazole and diazepam were introduced with a high percentage of rat plasma matrix and analyzed over an extended period to fulfill a thorough assessment of the mass spectrometer to support long-term bioanalysis studies. Mass Guard technology[1] was employed to minimize downstream ion path contamination, maintaining the highest levels of sensitivity and stability over an extended period on the SCIEX 7500+ system.

Key benefits of long-term analysis using the SCIEX 7500+ system

- **Enhanced robustness with Mass Guard technology:** Perform long-term bioanalysis seamlessly and reduce the risk of instrument downtime due to contaminating ions
- **Exceptional instrument stability:** The SCIEX 7500+ system achieved >2x improvement in robustness, as demonstrated by >10,000 injections of rat plasma matrix
- **User accessibility to the DJet+ assembly:** Easily perform front-end cleaning to minimize unscheduled downtime and maintain instrument performance
- **Built-in contamination check procedures in SCIEX OS software:** Enables easy monitoring of instrument performance for quick troubleshooting

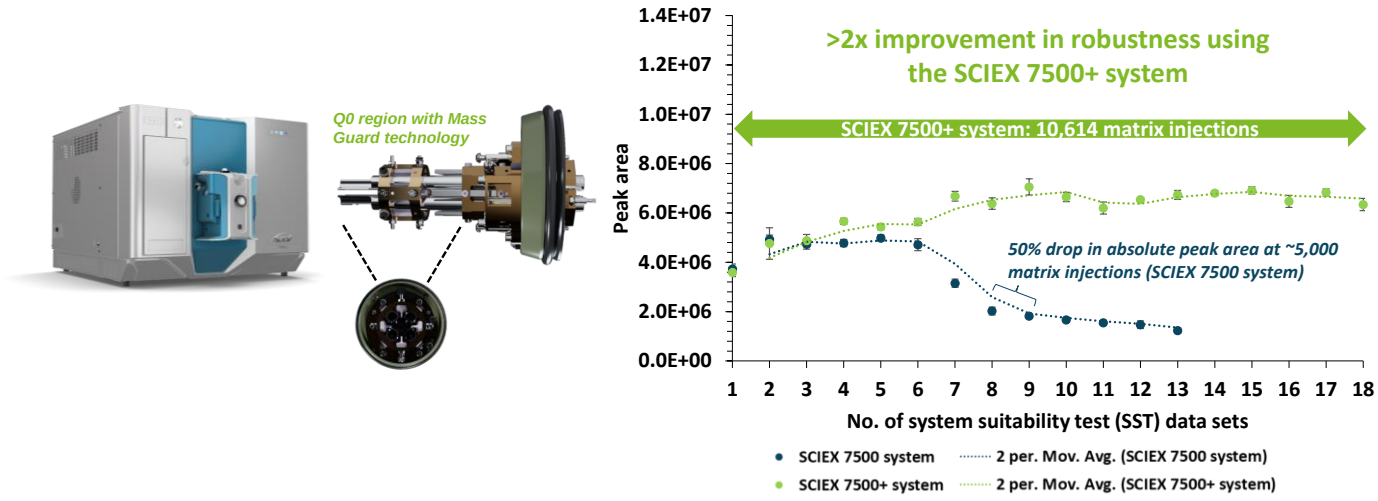

Figure 1: Comparison of raw peak areas for diazepam system suitability tests (SSTs) on the SCIEX 7500 system (blue) and on the SCIEX 7500+ system (green). Each data point represents the mean peak area with standard error bars (n = 8). Between each SST data point, >560 rat plasma extracts were consecutively injected with a total of 9,793 and 10,614 matrix injections on the SCIEX 7500 system and SCIEX 7500+ system, respectively. Trendlines based on moving averages (2 period) were calculated for the SCIEX 7500 system (blue) and SCIEX 7500+ system (green). Robustness was compared based on the total number of injections before the instrument sensitivity declined to 50% of the maxima. On the SCIEX 7500 system, the peak area remained stable to SST #6 (~3,700 matrix injections) until between SST #8 and SST #9 (~5,000 matrix injections) where there was a decline in 50% of the response. In comparison, the SCIEX 7500+ system surpassed and maintained stability by >2x, where diazepam peak area was stable over 10,000 matrix injections.

Introduction

Quantitation of pharmaceutical drugs is often performed in complex matrices. Because of challenging matrix contaminants, highly robust analytical techniques are needed to ensure accurate and precise measurements.

Systems such as triple quadrupole mass spectrometers are commonly used for quantitative bioanalysis. SCIEX triple quadrupole systems are renowned for extended uptime for bioanalysis. However, even longer durations of stable analytical performance are often advantageous in high throughput bioanalysis environments. Therefore, longer stable sensitivity and reduced downtime based on cleaning are significant benefits in such laboratories.

Mass Guard technology[1] was introduced on the SCIEX 7500+ system to minimize downstream contamination of the ion optics, maintaining instrument robustness over greater periods than the benchmark triple quadrupole mass spectrometers. Adding the T Bar assembly to the Q0 region actively filters out contaminating ions to create a cleaner ion beam (**Figure 2**). Visual examination of the downstream ion optics reveals less contamination markings on the IQ1 lens of the SCIEX 7500+ system compared to the SCIEX 7500 system. Therefore, there is a significant reduction in the impact of matrix contaminants on the SCIEX 7500+ system, leading to enhanced robustness over long-term analysis for this example assay.

In addition, the SCIEX 7500+ system features improved customer access to the Djet+ assembly for front-end cleaning as needed.[1] Here, the long-term robustness of the SCIEX 7500+ system and SCIEX 7500 system was evaluated under contamination-accelerated conditions using 2:1 (v/v) methanol/rat plasma protein precipitation.[2]

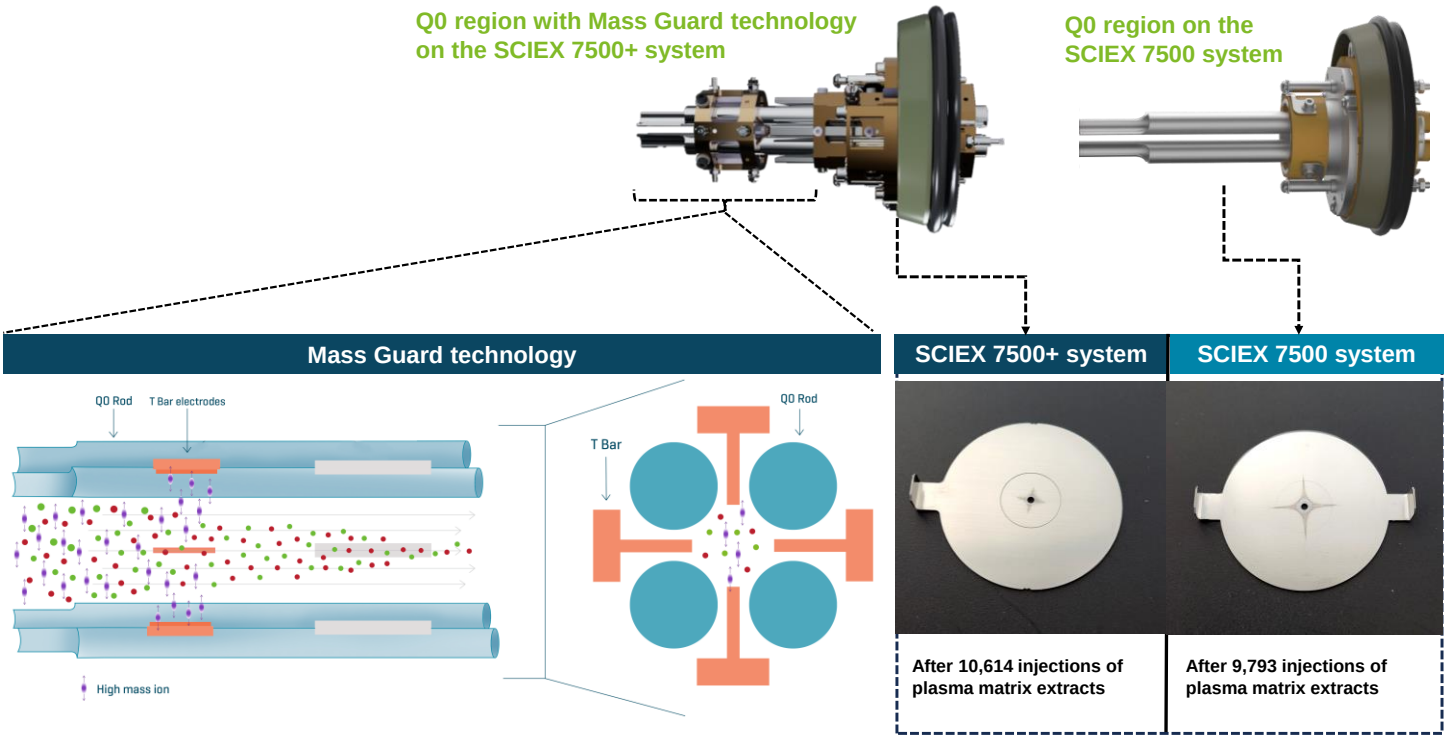

Figure 2: Hardware components of Mass Guard technology. The added T Bar assembly in the Q0 region of the SCIEX 7500+ system actively removes potentially contaminating ions (purple symbols), resulting in a much cleaner sample plume (red and green symbols) entering the instrument. Visual comparison of the ion optics downstream of the T Bar assembly showed significantly less impact from matrix contamination, when compared against the same component on the SCIEX 7500 system.

Methods

The following experimental regime was utilized to maximize the matrix load injected over consecutive weeks for evaluation of robustness on the SCIEX 7500+ system and SCIEX 7500 system:

- A modified sample preparation generated rat plasma matrix extracts that contain higher contaminant components to accelerate this test, compared to typical procedures
- Dedicated LCs to introduce rat plasma matrix and SST samples
- A short gradient to maximize the number of consecutive rat plasma matrix injections between SST samples
- Continuous acquisition of more than 10,000 matrix injections (no diverter valve) with intermittent SST sample analysis without any interim maintenance on the mass spectrometer

Sample preparation: The rat plasma matrix was prepared by extracting 500 µL of rat plasma with 1000 µL of methanol. The mixture was vortexed for a minute and centrifuged at 12000 rcf for 10 minutes. 1200 µL of supernatant was collected and diluted with 1200 µL of water. A mixture of alprazolam, diazepam and sulfamethoxazole and their respective deuterated internal standards (pharma mix) were spiked in rat plasma extract to achieve a final concentration of 0.5 ng/mL for analysis.

The solvent for SST samples was prepared as follows: a mixture of 1:2 (v/v), water/methanol was diluted with an equivalent volume of water. The solvent was spiked with pharma mix at a final concentration of 0.5 ng/mL for analysis.

Chromatography: The LC system used for SST injections was operated at a 0.8 mL/min flow rate (**Table 1**). SST samples were run on a Gemini C18 column (3 µm, 110 Å, 3 x 50 mm) with KrudKatcher ULTRA HPLC in-line Filter (2.0 µm depth filter x 0.004 in ID). A separate LC system was used to inject the rat plasma matrix, operated at a 1 mL/min flow rate (**Table 2**). Matrix samples were introduced using the Gemini C18 column (3 µm, 110 Å, 3 x 50 mm) and SecurityGuard ULTRA guard holder with cartridge (C18, 2.1 mm). Both gradients were run using 0.1% formic acid in water as mobile phase A and 0.1% formic acid in acetonitrile as mobile phase B. The column temperature was maintained at 40°C and an injection volume of 5 µL was used for analysis of matrix and SST samples. A 1:1:1 (v/v/v) mixture of acetonitrile/methanol/water was used as a needle wash solvent. Analysis was performed on a SCIEX 7500 system and a SCIEX 7500+ system in positive mode. Collision energy, source and MS parameters were optimized for MRM-based quantitation (**Table 3 and Table 4**).

Table 1: LC gradient for SST samples.

Time (min)	Mobile phase A (%)	Mobile phase B (%)
0.0	95	5
0.5	95	5
2.0	5	95
3.0	5	95
3.1	95	5
4.0	95	5

Table 2: LC gradient for rat plasma matrix samples.

Time (min)	Mobile phase A (%)	Mobile phase B (%)
0.0	95	5
0.1	95	5
0.9	5	95
1.5	5	95
1.51	95	5
2.0	95	5

Mass spectrometry: Table 3 lists the optimized source and gas parameters and **Table 4** includes the MRM parameters.

Table 3: Source and gas parameters for the SCIEX 7500 system and the SCIEX 7500+ system.

Parameter	Value
Polarity	Positive
Ion source gas 1	60 psi
Ion source gas 2	70 psi
Curtain gas	50 psi
Source temperature	650°C
Ion spray voltage	2000 V
CAD gas	10

Table 4: MRM parameters used for quantitation on the SCIEX 7500 system and SCIEX 7500+ system.

ID	Precursor ion (m/z)	Fragment ion (m/z)	CE (V)	CXP (V)
Alprazolam	309.2	205.1	55	10
Alprazolam-d_5	314.2	210.1	55	10
Diazepam	285.1	193.2	40	10
Diazepam-d_5	290.1	198.2	40	10
Sulfamethoxazole	254.1	156.0	19	10
Sulfamethoxazole-d_4	258.1	160.0	19	10

Data processing: Data collection and analysis were performed in SCIEX OS software, version 3.3.1. Peaks were integrated using the MQ4 algorithm.

Robustness on the SCIEX 7500+ system

Instrument robustness was evaluated by intermittently monitoring SST samples spiked with native and internal standards between large blocks of consecutive rat plasma matrix injections. More than 2x improvement in robustness for sulfamethoxazole and diazepam was demonstrated on the SCIEX 7500+ system with over 10,000 rat plasma matrix injections (**Figure 1 and Figure 3**). Moving averages (2 period) for both data sets highlight the trend across each

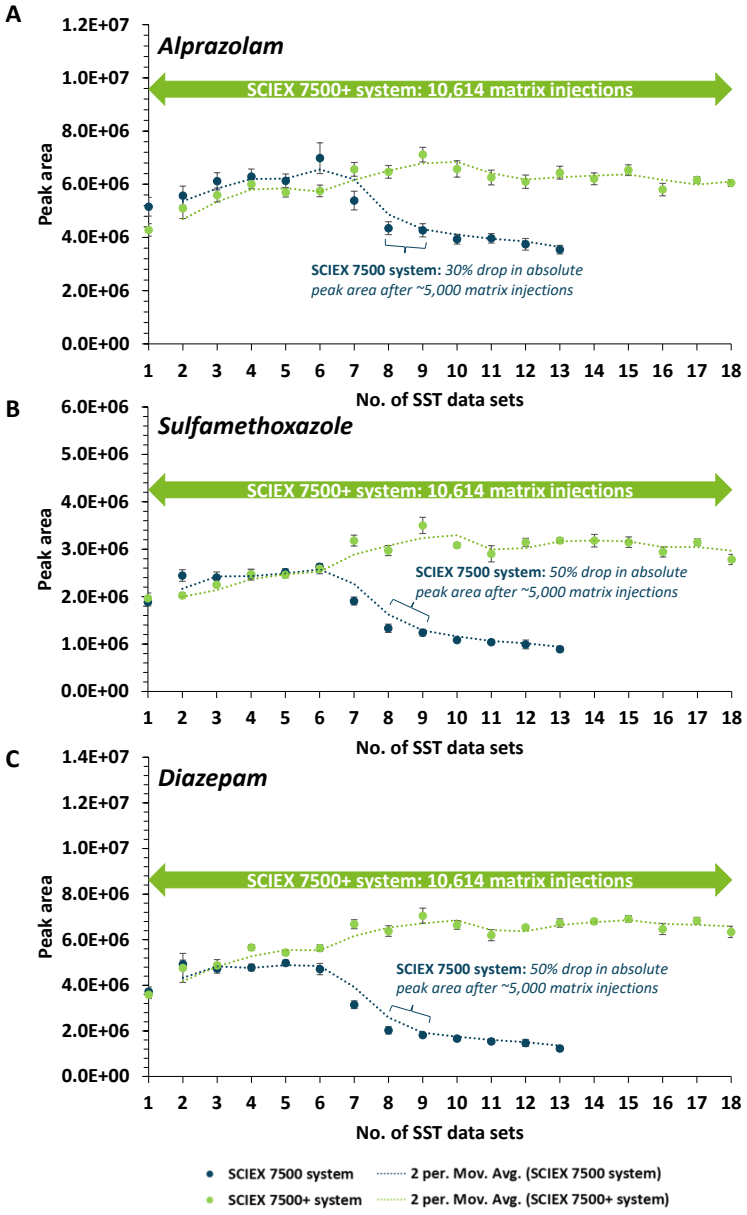

Figure 3: Comparison of raw peak areas for alprazolam (A), sulfamethoxazole (B) and diazepam (C) SSTs on the SCIEX 7500 system (blue) and on the SCIEX 7500+ system (green). Each data point represents the mean peak area with standard error bars (n = 8). Between each SST data point, >560 rat plasma extracts were consecutively injected with a total of 9,793 and 10,614 matrix injections on the SCIEX 7500 system and SCIEX 7500+ system, respectively. Trendlines based on moving averages (2 period) were calculated for the SCIEX 7500 system (blue) and SCIEX 7500+ system (green). Robustness was compared based on the total number of injections before the instrument sensitivity declined to 50% of the maxima. On the SCIEX 7500 system, there was a decline in 50% of the response for sulfamethoxazole (~5,000 matrix injections) and diazepam (~5,000 matrix injections) and a 30% drop in response for alprazolam (~5,000 matrix injections) between SST#8 and SST#9. In comparison, the SCIEX 7500+ system surpassed and maintained stability by >2x for sulfamethoxazole and diazepam which had stable peak area over 10,000 matrix injections.

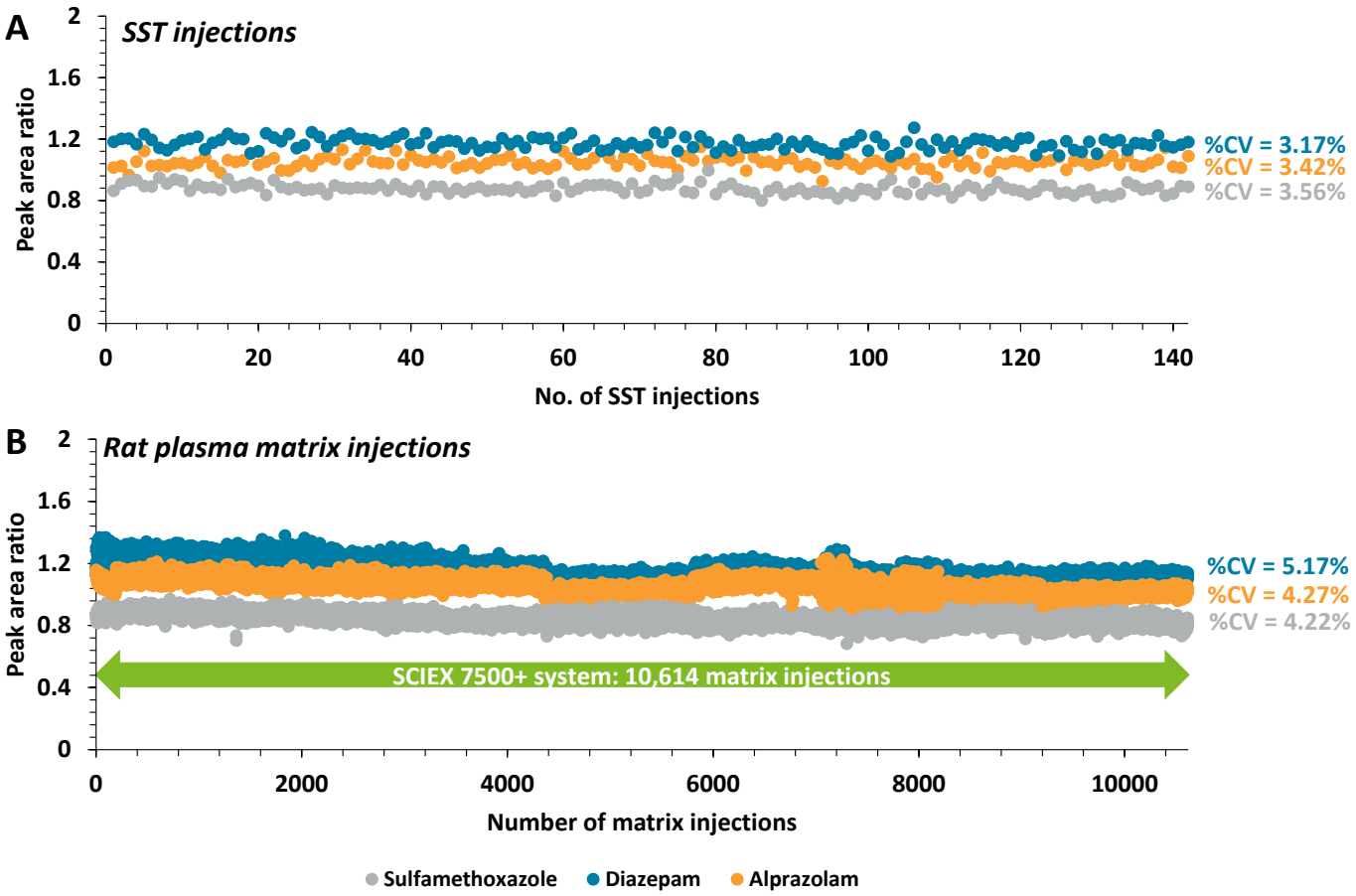

Figure 4: Peak area ratio (raw peak area normalized to IS) from analysis of alprazolam (orange), diazepam (blue) and sulfamethoxazole (grey) SST (A) and rat plasma matrix (B) injections on the SCIEX 7500+ system. The %CV from the SST samples was 3.17%, 3.42% and 3.56% for diazepam, alprazolam and sulfamethoxazole, respectively. The %CV from the rat plasma matrix samples was 5.17%, 4.27% and 4.22% for diazepam, alprazolam and sulfamethoxazole, respectively. Consistent peak area ratios were observed, demonstrating instrument stability and performance across 10,614 rat plasma matrix injections. A total of 8.8 mL of rat plasma was extracted and analyzed on the SCIEX 7500+ system, across 10,614 injections.

consecutive SST. The SSTs measured for all 3 small molecule compounds reflected similar sensitivity on the SCIEX 7500+ system and SCIEX 7500 system across approximately 4,000 rat plasma matrix injections. This demonstrated sensitivity effective equivalency between the SCIEX 7500+ system and SCIEX 7500 system.[3]

The peak area ratio was also calculated using the respective IS for each analyte. Figure 4 shows consistent IS-corrected peak area ratios for SSTs (**Figure 4A**) and rat plasma matrix samples (**Figure 4B**) on the SCIEX 7500+ system. Overall, %CV was <4% for the SST samples and <6% for the rat plasma matrix samples. The performance of the SCIEX 7500+ system remained stable throughout the experiment despite the introduction of >10,000 rat plasma matrix injections, given the consistent reproducibility of the peak area ratios.

Enhanced software tools for monitoring system performance

The SCIEX OS software provides a built-in automated workflow that enables the user to monitor the detector performance and system charging events with minimal manual intervention (**Figure 5**). The contamination check procedure enables system tests to be run in both the positive and negative polarities using the MS single tuning solution.

System tests for the contamination check procedure include verification of the detector voltage, MRM performance and Q1 and MRM charging tests. System reports are then generated and can be easily compared against previous contamination check results using the SCIEX OS software.

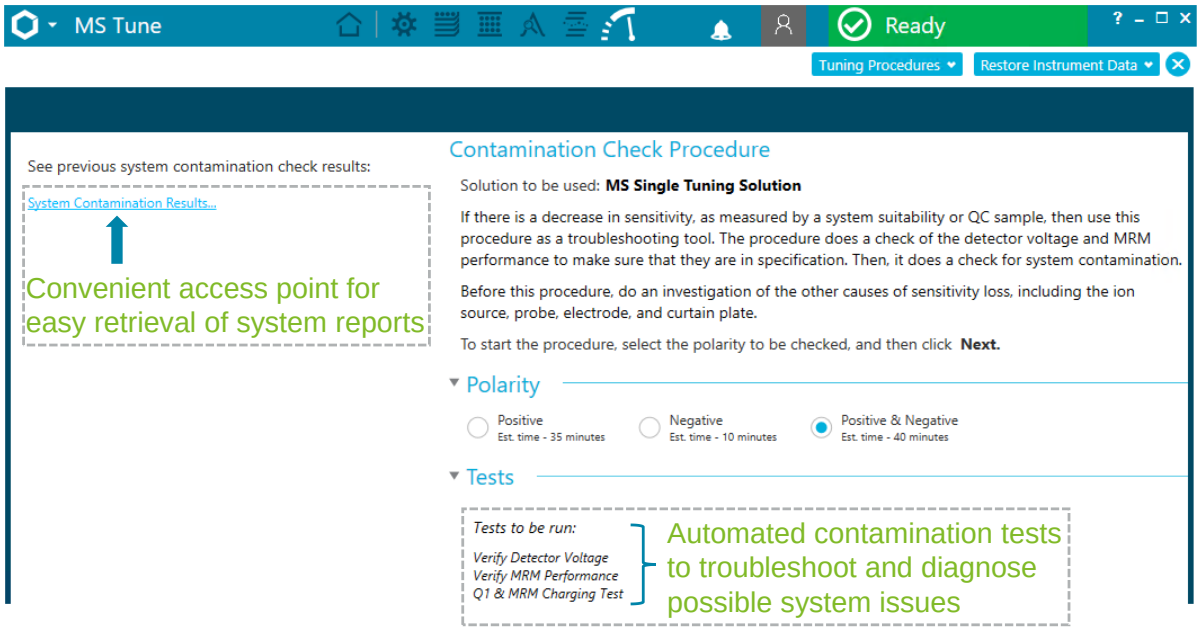

Figure 5: Built-in contamination check procedures in SCIEX OS software for easy troubleshooting. The MS Tune module in SCIEX OS software provides an automated contamination check procedure that allows the user to troubleshoot and monitor instrument performance during sensitivity loss. At the end of the procedure, the software generates a summary report of the instrument performance based on the tests ran.

Conclusion

- Mass Guard technology actively removed contaminating ions in the rat plasma matrix, leading to >2x improvement in robustness on the SCIEX 7500+ system for this assay
- The combination of SCIEX OS software enhancements for system performance tracking and the extractable DJet+ assembly offers increased efficiency for user-initiated management of system uptime
- Integrating the unparalleled sensitivity of the SCIEX 7500 system, the SCIEX 7500+ system demonstrates the highest levels of data stability, making it a powerful tool for bioanalysis in complex matrices for extended periods

References

1. Build resilience with the SCIEX 7500+ system. SCIEX brochure, MKT-31468-A.
2. Polson, C. *et al.* Optimization of protein precipitation based upon effectiveness of protein removal and ionization effect in liquid chromatography–tandem mass spectrometry. *J. Chromatogr. B. Analyt. Technol. Biomed. Life Sci.* **2003**, *785(2)*, 263-275.
3. Quantitative performance of a next-generation, highly robust triple quadrupole mass spectrometer. SCIEX technical note, MKT-30856-A.

Headquarters
500 Old Connecticut Path | Framingham, MA 01701
USA
Phone 508-383-7700
sciex.com

International Sales
For our office locations please all the division headquarters or refer to our website at
sciex.com/offices

Bioanalysis

ISSN: (Print) (Online) Journal homepage: www.tandfonline.com/journals/ibio20

Review on *In Vivo* Profiling of Drug Metabolites with Lc-Ms/Ms in the Past Decade

Gangireddy Navitha Reddy, Chenkual Laltanpuii & Rajesh Sonti

To cite this article: Gangireddy Navitha Reddy, Chenkual Laltanpuii & Rajesh Sonti (2021) Review on *In Vivo* Profiling of Drug Metabolites with Lc-Ms/Ms in the Past Decade, Bioanalysis, 13:22, 1697-1722, DOI: 10.4155/bio-2021-0144

To link to this article: https://doi.org/10.4155/bio-2021-0144

Review

For reprint orders, please contact: reprints@future-science.com

Bioanalysis

Review on *in vivo* profiling of drug metabolites with LC-MS/MS in the past decade

Gangireddy Navitha Reddy[1], Chenkual Laltanpuii[1] & Rajesh Sonti*,[1]

[1]Department of Pharmaceutical Analysis, National Institute of Pharmaceutical Education & Research (NIPER), Hyderabad, Balanagar, Telangana, 500037, India

*Author for correspondence: Tel.: +91 917 227 3849; rajesh.sonti@niperhyd.ac.in

Metabolite profiling is an indispensable part of drug discovery and development, enabling a comprehensive understanding of the drug's metabolic behavior. Liquid chromatography-mass spectrometry facilitates metabolite profiling by reducing sample complexity and providing high sensitivity. This review discusses the *in vivo* metabolite profiling involving LC-MS/MS and the utilization of QTOF, QQQ mass analyzers with a particular emphasis on a mass filter. Further, a summary of sample extraction procedures in biological matrices such as plasma, urine, feces, serum and hair as *in vivo* samples are outlined. toward the end, we present 15 case studies in biological matrices and their LC-MS/MS conditions to understand the metabolic disposition.

Graphical abstract:

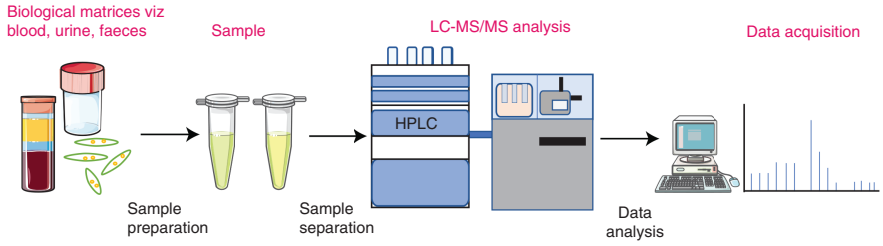

First draft submitted: 29 June 2021; Accepted for publication: 13 October 2021; Published online: 26 October 2021

Keywords: biotransformation • LC-MS • metabolite profiling • plasma • urine

Metabolomics investigates metabolome inside cells, biofluids, tissues or organisms engaged in clinical studies, pharmacology and toxicology [1]. It identifies small molecules (molecular weight <1500 Da) to empower a comprehensive understanding of the biological processes and biochemical mechanisms in a biological matrix [2,3]. Quantitative analysis was first performed on urine vapor and breath, leading to metabolite quantitation [4]. The first metabolome study was conducted on yeast, which further inspired reports on metabolic profiling of urinary constituents [5,6]. After oral administration of a drug, it passes through the GI tract and liver for metabolism by various enzymes before reaching the systemic circulation. As the liver is the primary drug metabolizing site, *in vitro* metabolite identification is carried out with liver microsomes to screen various drug candidates in the early stages of the drug discovery. Although hepatocytes and liver microsomes find extensive usage for *in vitro* studies, there is an absence of clear-cut metabolism for *in vitro* systems to reproduce *in vivo* conjugation reactions quantitatively. Therefore, metabolite identification plays a crucial role in drug discovery and development [7,8].

Metabolite profiling aims to analyze and identify the largest number of compounds produced by an organism after administering the exogenous drug in biological matrices such as serum, urine and plasma. The characterization of metabolites in any matrix of human or animal provides information about the biotransformation and drug clearance

newlands press

pathways [9–12]. Production of innovative medicines requires high-quality testing, analysis and proper technologies for the research. Identification of metabolites is a time-consuming task involving numerous chromatographic methods and sample pre-treatments. The most challenging task by liquid chromatography-mass spectrometry (LC-MS) in metabolite identification is to screen metabolites and separate them from the endogenous interfering compounds present in biological matrices. LC provides separation of the drug-related material from endogenous components and separation of isobaric compounds. MS allows for the characterization of the metabolite based on m/z value and known biotransformation [13].

Paul and Steinwedel published the basic principles of the mass spectrometer in 1953, laying the groundwork for metabolite profiling [14]. Initial studies on structure elucidation and metabolite identification with triple quadrupole mass analyzer were performed on antiepileptic drugs in plasma and urine samples [15]. The MS/MS method requires the parent structure/substructure of the drug to be intact, and the metabolites undergo similar fragmentation patterns as that of the parent drug [16,17]. Spectral overlap in complex metabolite mixtures occurs on quadrupole detectors in a single experiment. Substantial overlap often appears in the mass range $m/z > 400$, where many metabolites of interest and nonspecific impurities are present. To offset quadrupole's low mass resolution, improvements in chromatographic separation will result in increased sensitivity and specificity in complex mixtures [18]. On the other hand, LC-HRMS has remarkable specificity and selectivity for precise mass identification with an enormous impact on metabolites characterization from biological specimens [19]. Chromatographic separation of metabolites has offered advantages over direct MS analysis. It separates isomers by providing additional orthogonal data, reducing matrix effects, and allowing more accurate quantification of individual metabolites [20]. Nowadays, LC-MS and NMR spectroscopy are considered the two most widely used analytical techniques for metabolite profiling. However, the cost of an NMR spectrometer makes its usage and installation numbers less than MS [21,22]. Moreover, NMR sensitivity is very low compared with MS instruments, and hence analytes above significant threshold concentrations can be detected [21]. This review summarizes the sample preparation and mass spectrometric conditions applied for respective metabolite identification studies.

Sample preparation & extraction approaches

The sample preparation method influences the analysis of the metabolite profile and the quality of data. Preparation strategy in developing a reproducible sample that extracts and separates a group of metabolites is a significant challenge in metabolite profiling. Designing metabolite identification experiments with a particular biological question must precede an extensive literature survey to determine the metabolites of interest. In addition, collecting complete information about the individuals participating in the experimentation increases data interpretation confidence [23,24]. The main objective is to reproducibly alter the sample into a format fitted with LC-MS analysis while sustaining the original metabolite composition to a maximum extent.

Some of the ideal sample preparation methods for metabolite profiling of biological samples have the following points in consideration: nonselective, easy and fast with fewer steps, reproducible and employ a metabolism quenching step. The samples are either diluted or derivatized to isolate the metabolites in a matrix before the analysis. In the case of biofluids, initial preparation is often achieved first by protein precipitation (PPT) with organic solvents followed by solid-phase extraction (SPE) or liquid-liquid extraction (LLE) [23,25].

Solid-phase microextraction (SPME), a well-known technique, utilizes a needle coated with chemicals like hydrophilic lipophilic balanced (HLB), divinylbenzene (DVB), octadecylsilyl derivatized silica column packing material (C18), carbowax (CW), templated resin (TPR), polyacrylonitrile (PAN) and benzenesulfonic acid (BSA). The SPME method saves preparation time by creating a concentrated extract that is suitable for direct MS analyzes with high accuracy, low operational and disposal costs [26,27]. An *in vivo* study in rat employing molecular imprinted polymers (MIP-SPME) coupled with LC-QTOF-MS/MS method was used to identify luteolin and its metabolites included apigenin, chrysiderol and diosmetin [28]. Various *in vitro* and *in vivo* studies have applied SPME as a sample extraction tool, indicating it as a considerable need in metabolite analysis [29–31].

Dried blood spot sampling (DBS) is a new technique in bioanalytical methods for collecting whole blood samples on paper. The blood collection on DBS card is fast and less invasive. Further, this card behaves as a sample matrix from which analytes and metabolites are extracted following a suitable solvent extraction method [27,32]. A detailed methodology on DBS is discussed in the Section 3.1.

In some cases, metabolite standards are synthesized and later used to confirm the drug metabolites obtained in the desired matrix. Stanozolol and its metabolites are checked for identification in doping control of human urine sam-

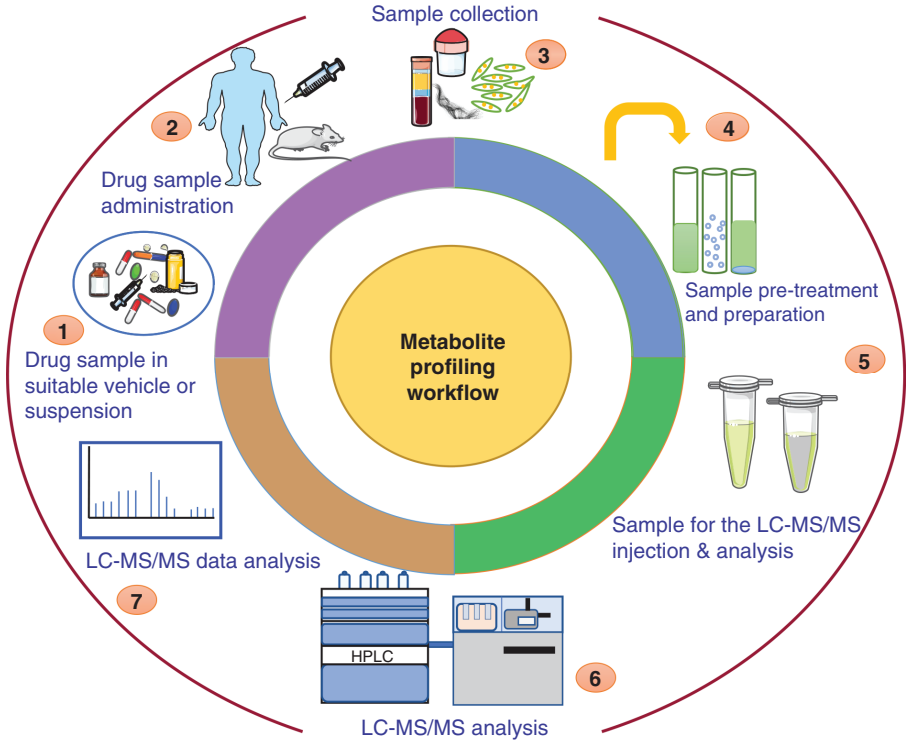

Figure 1. Illustration of metabolite profiling through LC-MS/MS. This comprises of drug administration, sample preparation, LC-MS analysis and structural data confirmation of unknown metabolites.
HPLC: High-performance liquid chromatography; LC-MS/MS: Liquid chromatography-tandem mass spectrometry; LLE: Liquid–liquid extraction, PPT: Protein precipitation; SPE: Solid-phase extraction.

ples using LC-ESI-MS/MS. Here, 4β-OH-stanozolol and 16β-OH-stanozolol are previously identified metabolites and are synthesized by established protocols [33]. Employing consecutive SPE and LLE for 16 doping control urine samples, these metabolites were in higher concentrations than the main metabolite 3-OH-stanozolol [34].

Optimally, in a true global metabolite profiling of drugs, samples are injected into an LC-MS system and analyzed for ions of all metabolites. Nonetheless, the sample complexation and endogenous substances form ion suppression/enhancement effect, disturbing the mass signal [25,35]. Therefore, most researchers implement a sample preparation/pre-treatment strategy to overcome this issue and proceed with chromatographic LC separation to remove the complex substances that negatively affect MS detection [24,25,35–44]. Recent literature studies show that about 65% of the metabolite profiling considered plasma as a sample type, whereas serum is about 20% for its less reproducibility. However, according to Dunn *et al.* and Yu *et al.* serum is the best-suited matrix for sample preparation and yields drug metabolites in significantly higher concentrations [24,45]. Apart from these sample types, urine, whole blood, tissues and hair are also employed to identify the metabolites. Table 1 documents the metabolite profiling of drugs in various matrices by GC-MS and LC-MS.

Analytical techniques for metabolite profiling studies

Metabolite profiling and identification consist of three crucial steps: separation, detection and structural elucidation of the metabolites that depends on the availability of analytical procedures and instruments [7,8]. Figure 1 shows the detailed presentation of metabolite profiling workflow by LC-MS/MS. HPLC and Ultra-Performance Liquid Chromatography (UPLC) offer great separation and higher efficiency in metabolite profiling for pharmaceutical research and are extensively used to analyze various biological samples [72]. Table 2 lists different chromatographic conditions utilized for drug metabolite analysis. Mass spectrometry (MS) and nuclear magnetic resonance (NMR) have become the state-of-the-art technology for metabolite profiling. These two techniques can be used as a detector and provide characteristic structural information of the analyte [7,22,73].

On the other hand, LC-MS (a hyphenation of HPLC/UPLC and mass spectrometry) has been a tremendously successful technique because of advancements in electrospray ionization (ESI), triple quadrupole and time of

Table 1. Studies on metabolite profiling of drugs in various matrices by GC-MS and LC-MS.

S. No.	Biological matrices	Species	Drugs	Mass spectrometry	Outcomes	Ref.
1	DBS	Wistar Han rats	Dasatinib	QTRAP-LC-MS/MS	A comparative study between the feasibility of plasma and DBS samples shows the similarity between them	[46]
2	DBS	Human	Nicotine and metabolites	DBS-Online-SPE-LC-HR-MS/MS	Nicotine and its major metabolites determined for sports drug testing	[47]
3	Urine, plasma and feces	Male Wistar rats	Amiodarone	QTRAP-LC-MS/MS and Q-TOF-LC-MS/MS	A total of 26 metabolites were identified, out of which 12 were novel	[48]
4	Urine	Male Sprague-Dawley rat	Acotiamide	Q-TOF-LC-MS/MS	MDF-based background subtraction for tracing metabolites and fragmentation pattern-based structure elucidation with accurate mass measurement was employed. Seven metabolites of acotiamide were identified	[49]
5	Urine, plasma and feces	Sprague-Dawley rats	Vilazodone	Q-TOF-LC-MS/MS	12 metabolites were identified	[50]
6	Urine	Sprague-Dawley rats	Entrectinib	QQQ-LC-MS/MS	6 metabolites were identified	[51]
7	Urine, plasma and feces	Male Sprague-Dawley rats	Palbociclib	Q-TOF-LC-MS/MS	14 metabolites were observed for both *in vitro* and *in vivo* samples	[52]
8	Urine, brain and plasma	Sprague-Dawley rats	Benzimidazole compound ZLN005	QTRAP-LC-MS/MS	22 metabolites were obtained, out of which 10 were novel	[53]
9	Plasma, urine and feces	Healthy male volunteers	Afatinib	QTOF-MS/MS	The study showed that minimal metabolism has occurred with plasma binding after 36 h of administration. In urine and feces, 89% of drug excretion was observed	[54]
10	Urine	Male Sprague–Dawley rats	Vandetanib	QQQ-LC-MS/MS	5 metabolites were identified	[55]
11	Urine	Male Sprague–Dawley rats	^{14}C-guadecitabine	Orbitrap HRMS	Mass balance and metabolite profiling are used in the clinical evaluation	[56]
12	Plasma	Male Sprague–Dawley rats	^{14}C-guadecitabine	QTRAP5500-QQQ-LC-MS/MS	Mass balance and metabolite profiling are used in the clinical evaluation	[56]
13	Plasma	Male Sprague–Dawley rats	Vipadenant	Q-TOF-LC-MS/MS	10 metabolites from *in vitro* and two metabolites from *in vivo* study were observed. The differences are possible due to the restriction of metabolic enzymes or cofactors existing in the *in vitro* liver microsomes to the *in vivo* system	[57]
14	Urine, plasma and feces	Male Sprague–Dawley rats	Abemaciclib	Q-TOF-LC-MS/MS	A total of 12 metabolites were identified, of these 7 were observed *in vivo* samples	[58]
15	Serum and urine	SPF male Sprague–Dawley rats	Febuxostat	Q-TOF-LC-MS/MS	A total of 10 metabolites were identified, in that 4 were novel	[59]
16	Urine, plasma and feces	Male Wistar rats	Verapamil	Q-TOF-LC-MS/MS	A total of 71 verapamil metabolites were identified, in which 2 were novel	[60]
17	Urine, plasma and bile	Male Sprague–Dawley rats	Carfilzomib	QTRAP4000- LC-MS/MS	A total of 24 metabolites were identified that helped in the knowledge disposition of carfilzomib	[61]
18	Urine	Dog, monkey, mouse, rabbit, rat and human	WCK 771	QQQ-LC-MS/MS	A total of 8 metabolites were identified in the various urine samples, where 5 were novel	[62]
19	Urine	Male Sprague–Dawley rats	Infigratinib	IT-LC-MS	7 metabolites were identified	[63]
20	Urine, plasma and feces	Male Wistar rat	Nintedanib	Q-TOF-LC-MS/MS	18 metabolites were identified, in that 10 were observed *in vivo* samples and 9 novel metabolites were identified	[64]

APB: 2-Amino-1-phenylbutane; DBS: Dried blood spot; EAPB: 2-Ethylamino-1-phenylbutane; EW: Electronic waste; GC-MS: Gas chromatography-mass spectrometry; HRMS: High-resolution mass spectrometry; IT-LC-MS: Liquid chromatography ion trap mass spectrometry; LC-MS/MS: Liquid chromatography-tandem mass spectrometry; MDF: Mass defect filter; PAH: Polycyclic aromatic hydrocarbon; QQQ: Triple quadrupole; Q-TOF: Quadrupole-time of flight; QTRAP: Hybrid triple-quadrupole linear ion trap; UPLC: Ultra-performance liquid chromatography.

Table 1. Studies on metabolite profiling of drugs in various matrices by GC-MS and LC-MS (cont.).

S. No.	Biological matrices	Species	Drugs	Mass spectrometry	Outcomes	Ref.
21	Plasma	Male patients treated with gefitinib	Gefitinib	UPLC-Q-TOF-MS/MS	18 tentative metabolites were identified, in which intestinal flora might be involved. The results further improved understanding of the toxic nature of *in vivo* products	[65]
22	Urine	Human	(EAPB) and (APB)	GC–MS	Detection of EAPB and its metabolite APB in dietary supplements intake and doping case study	[66]
23	Urine	Human	Oxandrolone, Danazol	LC-MS/MS and GC-MS	Sulphate conjugates of oxandrolone and danazol metabolites are determined	[67]
24	Hair	Human male athletes	Letrozole	XEVO™ G2XS Q-TOF-MS/MS nd confirmation with LC-HRMS	A doping agent is determined and suitable for testing in sports	[68]
25	Hair	Human	Cocaine	GC-QQQ-MS/MS	The method developed was used for authentic samples, and all the probable metabolites were identified	[69]
26	Nails	Human	PAHs and hydroxylated metabolite	LC-QQQ-MS/MS	The concentration of PAHs in EW was higher than non-EW workers	[70]
27	Nails	Human	Nicotine and its metabolite cotinine and *trans*-3′-hydroxycotinine (3-HCOT)	LC-QQQ-MS/MS	26 clinical samples obtained from infants were determined for the metabolites	[71]

APB: 2-Amino-1-phenylbutane; DBS: Dried blood spot; EAPB: 2-Ethylamino-1-phenylbutane; EW: Electronic waste; GC-MS: Gas chromatography-mass spectrometry; HRMS: High-resolution mass spectrometry; IT-LC-MS: Liquid chromatography ion trap mass spectrometry; LC-MS/MS: Liquid chromatography-tandem mass spectrometry; MDF: Mass defect filter; PAH: Polycyclic aromatic hydrocarbon; QQQ: Triple quadrupole; Q-TOF: Quadrupole-time of flight; QTRAP: Hybrid triple-quadrupole linear ion trap; UPLC: Ultra-performance liquid chromatography.

Table 2. Different chromatographic conditions in drug metabolite analysis.

Stationary phase			Mobile phase			Applied for the matrix
Column	Column length (mm)	Column particle size(μm)	Buffers and additives	Organic solvent	Elution pattern	
C18	100–200	1.7–3.5	Ammonium acetate/ammonium formate, formic acid	Acetonitrile/methanol	Gradient based on increasing the organic solvent	Plasma, feces, hair, nails and urine
HSS T3 C18	100	1.8	Ammonium acetate, formic acid	Acetonitrile	Gradient with a more organic solvent	Urine, plasma
C8	50–250	1.8–4.5	Ammonium formate	Acetonitrile in water	Gradient elution with decreasing organic solvent	Plasma, urine
HILIC	100–150	3–5	Ammonium formate, ammonium acetate, formic acid	Acetonitrile, methanol	Water as strong eluotropic solvent. Acetonitrile and methanol as weak eluotropic solvent	Urine, plasma

HILIC: Hydrophilic interaction liquid chromatography; HSS T3: High-strength silica tri-functional technology.

flight and ion-trap mass instruments. Using radioactivity or UV/Vis (photodiode array) detectors, the LC-MS can produce the metabolites structures and their quantitative estimation in a single run [72]. Further, the development of the latest tandem MS technologies like quadrupole time-of-flight accurate mass spectrometer (Q-TOF), triple quadrupole-linear ion trap (Q-trap), triple-quadrupole (QQQ) and linear trap quadrupole orbitrap (LTQ-Orbitrap) have significantly improved metabolites profiling in drug discovery and development process [7,74]. In addition, recent isotope labelling and isotope tagging permits increased ionization efficiency and quantifies metabolites separated by 1 Dalton difference [72,75].

Triple quadrupole

Paul and Steinwedel published basic quadrupole mass filter principles, which have become widely used in mass spectrometers for their small and low cost compared with other technologies [76]. In triple quadrupole (QQQ), there is a combination of two mass analyzers using RF-only collisions cell, and fragmentation occurs by the collision of DC accelerated ions with argon/nitrogen gas [77]. Ions selected in the first mass filter Q1 undergo collisional

activation in Q2, followed by analysis of fragmentation products in Q3. Achieving a stable trajectory for ions of specific m/z values in a hyperbolic electrostatic field is the primary means of mass separation in quadrupole mass filters [76].

QQQ mass spectrometers have wide usage in most analytical laboratories [78,79]. Due to its excellent MS/MS capability and mass resolution of 1000–5000, it is utilized to elucidate biotransformation sites in conjunction with accurate mass measurements obtained from Q-TOF [80,81]. Furthermore, QQQ has better sensitivity toward known compounds when run in multiple reaction monitoring (MRM) mode, in other words, when the two quadrupole mass analyzers are used as mass filters before and after the collision cell for precursor/molecular ion and fragment ion [72,82]. QQQ can produce fragment ion data, product ion scanning, including other full scan data acquisition modes, in other words, neutral loss (NL) and precursor ion (PI) scanning functions [82]. However, it produces accurate positive results only when the metabolites fragmentation pattern undergoes a similar pattern with the parent drug leading to the missing of the unexpected metabolites, in other words, metabolites having more than one site of biotransformation. One of the most often utilized screening methods using QQQ is scanning neutral loss of phase II conjugated metabolite, in other words, the neutral loss of 176 Da of a glucuronide [80,83].

Quadrupole time of flight

Quadrupole time of flight (QTOF) combines quadrupole technologies with a time-of-flight mass analyzer and differs from QQQ by replacing the last quadrupole with a time-of-flight mass analyzer. In 1955, Wiley and McLaren's team designed the first commercial time-of-flight (TOF) mass spectrometer [84,85]. After two decades, Glish and Goeringer developed a quadrupole/TOF-MS instrument where the quadrupole is employed for selecting the required precursor [86]. In QTOF, the first quadrupole (Q1) acts as a mass filter by choosing a specific ion depending upon the m/z ratio. Whereas in the second quadrupole, the ions bombard the neutral gas such as nitrogen or argon resulting in fragmentation of the ions by collision-induced dissociation (CID) process; thus, Q2 is called a collision cell [87]. Using quadrupole technology in conjunction with the TOF analyzer offers two distinct scan types for data acquisition. The first mode (MS mode) utilizes the two quadrupoles in the RF-only mode to produce an accurate mass of unfragmented precursor ions. The Q1 can also select a specific mass/charge range for transmission to the TOF analyzer. The second mode (MS/MS) can use either mass filter mode or Q1 in RF-only mode for ions transmission into Q2. The ions produced along with the unfragmented ones reaches the TOF analyzer for accurate mass measurement. The possibility of using these two modes enables the Q-TOF-MS to gather both precursor and product ion information simultaneously [88].

Hybrid-QTOF-MS instruments have excellent sensitivity, robustness and accuracy in full scan detection providing high data acquisition rate for screening and identifying metabolites. Utilizing information-dependent acquisition (IDA), the QTOF systems can acquire full-scan MS spectra and product-ion spectral data sets for the metabolites enabling the detection of targeted and non-targeted metabolites [89–91]. Moreover, QTOF mass spectrometers can detect wide mass ranges with resolution >10,000, facilitating them to reveal all the expected and unexpected metabolites even without prior knowledge of the molecular structures. Preadjustments are unnecessary as different metabolites may be detected even with a single run [74,92].

Even though TOF instruments can produce MS/MS details via insource fragmentation, hybrid QTOF has shown superiority over TOF for observing more comprehensive biotransformation sites. When both high and low collision energy data acquisition functions are used in a single LC/MS run, MSE data is produced, in which fragment ion data for all detected compounds are linked to their retention times. This operation is also applicable to TOF instruments by employing two parallel acquisition functions with low and high aperture/cone voltages without an actual collision cell, making it the main limitation [80].

Hybrid technologies

New hybrid technologies like the combination of quadrupole with linear ion-trap MS have enhanced its utilization in metabolites screening to an advanced level. This hybrid technology displaces the last quadrupole by a linear ion trap, enabling high sensitivity scanning. Structure-specific and data-dependent acquisition modes are possible with Q-trap. For metabolite screening, selected/multiple reaction monitoring (SRM/MRM) triggered enhanced product ion (EPI) MS/MS scanning is utilized [82,93,94]. The linear trap quadrupole (LTQ)-Orbitrap can produce MS/MS with high accuracy, enabling the instrument to identify the biotransformation sites. In LTQ-Orbitrap mass spectrometer, the high-resolution mass analyzer is connected to a linear ion trap where accurate mass measurements are combined with the linear ion trap high trapping capacity and MS^n scan function. On the other hand, due to

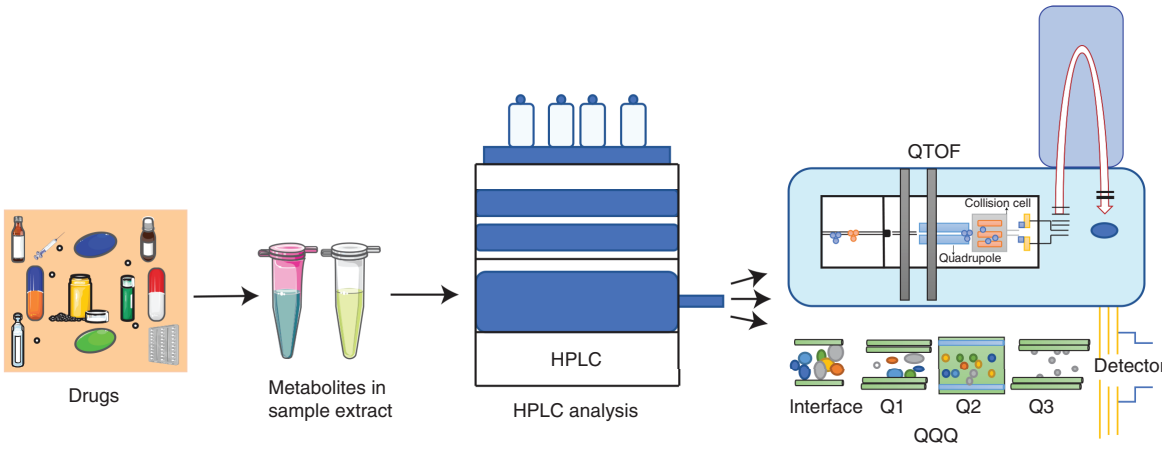

Figure 2. Metabolites identification by LC-QTOF and LC-QQQ. Screening of all possible metabolites by LC-QTOF helpful in drug discovery, LC-QQQ looks for certain metabolites by MRM mode.
HPLC: High-performance liquid chromatography; LC-QTOF: Liquid chromatography – quadrupole time of flight; LC-QQQ: Liquid chromatography – triple quadrupole; QTOF: Quadrupole time of flight; QQQ: Triple quadrupole.

the slow acquisition rate of LTQ-orbitrap, it becomes a rate-limiting step with the modern fast chromatography, especially for high throughput metabolite screening with a single LC-MS run [9,95,96]. Figure 2 depicts the representation of metabolite identification by QTOF and QQQ. Different softwares are available for post-acquisition processing and prediction based on the types of MS instruments employed. In the post-acquisition data processing, these software programs run by comparison of sample and control chromatograms [82,97,98].

Other analytical techniques in drug metabolite profiling

In recent years, NMR spectroscopy has played a vital role in unravelling drug metabolic processes. NMR is non-destructive, unbiased, identifies novel compounds without chemical modifications, and offers easy quantification as an analytical tool. NMR instruments with frequencies of 500 or 600 MHz are usually used in metabolite profiling because they are cost effective and easily accessible. However, high field instruments provide high sensitivity and resolution [72,99,100]. When coupled with chromatographic methods, in other words, LC-NMR has much greater resolving power to distinguish complex mixtures for structural elucidation of the components [100]. Several metabolite identification studies describe elegant chemoselective isotopic tagging approaches that introduce ^{15}N labels to amino groups via ^{15}N ethanolamine and ^{13}C labels to carboxylate groups via ^{13}C formic acid or ^{13}C acetic anhydride. Identification of metabolites uses deconvolution spectroscopy with a set of generated reference spectra with commercial and freeware tools such as Chenomx's NMR Suite, Bruker's AMIX and MetaboMiner [72,101]. NMR is insensitive with a lower detection limit of 1–5 µM. Advancements in cryogenically cooled probes have improved the sensitivity by approximately four times to room temperature probes. Using microcoil and cryogenically cooled enabled the identification of several natural products and metabolites that are previously unknown. Furthermore, Microcoil NMR and probes facilitated NMR-based metabolite identification on small volumes of biofluids up to 10–40 µl [72,102,103].

GC-MS is a powerful, reproducible, reliable, selective and robust tool that can assist with metabolite profiling. GC-TOF-MS is a sensitive HRMS technique for the analysis of polar metabolites as compared with LC–MS. When combined with GC, combustion isotope ratio mass spectrometry (GC/C/IRMS) increases sensitivity and enables the detection of natural and synthetic steroids by carbon isotope composition. This hyphenation helps identify the metabolites of drugs of abuse and doping agents efficiently [104]. A fundamental limitation of GC is the need for volatile analytes or derivatization to transform nonvolatile analytes into volatile ones [105,106]. Chemical derivatization is required to lower the boiling point of many endogenous metabolites, allowing them to pass through GC columns at temperatures greater than 350°C. Trimethylsilylation derivatization in GC-MS alters the functional groups like ketones hydroxyls, thiols, carboxylic acids and amines, providing adequate coverage of metabolites. *N*-methyl-*N*-(trimethylsilyl)trifluoroacetamide (MSTFA), N,O-Bis(trimethylsilyl) trifluoroacetamide (BSTFA) and *N*-tert-butyldimethylsilyl-*N*-methyltrifluoroacetamide (MTB-STFA) follow silylation mechanism [106,107]. *In vivo* metabolism of novel psychoactive substance APINAC (adamantan-1-yl-1-pentyl-1H-indazole-3-carboxylate) uti-

lized GC-MS technique for its metabolite detection, where samples are derivatized with BSTFA, TMS and ethyl acetate. A total of ten metabolites are identified with LC-QTOF-MS and GC-MS [72,108].

Direct coupling techniques are well versed in combining chromatographic or sample preparation strategies with mass spectrometry. Newer versions of SPME interface with ESI-MS like SPME-ESI-MS and SPME-Nano-ESI are currently in use. Similarly, DBS and SPE have improved coupling with MS leading to online-DBS, DBS-Online-SPE-LC-HR-MS/MS and online-SPE-MS/MS techniques [47,109–111].

Use of mass defect filters

The introduction of the mass defect filter (MDF) in 2003 had removed all the endogenous background noise by incorporating an algorithm leading to enormous data acquisition improvements [74]. However, as some endogenous compounds mask the metabolites, detecting biological matrix metabolites remains a challenging task. The detection of uncommon metabolites formed via multiple-step biotransformation is challenging to predict from parent drugs using either PI or NL scanning techniques, QQQ or hybrid QQQ-linear ion trap mass spectrometers [112]. Such a pattern-based data acquisition poses a limitation in detecting metabolites for which fragmentation patterns are unpredictable. The development of an MDF technique that detects drug metabolites via post-acquisition processing of HRMS data has rectified the limitation and significantly enhanced the role of HRMS in metabolite profiling [17,113].

The central concept of MDF is to neglect all the data outside a decided mass defect range from complex, high-resolution mass spectral data sets. The difference between the exact mass of the isotope and its nominal integer mass is called the mass defect of a single element or a chemical compound. Molecular exact mass can help in elucidating chemical formulas of unknown compounds with great precision. Therefore, mass defects serve as a filtering criterion for a known target compound as elemental formulae depend on their accurate mass. To measure the accurate masses of the product ions, modern HR-MS relies on a mass defect. Based on the mass defect, narrowing down to a distinct mass defect range of an analyte makes it more interesting to filter complex mass spectra. When a drug undergoes metabolism, it becomes more polar, simplifying its excretion process. However, the central core of the structure remains the same, making mass defects similar for the product metabolites. HRMS having a resolution of about 10,000 can easily differentiate two different ions. Overall, MDF has played a tremendous role in drug metabolite profiling by screening many metabolites out of the complex HRMS data [114].

Recent studies in the past decade for *in vivo* metabolite profiling

Drug metabolism and pharmacokinetics (DMPK) studies become challenging with the novel demands for new drug molecules. In this, metabolite profiling gained its importance with the detection of several metabolites in various biological matrices. The following section deals with the general approach for biological matrix sample preparation. Further, we highlight few case studies in the past decade detailing their analytical methodologies for metabolite profiling.

Dried blood spot samples

Dried blood spots (DBSs) have been used enormously as an alternate sample collection and extraction tool in bio-analytical, clinical and pharmaceutical communities. The procedure is less invasive and cost effective; hence it has more advantages over methods for blood, serum or plasma samples [27,115]. In 1960, Guthrie collected blood spot samples from neonates for the first time to detect phenylketonuria [116]. Since then, DBS has been employed to detect phenylketonuria and other metabolites for treatable metabolic disorders. The DBS preparation method is simple, where a patient finger is sterilised with isopropyl alcohol followed by pricking with a sterile, disposable lancet. After wiping off the immediate blood, the subsequent blood is then applied to the Whatman #903 filter paper. The samples were kept for drying over 4 h to overnight, followed by stacking and storing with a desiccant consisting of coloured humidity indicator in a sealed container [117]. Vu *et al.* developed an LC-MS method for rifampicin and clarithromycin metabolites using DBS that retains stability for 2 months at 25°C [118]. Figure 3 shows the chemical structures of the drug and major metabolite in DBS, plasma and feces samples discussed below with their respective m/z values.

Dasatinib

Dasatinib is a potent multi-targeted kinase inhibitor used to treat chronic myelogenous leukaemia by binding to BCR-Abl protein in an active state [119,120]. A study was performed to assess the feasibility of phase I and II

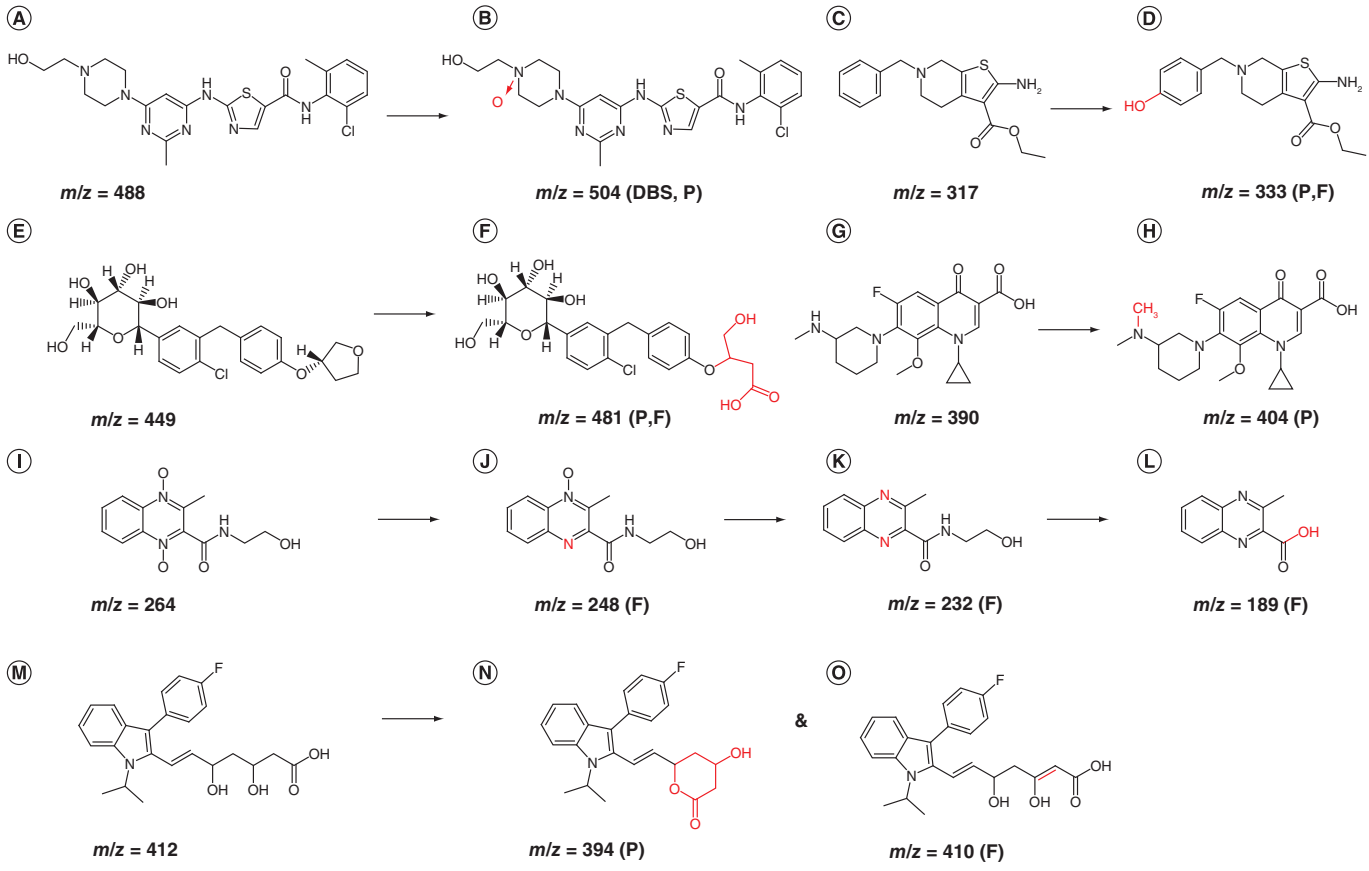

Figure 3. Structural representation with m/z value of parent molecule with their respective main metabolite in matrices. (A) Dasatinib; **(B)** M5: Piperazine N-oxide; **(C)** Tinoridine; **(D)** M10: oxidative metabolite; **(E)** Empagliflozin; **(F)** M482/1: Tetrahydrofuran ring-opened carboxylic metabolite; **(G)** Balofloxacin (BLFX); **(H)** B5: methylated metabolite; **(I)** Olaquidox; **(J)** M2: 4-deoxyolaquindox; **(K)** M3: 1,4-bideoxyolaquindox; **(L)** M5: 3-methylquinoxaline-2-carboxylic acid; **(M)** Fluvastatin (FLU); **(N)** FLU M15; **(O)** FLU M6.
DBS: Dried blood spot, P: Plasma, F: Feces.

metabolites of dasatinib in DBS and plasma, along with the difference between untreated and treated DMPK cards. The study included 200–250 g of Wistar-Han rats, to which a 50 mg/kg dose of dasatinib (dissolved in 0.5% of methylcellulose) was administered orally. Dilab accusampler, an autosampler device, collected 200 µl of blood and spotted two 20 µl of blood onto the DBS card (chemically treated DMPK-B and DMPK-A cards and untreated DBS cards) at predetermined intervals followed by drying at room temperature for 2 h and then transferring to a plastic bag in the desiccator. The remaining blood sample is placed in tubes containing sodium EDTA, where the plasma was collected and extracted by LLE. For metabolite profiling and qualitative analysis of dasatinib in DBS disc cards, samples at different intervals, i.e., 0.083, 0.25, 0.5, 1, 4, 7 and 24 h were pooled together, followed by extraction with 2 ml methanol. The supernatant was dried with nitrogen and reconstituted with 100 µl of 30% acetonitrile in water. An aliquot of 20 µl was injected into the Shimadzu SCL-10Avp stacked with a leap autosampler coupled to a Sciex API 4000 Qtrap mass spectrometer. A Phenomenex Synergy polar RP, 2.0 × 150 mm, 4.0 µm column was used with 0.1% formic acid and acetonitrile as the mobile phase at a flow rate of 0.25 ml/min in gradient mode. A positive turbo-ion spray set at 4.5 kV was utilized for mass spectral analysis.

MRM triggered enhanced product ion scan (MRM-EPI) was used for qualitative analysis, and MRM mode was used for quantitative analysis. Specific precursor ion→ product ion transitions of *m/z* 488→347 were used for dasatinib (Figure 3A) and *m/z* 494→394 for imatinib (internal standard) for quantitative analysis. Specific precursor ion→*m/z* product ion transitions of *m/z* 444→303, 502→401, 504→460, 664→488 and 568→401 for M4, M5, M6, M8 and M13 were the MRM transitions used for other identified significant metabolites. The acquisition of data and chromatographic peak integration was carried out using Analyst® software, version 1.5.1. Engaging both DBS and plasma samples leads to observing all expected metabolites from phase I and II. For the

DBS cards, untreated DBS cards show more consistency than the treated ones, which may be due to the infusion of anti-infective or anti-viral chemicals. Metabolites, namely M4, M5 (Figure 3B) and M6, have been identified for phase I metabolism. The sulphate conjugate M8 and glucuronide M13 were the metabolites obtained in phase II. In summary, using untreated DBS cards is advised over treated DBS cards [46].

Plasma & feces samples

Blood is collected in microcentrifuge tubes containing heparin, citrate, and tripotassium ethylenediaminetetraacetic acid (K_3EDTA) or K_3EDTA containing lavender-top tubes. Immediate storage of collected blood samples at -20°C is practised, and samples thawed more than twice are less recommended for routine analysis. Centrifuge with 3000 rpm is required to separate the plasma from collected blood samples, and immediate addition of liquid nitrogen halts the biological activity [24,25]. Dry ice maintains plasma stability during storage and transport and a -80°C freezer for long-term storage samples [121,122]. The co-occurrence of proteins/peptides and phospholipids in plasma increases the complexity, complicating the analytical procedures. In most cases, protein precipitation in plasma is carried out with organic solvents like methanol, acetonitrile or perchloric acid, and SPE technologies are used to remove phospholipids. For the PPT, at least three volumes of acetonitrile per plasma proved to be the best precipitating agent [7,123–125].

Fecal/stool samples are prepared by diluting the feces with methanol or acetonitrile followed by centrifugation to remove proteins. To avoid column frits blockage and damage to the LC-MS system, SPE is followed by filtration. Cao *et al.* performed a metabolite profiling study in fecal samples from healthy control and patient groups by extracting with methanol at a proportion of 3 ml/g. Following centrifugation, supernatants were filtered through a 0.2 μm pore size membrane [126,127].

Tinoridine

Male Sprague–Dawley rats of 190–210 g were utilized for metabolite structural characterization of tinoridine (TINO), a drug used to treat tonsillitis [128]. 10 mg/kg TINO dissolved in carboxymethyl cellulose (0.5% w/v in water) suspension was administered to six rats. 0.2 ml blood samples were collected in heparinized centrifuge tubes at 0.25, 0.5, 1, 2, 4, 8, 12 and 24 h. The feces were collected before the dosing and within a time interval of 4 h after dosing up to 24 h. All the urine, feces and blood plasma samples were pooled individually to obtain a single sample of each matrix. Protein precipitation followed by SPE was employed for the extraction of the drugs/metabolites. The aliquots of the sample were then injected into the LC-MS system. For the feces sample, the slurry was prepared by adding an equal volume of acetonitrile and water. The slurry was centrifuged for 10 min at 10,000 rpm, and the supernatant obtained was treated as the plasma sample.

Agilent 1200 series HPLC consisting of Acquity UPLC HSS C18 SB (2.1 × 100 mm, 1.7 μm) connected to Q-TOF LC/MS 6540 equipped with an ESI source, Agilent Technologies was operated in positive ion mode and Mass Hunter B.06.00 software was used for data acquisition. 10 mM ammonium acetate buffer at pH 5 and acetonitrile was used as the mobile phase with a 0.4 ml/min flow rate in gradient mode. The mass range was set at m/z 50–1000 for full scan MS mode with a scan time of 0.3 s^{-1}

The plasma sample contained three metabolites, whereas feces had four metabolites for tinoridine (Figure 3C). The ion peak at m/z 351(M5) in plasma with the elemental composition of $C_{17}H_{23}N_2O_4S^+$ suggested the addition of two oxygens to the parent structure. Missing of tropylium ion at m/z 91 and relatively intense fragment ions formed at m/z 152 and 198 indicated the occurrence of oxidation of the drug. The peak at m/z 287 obtained in feces having an elemental composition of $C_{15}H_{15}N_2O_2S^+$, proposed the elimination of two carbons and hydrogen from the parent drug. The product ion at m/z 269 obtained by the loss of 18 Da confirmed to be carboxylic moiety in M7, resulting in a dehydrogenated and dealkylated metabolite. Another peak at m/z 287 obtained in feces having an elemental composition of $C_{16}H_{19}N_2OS^+$ implied that decarboxylation followed acetylation. M8 was specified as N-(6-benzyl-4,5,6,7-tetrahydrothieno[2,3-c] pyridin-2-yl)acetamide, as there are no ions at m/z 198 and 152, which indicated that the ethyl carboxylate group of thiophene moiety might be metabolised into acetylated form. A peak at m/z 333 obtained in both plasma and feces with the elemental composition of $C_{17}H_{21}N_2O_3S^+$ was designated as metabolite M10 (Figure 3D). It was the most abundant oxidative metabolite having additional oxygen that is formed via phase I metabolism. A significant product ion formed at m/z 198 hinted the oxidation of the benzene moiety on the drug, whereas the 3-amino, ethyl thiophene carboxylate group was intact. A mass difference of 2 Da from the parent drug asserted that the metabolite M11 ($C_{17}H_{19}N_2O_2S^+$) was a dehydrogenated metabolite

obtained in both plasma and feces. Further, product ions at m/z 287 by loss of ethyne group and m/z 91 ($C_7H_7^+$) confirmed that benzyl moiety and ethyl carboxylate chain were intact [128].

Deductive Estimation of Risk from Existing Knowledge (DEREK) (Nexus v2.0, Lhasa Ltd., Leeds, UK) and TOPKAT (Discovery Studio 2.5, Accelrys, Inc., CA, USA) software were used for toxicity prediction. M10 was shown to have hepatotoxicity and might cause skin sensitization [128].

Empaglifozin

The excretion, metabolism and pharmacokinetic characterization of a single dose of [^{14}C]-empaglifozin, a potent and selective sodium-glucose co-transporter-2 (SGLT2) inhibitor, for the treatment of Type II diabetes mellitus was performed [75]. 50 mg of empagliflozin consisting of [^{14}C]-radiolabeled empagliflozin in solution was administered to eight male human subjects followed by a period of 4 h waiting, later standard foods were served at 4.5, 8 and 10.5 h. Blood samples were collected 1 h before the dosing for the metabolite profiling and at 2, 6 and 12 h after the administration. As there is low level of radioactivity for plasma samples after 12 h, they were pooled from all the subjects for further anlaysis. The samples collected at 2 and 6 h were profiled as an individual sample. The samples were diluted with equal amounts of water, and drugs were extracted by SPE using Oasis MCX SPE cartridges, and an aliquot of the samples was then injected into the LC-MS.

The feces were collected 24 h before the dosing and 24 h after dosing up to 168 h. The feces collected at all-time points were pooled together for each subject, and an aliquot of 10 ml feces was centrifuged for 15 min at 10°C at 10,000 rpm. Methanol and 10% acetic acid were used for the pellet extracts after removing supernatant acid and drying at 35°C under a nitrogen stream. The residue obtained was dissolved in 20 ml of water, mixed with the supernatant. The obtained mixture was eluted with Oasis MCX SPE cartridges, washed, eluted, dried (0.2 ml) and reconstituted with 1 ml of 50% methanol followed by injection into the LC-MS.

Identification of the metabolites was made based on radio chromatography, HPLC retention time and MS. The LC-MS system comprised of an Agilent 1200 HPLC system connected to Thermo Fisher Scientific LTQ Orbitrap XL operated with Xcalibur software 2.0 and a PerkinElmer 625 TR flow scintillation analyzer. ProFSA software was used to process radiochromatograms produced from the flow scintillation analyzer and Thermo Fisher Scientific MetWorks 1.1 software with a mass defect filter for metabolite identification. Empagliflozin authentic standards and three glucuronide conjugates were used for the confirmation. For the structural elucidation of the metabolites, accurate mass measurements, triple mass spectrometry (MS3), MS/MS and MS were performed.

As empagliflozin (Figure 3E) undergoes limited metabolism, most of the drug remained unchanged, with 41.2% excreted in feces. A total of six metabolites were observed, further emphasizing the limited metabolism of the drug. Of these, the most abundant drug-related component was the unchanged empagliflozin in both positive and negative mode, although the negative ion mode shows the majority. Loss of tetrahydrofuran ring was observed in a negative mode corresponding to the peak at m/z 379. The presence of one chlorine atom corresponded to the molecular ions at m/z 449 (negative mode) and 451 (positive mode), having [M + 2]/M isotope ratio of 0.35.

Furthermore, three radioactive glucuronide conjugates, M6261/1, M626/2 and M626/3, have similar m/z values with empagliflozin glucuronides authentic standards. An excess of 32 Da of empagliflozin was observed at m/z 481 in a negative mode that suggested the retention of chlorine atom with [M+2]/[M] ratio of 0.35. M482/1, i.e., m/z 481, was determined as a ring-opened tetrahydrofuran carboxylic metabolite (Figure 3F) based on the mass spectral analysis. An oxidation/dehydrogenation metabolite (M464/1) was formed in a positive mode corresponding to the elemental composition of $C_{23}H_{26}O_8Cl$. MS also showed a negative molecular ion at m/z 467, i.e., 18 Da more than empagliflozin mass corresponded to 2 hydrogen atoms and one oxygen atom [75].

Balofloxacin

The structural characterization and identification of balofloxacin (BLFX) metabolites, an antibiotic for the management and treatment of urinary tract infections, was performed using 200–250 g of female Sprague Dawley rats [129]. The study protocol was designed with three groups: two groups for blood, feces/urine and one group for control with three rats for each group. 10 mg/kg dose of BLFX dissolved in saline was administered to two groups of the animals. For the plasma sample, 0.2 ml of blood sample was collected at 0.25, 0.50, 1, 2, 8, 12, 24, 48 and 72 h. All the urine, blood plasma and feces samples were pooled to obtain a single sample of each matrix. Simple protein precipitation followed by SPE using Strata-X cartridges was used to extract the plasma BLFX metabolites. Plasma samples were mixed with three-times volume of acetonitrile, and a slurry of feces samples was made by

vortexing with 3× weight equivalent to the water used for SPE extraction. An aliquot of the sample was injected into the LC-MS system.

Agilent 1200 series HPLC consisting of XDB C-18 (4.6 × 50 mm, 5 μm) was connected to Agilent Q-TOF LC/MS 6545 and operated in a positive ion mode. Water with 0.1% formic acid (solvent A) and acetonitrile (solvent B) were used as the mobile phases with a flow rate of 0.4 ml/min in gradient mode. Mass Hunter workstation software was used for data acquisition and processing with the scan range set at 50–1750 *m/z*. A quadrupole ion trap mass spectrometer equipped with an ESI source was used to perform MS^n experiments with Xcalibur software for data acquisition.

Thirteen metabolites were identified in plasma, urine and feces samples, in which four metabolites are obtained in plasma and one metabolite from feces. Metabolite B3 with *m/z* 377 having 23 Da mass unit difference from BLFX (Figure 3G) is a highly abundant product ion at *m/z* 243 by loss of $C_6H_{10}FO_2$. By the consecutive loss of water molecules, the precursor ion at *m/z* 377 produced two product ions at *m/z* 359 and *m/z* 341, indicating a free OH group on the piperidine ring with the BLFX. Product ions with *m/z* 305 and *m/z* 226 also suggested that dealkylation occurred at the piperidine ring. Based on these observations, it was concluded that the hydroxylation of BLFX followed the dealkylation.

Metabolite B4 with *m/z* 406 obtained both in plasma and feces with a 16 Da higher mass than BLFX showed product ion *m/z* 218 with high abundance by loss of $C_9H_{17}FN_2O$ and low product ions at *m/z* 388, 370 and 233 by consecutive loss of water indicated that B4 is a hydroxylated metabolite. A mass difference of 14 Da from the parent drug suggested that the metabolite B5 (Figure 3H) formed was methylated form observed in plasma, feces and urine matrices. An intense product ion at *m/z* 359 due to the loss of C_2H_7N moiety from the precursor ion *m/z* 404 suggested methylation at the NH site on the piperidine. Summing up all these data, B5 metabolite was found to be 1-cyclopropyl-7-(3-(methylamino)piperidin-1-yl)-6-fluoro-8-methoxy-4-oxo-1,4-dihydroquinoline-3-carboxylic acid. Potential toxicity for both phase I and II plasma metabolites of BLFX were assessed by Protox-II. Out of the four metabolites assessed, B5 and B8 have immunotoxicity with a high probability score [129].

Olaquindox

Olaquindox (OLA) is a veterinary drug of synthetic quinoxalines used as an antimicrobial and growth-promoting agent [130]. Metabolite characterization of OLA (Figure 3I) was studied in 180–220 g of male Sprague Dawley rats by administering 20 mg/kg of OLA in 0.5% carboxymethyl-cellulose-sodium suspension [131]. Feces were collected in clean vials before dosing and after dosing at time intervals of 0–4, 4–8, 8–12 and 12–24 h and dried at a temperature of 40°C followed by mixing and crushing. Simple protein precipitation using acetonitrile was done, and 2 ml of aliquot was injected into the LC-MS/MS.

Acquity UPLC system consisting of Acquity HSS T3 column (2.1 × 100 mm, 1.7 μm) connected SYNAPT HDMS™ equipped with an ESI source was utilized and run in a positive ion mode. Water with 0.1% formic acid and acetonitrile were the mobile phases used at a flow rate of 0.45 ml/min in gradient mode. Sulfadimethoxine was used for the lock mass, and all the data were stored in centroid mode. Metabolynx XSTM software with MDF function for metabolite identification was used for the processing of the data.

A total of 20 metabolites were obtained for OLA, where five phase I metabolites were observed in feces and none from phase II. M1 was determined as 1-deoxyolaquindox as fragment ions were formed at *m/z* 159.0556 by retaining N→O groups at position 4. *m/z* 230, 213 and 205 were 16 Da less from fragment ions at *m/z* 246, 229 and 221 of OLA. M2 (Figure 3J) was also identified as 4-deoxyolaquindox as there is the formation of fragment ions at *m/z* 232.1078 and *m/z* 214.0972 corresponded to the cleavage of the weak N→O group at position 1. Metabolite M3, at *m/z* 232.1077 (Figure 3K) was similar to synthesized OLA and was identified as 1,4-bideoxyolaquindox as other product ions were also observed at *m/z* 214.0972, 189.0668, 171.0566 and 143.0611. Metabolite M4, at *m/z* 246.0879 was identified as 1,4-bideoxyolaquindox-20-carboxylic acid, $C_{12}H_{12}N_3O_3$, as fragment ion formed at *m/z* 200.0834 by losing HCOOH, confirmed the presence of carboxylic acid. Metabolite M5 (Figure 3L) at *m/z* 189.0669 was identified as metabolite M5, $C_{10}H_9N_2O_2$, as fragment ion was formed at *m/z* 145.0761 and 143.0612 hinted the presence of carboxylic acid [131].

Fluvastatin

Fluvastatin (FLU) is an HMG Co-A reductase inhibitor used to treat cardiovascular diseases and hypercholesterolemia. Metabolite profiling of the FLU (Figure 3M) was performed using male Sprague–Dawley rats weighing

200–220 g. 25 mg/kg dose of FLU in 0.5% carboxymethyl-cellulose suspension was administered to two groups of animals: six rats for plasma and six rats for urine and feces. For the plasma sample, 0.2 ml of blood was taken in an Eppendorf tube at a pre-dose and post-dose at 1, 2, 4, 8, 12 and 24 h. Feces were collected before dosing and after dosing at a time interval of 0–4, 4–8 and 8–24 h. The aliquots of each sample matrix were pooled together and then stored at -80°C until further analysis.

Simple protein precipitation was followed by solid-phase extraction using strata C18-E cartridges to extract the FLU metabolites from the plasma and feces, as explained for the previous drug, tinoridine. Agilent 1200 series HPLC consisting of Acquity UPLC BEH C18 (2.1 × 100 mm, 1.7 µm) connected to Agilent Technologies, Q-TOF LC/MS 6540, equipped with an ESI source in positive ion mode was used. The mobile phase consisted of water with 0.1% formic acid and acetonitrile pumped with a 0.3 ml/min flow rate in gradient mode. Mass Hunter workstation software was used for data acquisition and processing.

Out of 15 metabolites obtained from the various biological matrices, 8 metabolites were obtained in plasma and 6 in feces. M4 and M5 with *m/z* 428 obtained both in plasma and feces corresponded to $C_{24}H_{27}FNO_5^+$, which eluted at 14.4 and 15.0 min are hydroxylated metabolites. A mass difference of 2 Da from the parent drug suggested that the metabolite M6 (Figure 3O) formed was dehydrogenated. The molecular ion at *m/z* 448 was the metabolite M7 formed by the carboxyl groups sulphation and M11 with *m/z* 352 obtained both in plasma and feces having a mass difference of 18 Da ($C_{21}H_{19}FNO_3^+$) was a dehydrogenated metabolite obtained from the protonated metabolite M12. M12 (*m/z* 370), a metabolite with a molecular formula $C_{21}H_{21}FNO_4^+$ was des-isopropyl FLU, and metabolite M13 at *m/z* 459 was suggested as the taurine conjugate of pentanoic acid. The molecular ion at *m/z* 368 was M14 obtained in plasma and feces, and M15 (Figure 3N) with *m/z* 394 obtained both in plasma and feces having a mass difference of 18 Da from the protonated drug indicated that it was a dehydrogenated metabolite (lactonization) [132].

DEREK software tool was used for qualitative toxicity estimation. TOPKAT showed that metabolites M14, M13, M11 and M7 depicted higher probabilities, whereas M7, M11 and M14 also showed higher probability values for carcinogenicity due to pyrrolizidine alkaloids. Higher probability indicated the potential carcinogenicity [132].

Urine samples

Urine contains an enormous diversity of chemicals, including mammalian metabolites providing insights into system-wide changes due to physiological conditions and diseases [43]. Collecting urine samples at specified time points, transferring them to suitable containers and storing them at a temperature of -20°C lowers metabolic decay [43]. Centrifugation employed to remove particulates followed by dilution with water is the only requirement, thereby minimising the potential for analyte loss. The qualitative confirmation of synthetic cannabinoids and 20 metabolites in urine samples required a simple procedure by adjusting the pH with a 0.4 M ammonium acetate buffer followed by vortexing and incubation. PPT using acetonitrile followed by centrifugation and the injection of supernatant into the LC-MS/MS system lead to metabolite detection [43,133]. Another study collected urine samples separately from the feces and stabilized them with sodium fluoride for 24 h [134]. Figure 4 shows the chemical structures of the drug and major metabolite in urine and serum samples discussed below with their respective *m/z* values.

Ilaprazole

To determine ilaprazole and its metabolites in urine samples, six human subjects were hospitalized and fasted for 10 h overnight before the study. All the subjects were orally administered with a single dose of ilaprazole with 250 ml of water. Urine samples were collected before dosing, post-dosing within 0–24 h, and stored at -40°C before analysis. Urine samples of volunteers without any ilaprazole administration were considered as metabolite control samples for the study. For extraction of ilaprazole metabolites, LLE is conducted, and the resulting residue was dissolved with 50 µl mobile phase containing 7:3 v/v of ammonium acetate buffer-acetonitrile, and 20 µl of the sample subjected to HPLC-ESI-MS/MS system, Xcalibur 1.3 software was used for data acquisition of ilaprazole metabolites. Hypersil BDS C18, 4.6 × 200 mm, 5 µm column was employed with a 1 ml/min flow rate in a gradient mode. HPLC-ESI-MS/MS in a positive mode with 100–400 *m/z* range in tandem and full scan MS mode was used for the data acquisition. HPLC-NMR analysis was utilized to characterize metabolites and their structures.

Upon comparing human urinary samples with blank samples, four metabolites were identified from the methylene chloride extract lacking the parent compound ilaprazole (Figure 4A). The first metabolite (M1) was observed with

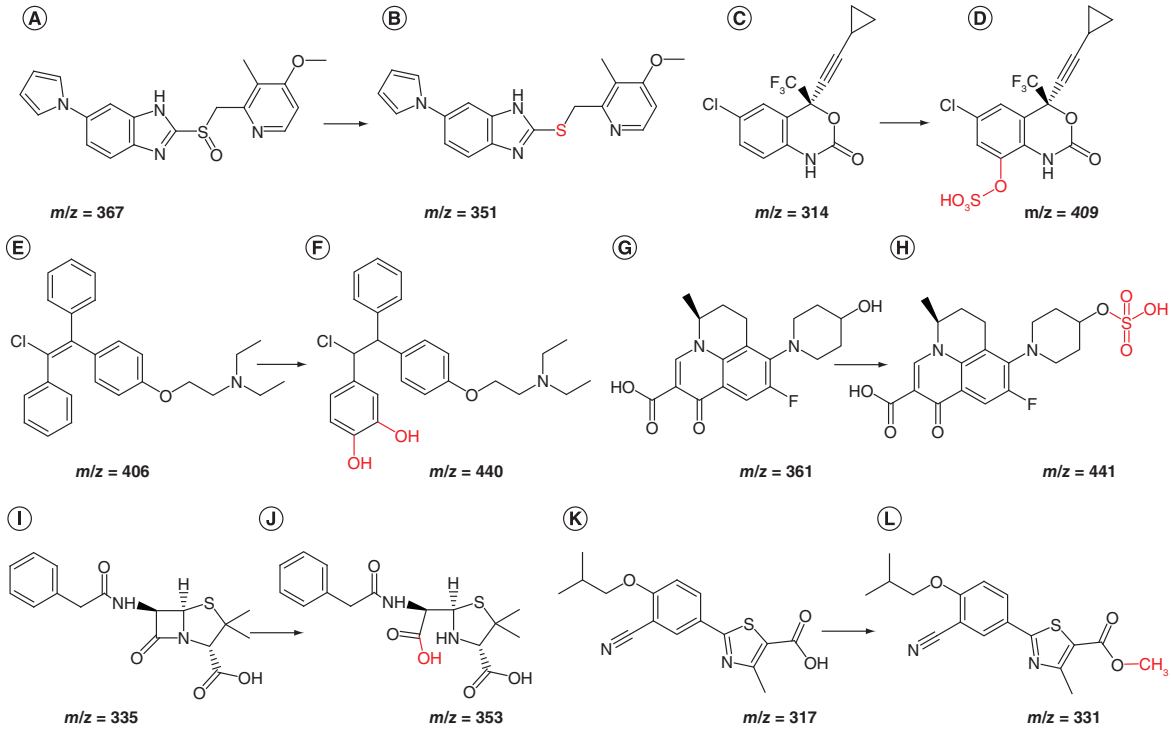

Figure 4. Structural representation with m/z value of parent molecule with their respective main metabolite in urine. (A) Ilaprazole; **(B)** M1: Ilaprazole sulfide; **(C)** Efavirenz (EFV); **(D)** 8-OH-EFV-sulfate; **(E)** Clomiphene; **(F)** Compound 2: 3,4-dihydroxy-dihydro-clomiphene; **(G)** Levonadifloxacin; **(H)** M6: O-sulfate metabolite and in serum; **(I)** Penicillin G; **(J)** M1: Penicilloate; **(K)** Febuxostat; **(L)** M7: Methylated metabolite.

m/z 351 (Figure 4B) obtained from the parent compound (*m/z* 367→351) by losing the oxygen group. *m/z* 351 gave an MS2 spectrum that showed product ions of *m/z* 318, 184 and 168. The 318 peak gave a clear idea that metabolite M1 contains a sulfide bond with a characteristic signature peak for many benzimidazoles with $–CH_2$-S– linked to a pyridine ring. A peak at *m/z* 184 was seen in fragmentation of M1 and the parent compound, revealing that the benzimidazole ring remains the same at pyrrole and pyridine rings.

Furthermore, metabolites 12-hydroxy-ilaprazole sulfide (M2), 11,12-dihydroxy-ilaprazole sulfide (M3), and ilaprazole sulfide A (M4) were observed in the fragmentation of the parent compound. Finally, a peak at *m/z* 168 was observed as a specific product ion in all the metabolite fragmentation peaks suggesting a lack of modification in the pyridine ring. Ilaprazole and metabolites M2, M3, and M4 were further confirmed with ^{1}H NMR using deuterated mobile phase solutions at a stopped-flow rate. The NMR spectrum was recorded with 12,000 Hz spectral width and 32 K data points. A biotransformation pathway showed all the metabolites M1 to M4 are formed by reducing the sulfoxide group in ilaprazole. Later, the resultant sulfide metabolites underwent hydroxylation or reduction, and the parent compound, ilaprazole was absent in urinary samples [135].

Efavirenz

The anti-viral drug efavirenz (EFV) metabolism pattern is complex with the involvement of different enzymes [136]. CYP2B6 metabolises EFV (Figure 4C) to 8-hydroxy-efavirenz (8OH-EFV), to a less extent by CYP2A6 to 7-hydroxy-efavirenz (7OH-EFV) and by UGT2B7 direct conjugation to efavirenz N-glucuronide. The primary metabolites 8OH-EFV and 7OH-EFV undergo secondary metabolism via phase II glucuronidation/ sulphation. The secondary metabolites of EFV observed in humans are 8OH-EFV–glucuronide (8OH-EFV-gln), 7OH-EFV–glucuronide (7OH-EFV-gln) and 7OH-EFV-sulfate. However, 8OH-EFV-sulfate is detected in only urine samples of cynomolgus monkeys and rats. Aouri *et al.* studied the *in vivo* profiling and distribution for novel phase I and II metabolites of EFV in urine, plasma and cerebrospinal fluid that may show neuropsychological toxicity [137]. This study enrolled 71 participants and also included the Swiss HIV cohort study for EFV observation. Urine samples

were collected from 8 healthy patients with normal renal and hepatic functions before EFV treatment (600 mg a day).

For the collected urine samples, pre-treatment and enzymatic hydrolysis was performed. 300 µl of acetonitrile was added to 100 µl of urine, centrifugated at 20,000 rpm and maintained at 4°C for 10 min. The supernatant obtained (150 µl) was placed in propylene tubes and subjected to nitrogen evaporation. Sulfatase and glucuronidase enzymatic treatment were performed on the urine samples and controls without the enzymes. Then, 20 µl of the collected supernatant was injected into the LC system. Thermo Fischer Scientific triple-stage quadrupole (TSQ) with an ESI, Xcalibur 2.0 software connected to the chromatographic system was employed to analyze samples. The sample analytical separation was done on Waters 2.1 × 50 mm, 3 µm Atlantis® dC18 analytical column and a gradient elution program with mobile phase II mM ammonium acetate and 0.1% formic acid in acetonitrile. Creatinine urinary levels normalized the metabolite concentrations in millimolar, and metabolites of phase II were observed in full fragmentation analysis. Precursor Q1 ion obtained in negative ESI conditions for *m/z* 330, 7-OH-EFV and their known product ions were compared with the data acquired in plasma and urine samples. Results showed that 7-OH-EFV-sulphate (*m/z* 409.59) metabolite was abundant and consistently observed in urine samples, whereas 8-OH-EFV-sulphate (Figure 4D) being predominant in plasma [137].

Clomiphene

A metabolic characterization study for clomiphene, a selective estrogen receptor modulator, was performed utilizing LC-QTOFMS, where all the newly reported metabolites are the products of the hydrogenation pathway [138]. Using QTOF technology, this study aimed to identify and characterize clomiphene metabolites targeting MS/MS and full scan mode. Clomiphene, prohibited by the world anti-doping agency (WADA), is metabolised by CYP2D6, including methoxylation, hydroxylation, *N*-demethylation and *N*-oxidation pathways. For urine metabolites identification, three healthy male volunteers were administered a 50 mg clomiphene citrate. After administration, urine collection was done at 8.5, 9 and 12 h, followed by the second sample collection after 1 week. First, 3 ml of urine samples were pre-treated by adjusting the pH to 7.0 with 1 ml of phosphate buffer and later 50 µl of β-glucuronidase from *E. coli*. Next, 200 ng of 17α-methyltestosterone was added and heated for 1 h at 50°C. After cooling the sample to room temperature, 0.5 ml of 1:1 potassium carbonate and potassium bicarbonate solution with pH 9.5 along with 4.5 ml of tert-butyl methyl ether were added, shaken, and centrifuged for 5 min. Organic layer constituents were subjected to dryness at 25°C, further constituted with mobile phase 90:10 v/v of 10 mM ammonium formate and acetonitrile, and 20 µl of this solution was subjected to LC-MS/MS system. Agilent LC system was used for the rapid chromatographic separation of clomiphene and metabolites using 2.0 × 150 mm, 3.5 µm zorbax eclipse C18 column with a constant flow of 0.3 ml/min gradient elution. Agilent 6538 QTOF-LC/MS is employed, while ESI was done in positive ion mode with full scan spectral data in the range of 100 to 1100 *m/z* at 1.5 scans/s rate.

Urine samples collected at 8.5, 9 and 12 h were devoid of unchanged clomiphene, therefore metabolites were distinguished with chlorine isotope pattern readily (Figure 4E). Among the seven newly identified metabolites 3,4-dihydroxy-dihydro-clomiphene (MW = 439); 3,4′,5-trihydroxy-4-methoxy-dihydro-clomiphene (MW = 487); 3-methoxy-4,4′,5-trihdroxy-dihydro-clomiphene (MW = 487); 3,4,5-trihydroxy-dihydro-clomiphene (MW = 455); 3-methoxy-4,4′-5-trihydroxy-dihydro-deethyl-clomiphene (MW = 457); 3,4-dihydroxydihydro-deethyl-clomiphene (MW = 411); 3,4,4′-trihydroxy-dihydro-deethyl-clomiphene (MW = 427); 2 important metabolites with *m/z* = 440.1991 and *m/z* 412.1674, were studied extensively with a proposed pathway for fragmentation. These new metabolites fragmentation further gave an understanding of N-diethylated side chain and N-deethylated side chain with an intense fragment ion *m/z* = 100.1125 and *m/z* = 72.0812. The study concluded that metabolites 3,4-dihydroxy-dihydro-deethyl-clomiphene and 3,4-dihydroxy-dihydro-clomiphene (Figure 4F) for their great abundance should be used as potential biomarkers supervising the clomiphene in human urine post oral administration for doping control [138].

Levonadifloxacin

WCK-771, a novel anti-methicillin-resistant *Staphylococcus aureus* (MRSA) and L-arginine salt of levonadifloxacin (LNF) pharmacokinetics was studied in rats, mice, rabbits, dogs, monkeys and humans after systemic administration in clinical and pre-clinical investigations [62]. Metabolite identification of LNF was performed using urine and serum samples and concluded that LNF undergoes primarily phase II biotransformation. Earlier studies on LNF have identified similar metabolites [139] that were identified in this study along with newly reported metabolites M8, M7, M5, M3 and M2. Serum and urine samples were collected from rats, mice, rabbits, dogs, monkeys and humans after

the intravenous administration of WCK 771. For the urine sample, the supernatant obtained after centrifugation was taken and analyzed.

Agilent 1100 HPLC with QQQ API 300 AB Sciex mass spectrometer was used with 4.6 × 250 mm, 5 µm YMC pack ODS A column and 50 mM ammonium acetate/ acetonitrile used as mobile phase for the identification of metabolites. A scan range of m/z 120 to 800 was performed in positive ionization mode with the turbo ion spray voltage of 3500V and the entrance potential 10 V at 550°C. LNF (Figure 4G) being lipophilic, is an ideal molecule for phase II metabolism, where it gets converted to polar metabolites. M1, M4, and M6 were identified in rabbits, mice and rats by Morita *et al.* with reference to the metabolic pathway of eight metabolites mentioned in the present study [139]

Collision-induced fragmentation studies of $(M+H)^+$ peaks confirmed all eight metabolites. M2 and M3 metabolites were synthesized in-company for confirming *in vivo* metabolites by correlating the retention time and mass. Identification of the structure of the three metabolites, in other words, M5, M7 and M8, was arduous owing to the plausibility of different structural isomers. Moreover, M5, M7 and M8 were challenging to synthesize; hence they were separated utilising preparative HPLC from dog urine. While product ions in MS verified the structures as O-glucuronide and acyl-glucuronide in M7 and M8, respectively. NMR studies further ensured proper confirmation on the isolated substances. Major metabolites of WCK-771 were M6 (O-sulphate, m/z = 441), M7 (O-glucuronide, m/z = 537) and M8 (acyl-glucuronide m/z = 537). In mouse urine, major metabolites detected were M7 and M8 followed by M5, while M6 (Figure 4H) was the major metabolite in rat urine succeeded by M1. Dog and rabbit urine showed similar metabolism patterns in which M7 and M8 were the intense metabolites and M1 and M5 were the minor components, whereas monkey urine exhibited an equivalent distribution of M1, M6, M7, and M8. Similar to rat urine, human urine showed M6 as the major metabolite in addition to M7 and M8. This biotransformation study of LNF helped to know the interspecies variation concerning metabolism and is further applied to serum and fecal samples with a suitable sample preparation procedure [62].

Oxandrolone & Danazol

Oxandralone and Danazol metabolite analyses are well established for glucuronide conjugates in the literature. In 2021, a study aimed to identify sulphate conjugates and their metabolites in urine [140]. Reference standards for metabolites ethisterone and 2α-hydroxymethylethisterone were synthesized and confirmed with Orbitrap XL mass spectrometer (Table 1). SPE was performed on one male volunteer's urine sample after administration of anabolic androgen steroids, and validation samples were prepared from urine samples of ten healthy volunteers by spiking reference sulphate conjugate metabolites. Preparative HPLC was done for the sulphate conjugates from excreted urine samples followed by HPLC-MS/MS. Sulphate conjugates of oxandrolone metabolite 4,2α-hydroxymethylethisterone, ethisterone, 2-hydroxy-1,2-dehydromethylethisterone and 6β-hydroxy-2-hydroxymethylethisterone were identified. Sulphate conjugates of ethisterone and 2β-hydroxymethylethisterone, 2-hydroxymethyl-1,2-dehydroethisterone (danazol metabolite 5) and 6β-hydroxy- 2-hydroxymethylethisterone (danazol metabolite 6) were identified, but danazol was undetected as a conjugate. Whereas sulphate conjugates of the danazol metabolites such as 6β-hydroxyethisterone (danazol metabolite 4), 6 β-hydroxy-2-hydroxymethyl-1,2-dehydroethisterone (danazol metabolite 7) and 6β,16-dihydroxy-2-hydroxymethylethisterone (danazol metabolite 8) were detected [67,140].

Serum sample

The serum contains less protein than the plasma and is obtained by clotting at room temperature for 30–60 min. During the clotting time, there is a high possibility of degradation and loss of more liable metabolites. Dunn *et al.* has suggested that clotting on ice and standard serum-clot contact time be followed to address concerns while using NMR and LC-MS analysis [24,25]. Serum holds an inherent advantage for detecting drugs of abuse as it can be immediately observed after exposure. However, the serum is unsuitable as a viable matrix for routine screening on drugs of abuse [141].

Penicillin G

Penicillin is one of the most prescribed β -lactam antibiotics; however, *in vivo* metabolites cause allergic reactions [142]. Therefore, for the structural characterization of penicillin G (PCN G), a study was performed with 3 authentic serum samples, in other words, S1, S2 and S3 collected before (blank) and after intravenous administration of 1 million units of PCN G and stored at -30°C before analysis. 100 ml aliquots of each sample were then collected

into a Microcon YM-3 filtration tube, subjected to centrifugation for 10 min at 12,000 rpm at 48°C. An aliquot of 5 µl sample was then injected into the LC-MS/MS system [143].

Agilent 1100 series HPLC consisting of Phenomenex Luna C18 column (2.0 × 150 mm, 5 µm) protected by a C18 guard column (4.0 × 2.0 mm) connected to LTQ linear ion trap mass spectrometer equipped with an ESI source was used. Water with 0.1% formic acid (solvent A) and acetonitrile (solvent B) were the mobile phases used at a flow rate of 0.2 ml/min in gradient mode. Penicilloate solutions and PCN G (1 mg/ml) were directly injected into the ESI source in a positive mode with a mobile phase flow rate of 40% A at 0.2 ml/min. For data-dependent scanning, four scan events design was used where full scan mode was the first scan event operated from *m/z* 148 to 1000, and the following scans were set as data-dependent product ion MSn scans: 104 for MS2, 102 for MS3 and MS4. Xcalibur™ software was used for the interpretation of data-dependent MS^n experiments.

The results showed that 7 metabolites of PCN G (Figure 4I) were identified from the serum samples. M1 (Figure 4J) and M2 were identified as penicilloate and penilloate. M3 was confirmed with an intense fragment ion at *m/z* 160, minor fragments at *m/z* 266 and 335 by loss of *m/z* 90, glycerone fragment ion. M4 was found to be derived from M3 by reducing glycerone and giving protonated molecule at *m/z* 427. Intense fragment ion was formed at *m/z* 250 by loss of *m/z* 159 and water. Other minor fragments are observed at *m/z* 409 by loss of water, 335 by loss of glycerine, *m/z* 92, and 160 by a thiazolidine ring fragment. The MS^2 spectra of M5(a)–M5(d) showed characteristic fragments at *m/z* 325 by losing a carbonyl group, *m/z* 351 by water loss, *m/z* 160, a thiazolidine ring fragment was deducing that these 4 metabolites are isomers. M6 undergoes the $[M+H-193]^+$ fragmentation of *m/z* 336 by loss of glucuronic acid. Furthermore, the MS2 spectrum of the protonated ion *m/z* 529 showed a fragment ion at *m/z* 511 by loss of H_2O and a base peak fragment ion at *m/z* 485 by neutral loss of CO_2 from the hydrolysed β-lactam ring. M7 is shown to exhibit $[M+H]^+$ at *m/z* 575 and $[M+H]^{2+}$ at 288. Overall, the data-dependent LC/MS^n yields a basic fragmentation pattern of each metabolite for the complete structural characterization in one chromatographic run proving its advantages for metabolite identification work [143].

Febuxostat

Febuxostat is a nonpurine selective inhibitor of xanthine oxidoreductase used to treat hyperuricemia in adults with gout [144–146]. For the metabolite characterization of febuxostat, a study was performed using 200–220 g of SPF male Sprague-Dawley rats [59]. 10 mg/kg dose of febuxostat in solution (0.5 mg/ml, 0.5% carboxymethyl cellulose sodium in water) was administered to the animals. 0.5 ml of the blood was collected at 0, 1, 2, 4, 8, and 12 h from the posterior orbital veins and kept for 10 min at 4°C followed by centrifugation for 5 min at 10,000 rpm. All the serum samples collected from different animals at a similar time point were pooled together, and 100 µl of each was stored at -80°C before analysis. After freeze-thawing, simple protein precipitation using methanol was employed for the sample preparation, and a 2 µl of the aliquot was injected into the UHPLC–QTOF/MS.

Agilent 1290 series UHPLC consists of an Infinity Lab Poroshell EC-C18 column (3.0 × 150 mm, 2.7 µm) connected to QTOF/MS 6545, Agilent Technologies jet stream ESI source was used in a positive ion mode. Water with 0.1% formic acid and acetonitrile were the mobile phases used at a 0.4 ml/min flow rate in gradient mode.

Five phase I (M1, M2, M3-1/M3-2, M4, M5) and two phase II metabolites are detected in serum individually for febuxostat (Figure 4K). Some identified metabolites were similar to the previously reported studies, but four novel metabolites, M7 (Figure 4L), M6, M5, M2, were obtained from this study. Two fragments with a slight difference in retention times but having the same fragment ion were labeled as M3-1 and M3-2. M3-1 is the most probable hydroxylation product because tertiary hydrogen was more active than para hydrogen and primary hydrogen. ProTox-II was used for the *in-silico* toxicity prediction of febuxostat and its metabolites. M1, M2, M3-1, M3-2, M5, M7 and M9 showed lower potential toxicity than febuxostat toward ATPase family AAA domain-containing protein 5 and androgen receptor. In addition, M3-1, M5, M7 and M9 possessed lower potential toxicity than febuxostat toward aryl hydrocarbon receptor. In essence, metabolites have no toxicity on nuclear receptor signalling and stress response pathways [59].

Hair samples & nail samples

The body's natural mechanism of metabolism and excretion diminishes the presence of most of the drug and metabolites from the body within a few minutes or hours. As the hair grows further, the drug-fixed hair becomes farther to the hair root leaving a chance to detect the drug's chronological exposure [147–149]. With advancements in analytical technologies, it is now possible to detect a minute quantity of drugs dissipated into the hair keratin at ever-decreasing concentrations [147]. The sample preparation for hair involves removing exogenous substances,

such as cosmetics, sweat, and sebum resulting in improved analytical performance. Dichloromethane is a choice for wash solvent as hair swelling is absent. Alkaline and acidic conditions can enhance the interaction surface and cause metabolite formation from parent substances, thus less recommended for dissolving hair [149,150].

Nails

Hair and nails are primarily used to identify illicit drugs. Nails are used as an alternate matrix source on the unavailability of hairs. Due to the convenience and non-invasiveness of sample collection and a longer detection time, nails offer similar benefits to the hair as a valuable matrix in forensic toxicology. However, because of the sample matrix's complexity and the low amount of drugs present, extraction and developing an analytical method are tedious [151]. Before proceeding with the LC-MS, they are subjected to alkaline hydrolysis, followed by LLE/SPE or a combination of both extraction procedures [152–154]. Representative examples of nail metabolite analysis of drugs are listed in Table 1.

JWH-018 & JWH-073

JWH-018 is Korea's most abused synthetic cannabinoid, with JWH-073 as a minor component [155,156]. Authentic hair samples up to 12 cm of length from 18 synthetic cannabinoid human suspects and 5 male lean Zucker rats about 6 weeks old were used to develop and determine JWH-018 and its metabolites for their effect on pigmentation. Pigmented and non-pigmented samples were collected by shaving the hairs from the rat's dorsal region before the drug administration. After three days, 10 mg/kg of JWH-073 was suspended in 2% Tween-80 and administered to the rats intraperitoneally. The drug was administered daily for four weeks for twenty weekdays, and the hair samples were again collected. The hair samples were washed thoroughly with methanol and water followed by weighing 10 mg, and 20 mg from human and rat hair, respectively. Then, methanol was added and then subjected to magnetic stirring for 16 h at 38°C. The extracts were then evaporated to dryness at 45°C under a stream of nitrogen, and the residue was added to 100 µl of 1:1 ratio of methanol and aqueous ammonium formate (2 mmol/l) containing 0.2% (v/v) formic acid. 5 µl of the aliquot was then injected into the LC-MS/MS system.

Agilent 1290 series UHPLC consisting of an Eclipse plus C18 column (RRHD 2.1 × 100 mm, 1.8 µm) with a 1290 in-line filter maintained at 40°C was used for the separation. Aqueous ammonium formate (2 mmol/l) containing 0.2% (v/v formic acid and ammonium formate (2 mmol/l) in acetonitrile containing 0.2% (v/v) formic acid were the mobile phases used at a flow rate of 500 µl/min in gradient mode with a total run time of 11 min. The UHPLC was connected to AB Sciex Qtrap 5500 MS/MS. For each analyte, two (MRM) transitions were selected. Analyst 1.6 software was then used for the processing of the data.

A UHPLC-MS/MS method was developed to determine JWH-018, JWH-073 and their metabolites to determine 18 authentic samples. Monohydroxylated and carboxylated metabolites are the most common metabolites obtained in hair. Only JWH-073, JWH-018 and JWH-018 N-5-OH M were detected in the human hair samples of all the metabolites. Although there is a vast difference in the quantitative results from the various individuals, JWH-073 N-COOH M and JWH-073 N-3-OH M, the two metabolites of JWH-073 were detected in all pigmented and non-pigmented hairs leading to a conclusion that pigmentation has few effects on the results [157].

XLR-11

The UHPLC-QTRAP MS/MS method was developed to characterize a popular synthetic cannabinoid XLR-11 and its metabolites to 14 authentic hair samples. The hair samples for the analysis were prepared and extracted in the same way as done for JWH-018. 5 µl of the aliquot was then injected into the LC-MS/MS system.

An Agilent 1290 Infinity UHPLC system and column compartment (Zorbax Eclipse plus C18 RRHD 2.1 × 100 mm, 1.8 µm fitted with 0.3 m in-line filter) was maintained at 40°C for the successful separation. The chromatographic separation was performed with aqueous ammonium formate (2 mmol/l) containing 0.2% (v/v) formic acid (Solvent A) and ammonium formate (2 mmol/l) in acetonitrile containing 0.2% (v/v) formic acid (Solvent B) used at a flow rate of 500 µl/min in gradient mode with a total run time of 15 min. The UHPLC was connected to AB SCIEX QTRAP® 5500 MS/MS. Two MRM transitions were selected for each analyte, and analyst 1.6 software was used to process the data. XLR-11, UR-144, UR-144 N-5-OH M, UR-144 N-COOH M and XLR-11 N-4-OH M were observed with a high difference in the quantity of the metabolites in various samples. However, the parent drug XLR-11 remained the most abundant component up on comparison [158].

Conclusion

The recent advancements in technologies have led to drastic improvements in metabolite profiling studies. High investments and core research have been conducted enormously with the aid of LC-MS/MS technologies. Progresses in technologies with high sensitivity, specificity, and functionality with ease of operation have led to substantial improvements in metabolite profiling with the availability to produce relevant results upon mining complex data sets. Biological matrices offer a great source of identifying metabolites of various drugs that provide deep insights into drug metabolism pathways. Plasma, feces and urine are still the most used matrix for metabolite profiling as they offer ease of sample extraction and preparation. However, a high throughput simple extraction method is the need of the hour. Regarding the use of different *in vivo* samples, urine samples still hold significant importance as almost all the metabolites unseen in other biological matrices can be observed. Further, it exhibits the most complex compounds, making it more challenging for data analysis and interpretation. It can reflect metabolic dysregulation as it is not under homeostatic regulation. Hence it provides insights into system-wide changes in retaliation to physiological challenges and diseases. Even though sample collection is easy for DBS, it still requires improvements for regular use. The advancements and improvements in chromatographic and mass spectrometric techniques have also contributed to increased hair analysis in modern forensic toxicology. Metabolite profiling using LC-MS/MS has enabled the researchers to predict the identified metabolites *in silico* toxicological activities and even pharmacokinetics. In the last decade, advances in metabolite profiling of anti-cancer and doping agents have gained immense interest in studying their metabolites and toxic nature.

QTOF and QQQ will be mass analyzers of choice for metabolite profile studies due to their sensitivity and ease of operation compared with other techniques. QTOF has found its enormous application in the quantification of metabolites at a significant level. It can acquire full-scan MS spectra and product-ion spectral data sets for the metabolites by utilising IDA to detect targeted and non-targeted metabolites. Its excellent MS/MS capability is frequently used to further elucidate the site of biotransformation in combination with accurate mass measurements obtained from different instruments.

QQQ has broad application for quantitative analysis due to its high detection sensitivity toward known analytes of various biological matrices when run in MRM. However, when run for full scan data acquisition mode, its sensitivity is limited compare to other MS instruments. QQQ is widely used to produce fragment ion data and product ion scanning, including other full scan data acquisition modes, i.e., neutral loss (NL) and precursor ion (PI) scanning functions. Thus, Q-TOF/MS will be the better choice for the determination of unknown metabolites than QQQ.

Future perspective

MS-based metabolite profiling is a burgeoning research field with notable investments in technology, resources and research time. There have been significant developments in analytical tools that include user-friendly software to generate pragmatic and valuable data. However, there is an absence of a complete fit method to generate high-quality data to make firm conclusions. Workflow decisions made during experiments influence the quality of data, in other words, sample preparation, LC-MS analysis, and data pre-processing. The field is likely to consolidate soon, with techniques reaching a degree of stability that will allow for inter-laboratory comparisons and data exchange. As stable pathways for detecting and characterising the unknown metabolites become available, these may add strength to the experimental metabolomics. Standard sample preparation and analysis methods should be available soon, paving the way for the routine identification and measurement of 70–100% of any given biofluid/ metabolome within the next decade.

Financial & competing interests disclosure

GN Reddy and C Laltanpuii are grateful to the Department of Pharmaceuticals, Ministry of Chemicals & Fertilizers, Government of India, New Delhi, for the NIPER fellowship award. The manuscript bears the NIPER-Hyderabad communication number NIPER-H/2021/176. The authors have no other relevant affiliations or financial involvement with any organization or entity with a financial interest in or financial conflict with the subject matter or materials discussed in the manuscript apart from those disclosed.

No writing assistance was utilized in the production of this manuscript.

Executive summary

Background

- Metabolite profiling is an essential part of drug discovery and development as it allows for a comprehensive understanding of the mechanisms of biochemical processes in a biological matrix.
- The most extensively used analytical approach for metabolite profiling is liquid chromatography-mass spectrometry.

Sample preparation & extraction approaches

- The sample from various biological matrices requires the preparation and technique that significantly impact the metabolite profile and data quality.
- The primary goal of the sample preparation technique is to convert the sample into a format suitable for LC-MS analysis while preserving as much of the sample's original metabolite composition as possible.

Analytical techniques for metabolite identification studies

- Because of developments in electrospray triple quadrupole and ion-trap mass instruments, LC-MS has been a highly successful approach.
- Recent tandem MS technologies such as the QTOF, Q-trap, QQQ, and LTQ-Orbitrap have significantly improved metabolites profiling and identification in drug discovery and development. GC-MS, LC-NMR and direct coupling to MS have emerged a lot in drug metabolite profiling.

Use of mass defect filters

- The primary idea of mass defect filters (MDF) is to remove all data from complex, high-resolution mass spectral data sets that fall outside of a predetermined mass defect range.

Recent studies in the past decade for *in vivo* metabolite profiling

- The topic of DMPK metabolite profiling/identification has grown in importance with numerous metabolites found in various biological matrices over the last decade.
- A total of 15 complete *in vivo* metabolite profiling studies were discussed in this section.

Conclusion

- Technological advancements that combine high levels of sensitivity, specificity, and functionality with ease of use have resulted in significant gains in metabolite profiling and the capacity to mine meaningful data from highly complicated data sets.

References

1. Nalbantoglu S. Metabolomics: Basic principles and strategies. *Mol. Med.* IntechOpen DOI:10.5772/intechopen.88563 (2019). https://www.intechopen.com/chapters/68486
2. Bowen BP, Northen TR. Dealing with the unknown: metabolomics and metabolite atlases. *J. Am. Soc. Mass Spectrom.* 21(9), 1471–1476 (2010).
3. Kwak M, Kang K, Wang Y. Methods of metabolite identification using MS/MS data. *J. Comput. Inf. Syst.* 1–7 https://doi.org/10.1080/08874417.2019.1681328 (2019).
4. Pauling L, Robinson AB, Teranishi R, Cary P. Quantitative analysis of urine vapor and breath by gas-liquid partition chromatography. *Proc. Natl Acad. Sci. USA* 68(10), 2374–2376 (1971).
5. Horning EC, Horning M-G. Metabolic profiles: gas-phase methods for analysis of metabolites. *Clin. Chem.* 17(8), 802–809 (1971).
6. Oliver SG, Winson MK, Kell DB, Baganz F. Systematic functional analysis of the yeast genome. *Trends Biotechnol.* 16(9), 373–378 (1998).
7. Zhang Z, Zhu M, Tang W. Metabolite identification and profiling in drug design: current practice and future directions. *Curr. Pharm. Des.* 15(19), 2220–2235 (2009).
8. Prasad B, Garg A, Takwani H, Singh S. Metabolite identification by liquid chromatography-mass spectrometry. *Trends Anal. Chem.* 30(2), 360–387 (2011).
9. Xiao JF, Zhou B, Ressom HW. Metabolite identification and quantitation in LC-MS/MS-based metabolomics. *Trends Anal. Chem.* 32, 1–14 (2012).
10. Roessner U, Bowne J. What is metabolomics all about? *BioTechniques* 46(5), 363–365 (2009).
11. Want EJ, Cravatt BF, Siuzdak G. The expanding role of mass spectrometry in metabolite profiling and characterization. *Chembiochem* 6(11), 1941–1951 (2005).
12. Muhamad N, Na-Bangchang K. Metabolite profiling in anticancer drug development: a systematic review. *Drug Des. Devel. Ther.* 14, 1401 (2020).
13. Clarke NJ, Rindgen D, Korfmacher WA, Cox KA. Peer reviewed: systematic LC/MS metabolite identification in drug discovery. *Anal. Chem.* 73(15), 430 A–439 A (2001).

14. Paul W, Steinwedel H. A new mass spectrometer without a magnetic field. *Zeitschrift fuer Naturforschung (West Germany) Divided into Z. Nautrforsch., A, and Z. Naturforsch., B: Anorg. Chem., Org. Chem., Biochem., Biophys.* 8 (1953).
15. Perchalski RJ, Yost RA, Wilder B. Structural elucidation of drug metabolites by triple-quadrupole mass spectrometry. *Anal. Chem.* 54(9), 1466–1471 (1982).
16. Lee MS, Yost RA. Rapid identification of drug metabolites with tandem mass spectrometry. *Biomed. Environ. Mass Spectrom.* 15(4), 193–204 (1988).
17. Bateman KP, Castro-Perez J, Wrona M *et al.* MSE with mass defect filtering for *in vitro* and *in vivo* metabolite identification. *Rapid Commun. Mass Spectrom.* 21(9), 1485–1496 (2007).
18. Gajula SNR, Nadimpalli N, Sonti R. Drug metabolic stability in early drug discovery to develop potential lead compounds. *Drug Metab. Rev.* (just-accepted), 1–47 (2021).
19. Lu D, Zhang S, Wang D *et al.* Identification of flurochloridone metabolites in rat urine using liquid chromatography/high resolution mass spectrometry. *J. Chromatogr. A* 1445, 80–92 (2016).
20. Lei Z, Huhman DV, Sumner LW. Mass spectrometry strategies in metabolomics. *J. Biol. Chem.* 286(29), 25435–25442 (2011).
21. Theodoridis GA, Gika HG, Want EJ, Wilson ID. Liquid chromatography–mass spectrometry based global metabolite profiling: a review. *Anal. Chim. Acta* 711, 7–16 (2012).
22. Beckonert O, Keun HC, Ebbels TM *et al.* Metabolic profiling, metabolomic and metabonomic procedures for NMR spectroscopy of urine, plasma, serum and tissue extracts. *Nat. Protoc.* 2(11), 2692–2703 (2007).
23. Dunn WB, Ellis DI. Metabolomics: current analytical platforms and methodologies. *Trends Anal. Chem.* 24(4), 285–294 (2005).
24. Dunn WB, Broadhurst D, Begley P *et al.* Procedures for large-scale metabolic profiling of serum and plasma using gas chromatography and liquid chromatography coupled to mass spectrometry. *Nat. Protoc.* 6(7), 1060–1083 (2011).
25. Vuckovic D. Current trends and challenges in sample preparation for global metabolomics using liquid chromatography–mass spectrometry. *Anal. Bioanal. Chem.* 403(6), 1523–1548 (2012).
26. Zhang Q-H, Zhou L-D, Chen H, Wang C-Z, Xia Z-N, Yuan C-S. Solid-phase microextraction technology for *in vitro* and *in vivo* metabolite analysis. *Trends Anal. Chem.* 80, 57–65 (2016).
27. Navitha Reddy G, Dilip Zagade A, Sengupta P. Current direction and advances in analytical sample extraction techniques for drugs with special emphasis on bioanalysis. *Bioanalysis* 11(04), 313–332 (2019).
28. Gao D, Wang D-D, Zhang Q *et al. In vivo* selective capture and rapid identification of luteolin and its metabolites in rat livers by molecularly imprinted solid-phase microextraction. *J. Agric. Food Chem.* 65(6), 1158–1166 (2017).
29. Simões RA, Bonato PS, Mirnaghi FS, Bojko B, Pawliszyn J. Bioanalytical method for *in vitro* metabolism study of repaglinide using 96-blade thin-film solid-phase microextraction and LC–MS/MS. *Bioanalysis* 7(1), 65–77 (2015).
30. Wang C, Li P, Lian A *et al.* Blood volatile compounds as biomarkers for colorectal cancer. *Cancer Biol. Ther.* 15(2), 200–206 (2014).
31. Wang D-D, Gao D, Huang Y-K, Xu W-J, Xia Z-N. Preparation of restricted access molecularly imprinted polymers based fiber for selective solid-phase microextraction of hesperetin and its metabolites *in vivo*. *Talanta* 202, 392–401 (2019).
32. Jager NG, Rosing H, Schellens JH, Beijnen JH. Procedures and practices for the validation of bioanalytical methods using dried blood spots: a review. *Bioanalysis* 6(18), 2481–2514 (2014).
33. Schänzer W, Opfermann G, Donike M. Metabolism of stanozolol: identification and synthesis of urinary metabolites. *J. Steroid Biochem.* 36(1–2), 153–174 (1990).
34. Thevis M, Fußhöller G, Geyer H *et al.* Detection of stanozolol and its major metabolites in human urine by liquid chromatography-tandem mass spectrometry. *Chromatographia* 64(7), 441–446 (2006).
35. Engskog MK, Haglöf J, Arvidsson T, Pettersson C. LC–MS based global metabolite profiling: the necessity of high data quality. *Metabolomics* 12(7), 114 (2016).
36. Bruce SJ, Tavazzi I, Parisod VR, Rezzi S, Kochhar S, Guy PA. Investigation of human blood plasma sample preparation for performing metabolomics using ultrahigh performance liquid chromatography/mass spectrometry. *Anal. Chem.* 81(9), 3285–3296 (2009).
37. León Z, García-Cañaveras JC, Donato MT, Lahoz A. Mammalian cell metabolomics: experimental design and sample preparation. *Electrophoresis* 34(19), 2762–2775 (2013).
38. Michopoulos F, Lai L, Gika H, Theodoridis G, Wilson I. UPLC-MS-based analysis of human plasma for metabonomics using solvent precipitation or solid phase extraction. *J. Proteome Res.* 8(4), 2114–2121 (2009).
39. Pereira H, Martin J-F, Joly C, Sébédio J-L, Pujos-Guillot E. Development and validation of a UPLC/MS method for a nutritional metabolomic study of human plasma. *Metabolomics* 6(2), 207–218 (2010).
40. Rico E, González O, Blanco ME, Alonso RM. Evaluation of human plasma sample preparation protocols for untargeted metabolic profiles analyzed by UHPLC-ESI-TOF-MS. *Anal. Bioanal. Chem.* 406(29), 7641–7652 (2014).

41. Sarafian MH, Gaudin M, Lewis MR *et al.* Objective set of criteria for optimization of sample preparation procedures for ultra-high throughput untargeted blood plasma lipid profiling by ultra performance liquid chromatography–mass spectrometry. *Anal. Chem.* 86(12), 5766–5774 (2014).
42. Tulipani S, Llorach R, Urpi-Sarda M, Andres-Lacueva C. Comparative analysis of sample preparation methods to handle the complexity of the blood fluid metabolome: when less is more. *Anal. Chem.* 85(1), 341–348 (2013).
43. Want EJ, Wilson ID, Gika H *et al.* Global metabolic profiling procedures for urine using UPLC–MS. *Nat. Protoc.* 5(6), 1005 (2010).
44. Vorkas PA, Isaac G, Anwar MA *et al.* Untargeted UPLC-MS profiling pipeline to expand tissue metabolome coverage: application to cardiovascular disease. *Anal. Chem.* 87(8), 4184–4193 (2015).
45. Yu Z, Kastenmüller G, He Y *et al.* Differences between human plasma and serum metabolite profiles. *PLoS ONE* 6(7), e21230 (2011).
46. Shen Z, Kang P, Rahavendran SV. Metabolite profiling of dasatinib dosed to Wistar Han rats using automated dried blood spot collection. *J. Pharm. Biomed. Anal.* 67, 92–97 (2012).
47. Tretzel L, Thomas A, Piper T *et al.* Fully automated determination of nicotine and its major metabolites in whole blood by means of a DBS online-SPE LC-HR-MS/MS approach for sports drug testing. *J. Pharm. Biomed. Anal.* 123, 132–140 (2016).
48. Varkhede NR, Jhajra S, Ahire DS, Singh S. Metabolite identification studies on amiodarone in *in vitro* (rat liver microsomes, rat and human liver S9 fractions) and *in vivo* (rat feces, urine, plasma) matrices by using liquid chromatography with high-resolution mass spectrometry and multiple-stage mass spectrometry: characterization of the diquinone metabolite supposedly responsible for the drug's hepatotoxicity. *Rapid Commun. Mass Spectrom.* 28(4), 311–331 (2014).
49. Patel PN, Kalariya PD, Swamy CV, Gananadhamu S, Srinivas R. Quantitation of acotiamide in rat plasma by UHPLC-Q-TOF-MS: method development, validation and application to pharmacokinetics. *Biomed. Chromatogr.* 30(3), 363–368 (2016).
50. Chavan BB, Kalariya PD, Tiwari S *et al.* Identification and characterization of vilazodone metabolites in rats and microsomes by ultrahigh-performance liquid chromatography/quadrupole time-of-flight tandem mass spectrometry. *Rapid Commun. Mass Spectrom.* 31(23), 1974–1984 (2017).
51. Attwa MW, Kadi AA, Alrabiah H, Darwish HW. LC–MS/MS reveals the formation of iminium and quinone methide reactive intermediates in entrectinib metabolism: *in vivo* and *in vitro* metabolic investigation. *J. Pharm. Biomed. Anal.* 160, 19–30 (2018).
52. Chavan BB, Tiwari S, Shankar G *et al. In vitro* and *in vivo* metabolic investigation of the Palbociclib by UHPLC-Q-TOF/MS/MS and *in silico* toxicity studies of its metabolites. *J. Pharm. Biomed. Anal.* 157, 59–74 (2018).
53. Sun W, Nguyen KD, Fitch WL *et al. In vitro* and *in vivo* metabolite identification of a novel benzimidazole compound ZLN005 by liquid chromatography/tandem mass spectrometry. *Rapid Commun. Mass Spectrom.* 32(6), 480–488 (2018).
54. Stopfer P, Marzin K, Narjes H *et al.* Afatinib pharmacokinetics and metabolism after oral administration to healthy male volunteers. *Cancer Chemother. Pharmacol.* 69(4), 1051–1061 (2012).
55. Attwa MW, Kadi AA, Darwish HW, Amer SM, Al-Shakliah NS. Identification and characterization of *in vivo*, *in vitro* and reactive metabolites of vandetanib using LC–ESI–MS/MS. *Chem. Cent. J.* 12(1), 1–16 (2018).
56. Roosendaal J, Rosing H, Lucas L *et al.* Mass balance and metabolite profiling of 14 C-guadecitabine in patients with advanced cancer. *Invest. New Drugs* 38(4), 1–11 (2019).
57. Shin S-H, Park M-H, Byeon J-J *et al.* Analysis of vipadenant and its *in vitro* and *in vivo* metabolites via liquid chromatography-quadrupole-time-of-flight mass spectrometry. *Pharmaceutics* 10(4), 260 (2018).
58. Thakkar D, Kate AS. Update on metabolism of abemaciclib: *in silico*, *in vitro*, and *in vivo* metabolite identification and characterization using high resolution mass spectrometry. *Drug test. Anal.* 12(3), 331–342 (2020).
59. Zhou L, Liu H, Xu Z, Guan S, Zhang L. Identification and structural characterization of febuxostat metabolites in rat serum and urine samples using UHPLC–QTOF/MS. *Biomed. Chromatogr.* 33(9), e4568 (2019).
60. Zhu C, Wan M, Cheng H, Wang H, Zhu M, Wu C. Rapid detection and structural characterization of verapamil metabolites in rats by UPLC–MSE and UNIFI platform. *Biomed. Chromatogr.* 34(1), e4702 (2020).
61. Yang J, Wang Z, Fang Y *et al.* Pharmacokinetics, pharmacodynamics, metabolism, distribution, and excretion of carfilzomib in rats. *Drug Metab. Dispos.* 39(10), 1873–1882 (2011).
62. Yeole RD, Rane VP, Ahirrao VK *et al.* Identification of metabolites of novel Anti-MRSA fluoroquinolone WCK 771 in mouse, rat, rabbit, dog, monkey and human urine using liquid chromatography tandem mass spectrometry. *Biomed. Chromatogr.* 33(7), e4532 (2019).
63. Al-Shakliah NS, Attwa MW, Kadi AA, Alrabiah H. Identification and characterization of *in silico*, *in vivo*, *in vitro*, and reactive metabolites of infigratinib using LC-ITMS: bioactivation pathway elucidation and *in silico* toxicity studies of its metabolites. *RSC Advances* 10(28), 16231–16244 (2020).
64. Tiwari SS, Dhiman V, Mukesh S, Sangamwar AT, Srinivas R, Talluri MK. Identification and characterization of novel metabolites of nintedanib by ultra-performance liquid chromatography/quadrupole time-of-flight tandem mass spectrometry with *in silico* toxicological assessment. *Rapid Commun. Mass Spectrom.* 34(22), e8915 (2020).

65. Wang C, Zhang J, Zhou S *et al.* Tentative identification of gefitinib metabolites in non-small-cell lung cancer patient plasma using ultra-performance liquid chromatography coupled with triple quadrupole time-of-flight mass spectrometry. *PLoS ONE* 15(7), e0236523 (2020).
66. Wójtowicz M, Jarek A, Chajewska K, Turek-Lepa E, Kwiatkowska D. Determination of designer doping agent–2-ethylamino-1-phenylbutane–in dietary supplements and excretion study following single oral supplement dose. *J. Pharm. Biomed. Anal.* 115, 523–533 (2015).
67. Rzeppa S, Viet L. Analysis of sulfate metabolites of the doping agents oxandrolone and danazol using high performance liquid chromatography coupled to tandem mass spectrometry. *J. Chromatogr. B.* 1029, 1–9 (2016).
68. Ameline A, Gheddar L, Raul J-S, Kintz P. Characterization of letrozole in human hair using LC-MS/MS and confirmation by LC-HRMS: application to a doping case. *J. Chromatogr. B.* 1162, 122495 (2021).
69. La Maida N, Mannocchi G, Giorgetti R, Sirignano A, Ricci G, Busardò FP. Optimization of a rapid sample pretreatment for the quantification of COCAINE and its main metabolites in hair through a new and validated GC-MS/MS method. *J. Pharm. Biomed. Anal.* 204, 114282 (2021).
70. Ma S, Zeng Z, Lin M *et al.* PAHs and their hydroxylated metabolites in the human fingernails from e-waste dismantlers: implications for human non-invasive biomonitoring and exposure. *Environ. Pollut.* 283, 117059 (2021).
71. Kim J, Cho H-D, Suh JH *et al.* Analysis of nicotine metabolites in hair and nails using QuEChERS method followed by liquid chromatography–tandem mass spectrometry. *Molecules* 25(8), 1763 (2020).
72. Wishart DS. Advances in metabolite identification. *Bioanalysis* 3(15), 1769–1782 (2011).
73. Gajula SNR, Nanjappan S. Metabolomics: a recent advanced omics technology in herbal medicine research. In: *Medicinal and Aromatic Plants*. Elsevier, 97–117 (2021).
74. Zhang H, Zhang D, Ray K. A software filter to remove interference ions from drug metabolites in accurate mass liquid chromatography/mass spectrometric analyzes. *J. Mass Spectrom.* 38(10), 1110–1112 (2003).
75. Chen L-Z, Jungnik A, Mao Y *et al.* Biotransformation and mass balance of the SGLT2 inhibitor empagliflozin in healthy volunteers. *Xenobiotica* 45(6), 520–529 (2015).
76. Picó Y, Blasco C, Font G. Environmental and food applications of LC–tandem mass spectrometry in pesticide-residue analysis: an overview. *Mass Spectrom. Rev.* 23(1), 45–85 (2004).
77. Soler C, Mañes J, Picó Y. Comparison of liquid chromatography using triple quadrupole and quadrupole ion trap mass analyzers to determine pesticide residues in oranges. *J. Chromatogr. A* 1067(1–2), 115–125 (2005).
78. Gautam N, Lin Z, Banoub MG *et al.* Simultaneous quantification of intracellular lamivudine and abacavir triphosphate metabolites by LC–MS/MS. *J. Pharm. Biomed. Anal.* 153, 248–259 (2018).
79. Rashid MM, Lee H, Jung BH. Metabolite identification and pharmacokinetic profiling of PP242, an ATP-competitive inhibitor of mTOR using ultra high-performance liquid chromatography and mass spectrometry. *J. Chromatogr. B.* 1072, 244–251 (2018).
80. Rousu T, Herttuainen J, Tolonen A. Comparison of triple quadrupole, hybrid linear ion trap triple quadrupole, time-of-flight and LTQ-Orbitrap mass spectrometers in drug discovery phase metabolite screening and identification *in vitro*–amitriptyline and verapamil as model compounds. *Rapid Commun. Mass Spectrom.* 24(7), 939–957 (2010).
81. Hakala KS, Kostiainen R, Ketola RA. Feasibility of different mass spectrometric techniques and programs for automated metabolite profiling of tramadol in human urine. *Rapid Commun. Mass Spectrom.* 20(14), 2081–2090 (2006).
82. Tolonen A, Turpeinen M, Pelkonen O. Liquid chromatography–mass spectrometry in *in vitro* drug metabolite screening. *Drug Discov. Today* 14(3–4), 120–133 (2009).
83. Jemal M, Ouyang Z, Zhao W, Zhu M, Wu WW. A strategy for metabolite identification using triple-quadrupole mass spectrometry with enhanced resolution and accurate mass capability. *Rapid Commun. Mass Spectrom.* 17(24), 2732–2740 (2003).
84. Cotter RJ. *Time-of-flight mass spectrometry*. ACS Publications (1993).
85. Wiley W, Mclaren IH. Time-of-flight mass spectrometer with improved resolution. *Rev. Sci. Instrum.* 26(12), 1150–1157 (1955).
86. Glish GL, Goeringer DE. A tandem quadrupole/time-of-flight instrument for mass spectrometry/mass spectrometry. *Anal. Chem.* 56(13), 2291–2295 (1984).
87. El-Aneed A, Cohen A, Banoub J. Mass spectrometry, review of the basics: electrospray, MALDI, and commonly used mass analyzers. *Appl. Spectrosc. Rev.* 44(3), 210–230 (2009).
88. Allen DR, Mcwhinney BC. Quadrupole time-of-flight mass spectrometry: a paradigm shift in toxicology screening applications. *Clin Biochem Rev* 40(3), 135 (2019).
89. Kim J, Basiri B, Hassan C *et al.* Metabolite profiling of the antisense oligonucleotide eluforsen using liquid chromatography-mass spectrometry. *Mol. Ther. Nucleic Acids* 17, 714–725 (2019).
90. Vishnuvardhan C, Baikadi S, Borkar RM, Srinivas R, Satheeshkumar N. *In vivo* metabolic investigation of silodosin using UHPLC–QTOF–MS/MS and *in silico* toxicological screening of its metabolites. *J. Mass Spectrom.* 51(10), 867–882 (2016).

91. Li X, Tang M, Wang H *et al. In Vitro* and *In Vivo* Primary Metabolic Characterization of F18, a Novel Histone Deacetylase-6 (HDAC6) Inhibitor, Using UHPLC–QqQ–MS/MS and Q-TOF–MS Methods. *Chromatographia* 79(21), 1479–1490 (2016).
92. Tian T, Jin Y, Ma Y *et al.* Identification of metabolites of oridonin in rats with a single run on UPLC-Triple-TOF-MS/MS system based on multiple mass defect filter data acquisition and multiple data processing techniques. *J. Chromatogr. B.* 1006, 80–92 (2015).
93. Ludwig F-A, Fischer S, Smits R *et al.* Exploring the metabolism of (+)-[18f] flubatine *in vitro* and *in vivo*: lc-ms/ms aided identification of radiometabolites in a clinical pet study. *Molecules* 23(2), 464 (2018).
94. Pan H, Li Y, Huang L, Zhou X, Lu Y, Shi F. Development and validation of a rapid LC–MS/MS method for simultaneous quantification of arecoline and its two active metabolites in rat plasma and its application to a pharmacokinetic study. *J. Pharm. Biomed. Anal.* 154, 397–403 (2018).
95. Dunn WB, Broadhurst D, Brown M *et al.* Metabolic profiling of serum using Ultra Performance Liquid Chromatography and the LTQ-Orbitrap mass spectrometry system. *J. Chromatogr. B.* 871(2), 288–298 (2008).
96. Hu Q, Noll RJ, Li H, Makarov A, Hardman M, Graham Cooks R. The Orbitrap: a new mass spectrometer. *J. Mass Spectrom.* 40(4), 430–443 (2005).
97. Pelkonen O, Tolonen A, Korjamo T, Turpeinen M, Raunio H. From known knowns to known unknowns: predicting *in vivo* drug metabolites. *Bioanalysis* 1(2), 393–414 (2009).
98. Nassar A-EF, Talaat RE. Strategies for dealing with metabolite elucidation in drug discovery and development. *Drug Discov. Today* 9(7), 317–327 (2004).
99. Viant MR, Bearden DW, Bundy JG *et al.* International NMR-based environmental metabolomics intercomparison exercise. *Environ. Sci. Technol.* 43(1), 219–225 (2009).
100. Zhang S, Gowda GN, Ye T, Raftery D. Advances in NMR-based biofluid analysis and metabolite profiling. *Analyst* 135(7), 1490–1498 (2010).
101. Ye T, Mo H, Shanaiah N, Gowda GN, Zhang S, Raftery D. Chemoselective 15N tag for sensitive and high-resolution nuclear magnetic resonance profiling of the carboxyl-containing metabolome. *Anal. Chem.* 81(12), 4882–4888 (2009).
102. Grimes JH, O'connell TM. The application of micro-coil NMR probe technology to metabolomics of urine and serum. *J. Biomol. NMR* 49(3–4), 297–305 (2011).
103. Putzbach K, Krucker M, Grynbaum MD, Hentschel P, Webb AG, Albert K. Hyphenation of capillary high-performance liquid chromatography to microcoil magnetic resonance spectroscopy – determination of various carotenoids in a small-sized spinach sample. *J. Pharm. Biomed. Anal.* 38(5), 910–917 (2005).
104. Polet M, Van Eenoo P. GC-C-IRMS in routine doping control practice: 3 years of drug testing data, quality control and evolution of the method. *Anal. Bioanal. Chem.* 407(15), 4397–4409 (2015).
105. Looser R, Krotzky AJ, Trethewey RN. Metabolite profiling with GC-MS and LC-MS. In: *Metabolome analyzes: Strategies for Systems Biology.*Springer, 103–118 (2005).
106. Zeki ÖC, Eylem CC, Reçber T, Kır S, Nemutlu E. Integration of GC-MS and LC-MS for untargeted metabolomics profiling. *J. Pharm. Biomed. Anal.* 113509 (2020).
107. Kopka J. Current challenges and developments in GC–MS based metabolite profiling technology. *J. Biotechnol.* 124(1), 312–322 (2006).
108. Savchuk S, Appolonova S, Pechnikov A, Rizvanova L, Shestakova K, Tagliaro F. *In vivo* metabolism of the new synthetic cannabinoid APINAC in rats by GC–MS and LC–QTOF-MS. *Forensic Toxicol.* 35(2), 359–368 (2017).
109. Ooms JA, Knegt L, Koster EHM. Exploration of a new concept for automated dried blood spot analysis using flow-through desorption and online SPE–MS/MS. *Bioanalysis* 3(20), 2311–2320 (2011).
110. Hu B, Zheng B, Rickert D *et al.* Direct coupling of solid phase microextraction with electrospray ionization mass spectrometry: a case study for detection of ketamine in urine. *Anal. Chim. Acta* 1075, 112–119 (2019).
111. Ng TT. Rapid determination of drugs-of-abuse in urine and oral fluid and rapid authentication of edible oils by mass spectrometry (2018). https://theses.lib.polyu.edu.hk/handle/200/9596
112. Zhu M, Ma L, Zhang D *et al.* Detection and characterization of metabolites in biological matrices using mass defect filtering of liquid chromatography/high resolution mass spectrometry data. *Drug Metab. Dispos.* 34(10), 1722–1733 (2006).
113. Zhang H, Zhang D, Ray K, Zhu M. Mass defect filter technique and its applications to drug metabolite identification by high-resolution mass spectrometry. *J. Mass Spectrom.* 44(7), 999–1016 (2009).
114. Sleno L. The use of mass defect in modern mass spectrometry. *J. Mass Spectrom.* 47(2), 226–236 (2012).
115. Déglon J, Thomas A, Daali Y *et al.* Automated system for on-line desorption of dried blood spots applied to LC/MS/MS pharmacokinetic study of flurbiprofen and its metabolite. *J. Pharm. Biomed. Anal.* 54(2), 359–367 (2011).
116. Guthrie R. Blood screening for phenylketonuria. *JAMA* 178(8), 863–863 (1961).
117. Mcdade TW, Williams S, Snodgrass JJ. What a drop can do: dried blood spots as a minimally invasive method for integrating biomarkers into population-based research. *Demography* 44(4), 899–925 (2007).

118. Vu D, Koster R, Bolhuis M *et al.* Simultaneous determination of rifampicin, clarithromycin and their metabolites in dried blood spots using LC–MS/MS. *Talanta* 121, 9–17 (2014).
119. Sonti R, Hertel-Hering I, Lamontanara AJ, Hantschel O, Grzesiek S. ATP site ligands determine the assembly state of the Abelson kinase regulatory core via the activation loop conformation. *J. Am. Chem. Soc.* 140(5), 1863–1869 (2018).
120. Hantschel O, Grebien F, Superti-Furga G. The growing arsenal of ATP-competitive and allosteric inhibitors of BCR–ABL. *Cancer Res.* 72(19), 4890–4895 (2012).
121. Fiehn O, Kind T. Metabolite profiling in blood plasma. In: *Metabolomics*, Springer (Eds). 3–17 (2007).
122. Kulkarni P, Karanam A, Gurjar M *et al.* Effect of various anticoagulants on the bioanalysis of drugs in rat blood: implication for pharmacokinetic studies of anticancer drugs. *Springerplus* 5(1), 1–8 (2016).
123. Skov K, Hadrup N, Smedsgaard J, Frandsen H. LC–MS analysis of the plasma metabolome—A novel sample preparation strategy. *J. Chromatogr. B.* 978, 83–88 (2015).
124. Psychogios N, Hau DD, Peng J *et al.* The human serum metabolome. *PLoS ONE* 6(2), e16957 (2011).
125. Josefsson M, Sabanovic A. Sample preparation on polymeric solid phase extraction sorbents for liquid chromatographic-tandem mass spectrometric analysis of human whole blood—A study on a number of beta-agonists and beta-antagonists. *J. Chromatogr. A* 1120(1–2), 1–12 (2006).
126. Deda O, Gika HG, Wilson ID, Theodoridis GA. An overview of fecal sample preparation for global metabolic profiling. *J. Pharm. Biomed. Anal.* 113, 137–150 (2015).
127. Cao H, Huang H, Xu W *et al.* Fecal metabolome profiling of liver cirrhosis and hepatocellular carcinoma patients by ultra performance liquid chromatography–mass spectrometry. *Anal. Chim. Acta* 691(1–2), 68–75 (2011).
128. Kalariya PD, Patel PN, Kavya P *et al.* Rapid structural characterization of *in vivo* and *in vitro* metabolites of tinoridine using UHPLC–QTOF–MS/MS and *in silico* toxicological screening of its metabolites. *J. Mass Spectrom.* 50(11), 1222–1233 (2015).
129. Shankar G, Borkar RM, Udutha S, Anagoni SP, Srinivas R. Identification and structural characterization of *in vivo* metabolites of balofloxacin in rat plasma, urine and feces samples using Q-TOF/LC/ESI/MS/MS: *in silico* toxicity studies. *J. Pharm. Biomed. Anal.* 159, 200–211 (2018).
130. Linton A, Hedges A, Bennett P. Monitoring for the development of antimicrobial resistance during the use of olaquindox as a feed additive on commercial pig farms. *J. Appl. Bacteriol.* 64(4), 311–327 (1988).
131. Bi Y, Wang X, Xu S *et al.* Metabolism of olaquindox in rat and identification of metabolites in urine and feces using ultra-performance liquid chromatography/quadrupole time-of-flight mass spectrometry. *Rapid Commun. Mass Spectrom.* 25(7), 889–898 (2011).
132. Chavan BB, Kalariya PD, Nimbalkar RD, Garg P, Srinivas R, Kumar Talluri M. Identification and characterization of fluvastatin metabolites in rats by UHPLC/Q-TOF/MS/MS and *in silico* toxicological screening of the metabolites. *J. Mass Spectrom.* 52(5), 296–314 (2017).
133. Wohlfarth A, Scheidweiler KB, Chen X, Liu H-F, Huestis MA. Qualitative confirmation of 9 synthetic cannabinoids and 20 metabolites in human urine using LC–MS/MS and library search. *Anal. Chem.* 85(7), 3730–3738 (2013).
134. Wissenbach DK. Development of the first metabolite-based LC-MS^n urine drug screening procedure. 400(1), 79–88 (2012).
135. Zhou G, Shi S, Zhang W *et al.* Identification of ilaprazole metabolites in human urine by HPLC-ESI-MS/MS and HPLC-NMR experiments. *Biomed. Chromatogr.* 24(10), 1130–1135 (2010).
136. Csajka C, Marzolini C, Fattinger K *et al.* Population pharmacokinetics and effects of efavirenz in patients with human immunodeficiency virus infection. *Clin. Pharmacol. Ther.* 73(1), 20–30 (2003).
137. Aouri M, Barcelo C, Ternon B *et al. In vivo* profiling and distribution of known and novel phase I and phase II metabolites of efavirenz in plasma, urine, and cerebrospinal fluid. *Drug Metab. Dispos.* 44(1), 151–161 (2016).
138. Lu J, He G, Wang X *et al.* Mass spectrometric identification and characterization of new clomiphene metabolites in human urine by liquid chromatography–quadrupole time-of-flight tandem mass spectrometry. *J. Chromatogr. A* 1243, 23–32 (2012).
139. Morita S, Otsubo K, Uchida M, Kawabata S, Tamaoka H, Shimizu T. Synthesis and antibacterial activity of the metabolites of 9-fluoro-6, 7-dihydro-8-(4-hydroxy-1-piperidyl)-5-methyl-1-oxo-1H, 5H-benzo [i, j] quinolizine-2-carboxylic acid (OPC-7251). *Chem. Pharm. Bull. (Tokyo)* 38(7), 2027–2029 (1990).
140. Thevis M, Piper T, Thomas A. Recent advances in identifying and utilizing metabolites of selected doping agents in human sports drug testing. *J. Pharm. Biomed. Anal.* 205, 114312 (2021).
141. De Jager AD, Warner JV, Henman M, Ferguson W, Hall A. LC–MS/MS method for the quantitation of metabolites of eight commonly-used synthetic cannabinoids in human urine – an Australian perspective. *J. Chromatogr. B.* 897, 22–31 (2012).
142. Basomba A, Pelaez A, Villalmanzo I, Campos A. Allergy to penicillin unsuccessfully treated with a haptenic inhibitor (benzyl-penicilloyl-N2-formil-lysine; BPO-Flys): a case report. *Clin. Exp. Allergy* 8(4), 341–345 (1978).
143. Ho HP, Lee RJ, Chen CY, Wang SR, Li ZG, Lee MR. Identification of new minor metabolites of penicillin G in human serum by multiple-stage tandem mass spectrometry. *Rapid Commun. Mass Spectrom.* 25(1), 25–32 (2011).
144. Frampton JE. Febuxostat: a review of its use in the treatment of hyperuricaemia in patients with gout. *Drugs* 75(4), 427–438 (2015).

145. Schumacher H Jr, Becker M, Lloyd E, Macdonald P, Lademacher C. Febuxostat in the treatment of gout: 5-yr findings of the FOCUS efficacy and safety study. *Rheumatology (Oxford)* 48(2), 188–194 (2009).

146. Edwards NL. Febuxostat: a new treatment for hyperuricaemia in gout. *Rheumatology (Oxford)* 48(Suppl. 2), ii15–ii19 (2009).

147. Vincenti M, Salomone A, Gerace E, Pirro V. Application of mass spectrometry to hair analysis for forensic toxicological investigations. *Mass Spectrom. Rev.* 32(4), 312–332 (2013).

148. Pragst F, Balikova MA. State of the art in hair analysis for detection of drug and alcohol abuse. *Clin. Chim. Acta* 370(1–2), 17–49 (2006).

149. Koster RA, Alffenaar J-WC, Greijdanus B, Vandernagel JE, Uges DR. Fast and highly selective LC-MS/MS screening for THC and 16 other abused drugs and metabolites in human hair to monitor patients for drug abuse. *Ther. Drug Monit.* 36(2), 234–243 (2014).

150. Musshoff F, Madea B. Analytical pitfalls in hair testing. *Anal. Bioanal. Chem.* 388(7), 1475–1494 (2007).

151. Cappelle D, Yegles M, Neels H *et al.* Nail analysis for the detection of drugs of abuse and pharmaceuticals: a review. *Forensic Toxicol.* 33(1), 12–36 (2015).

152. Cappelle D, De Doncker M, Gys C *et al.* A straightforward, validated liquid chromatography coupled to tandem mass spectrometry method for the simultaneous detection of nine drugs of abuse and their metabolites in hair and nails. *Anal. Chim. Acta* 960, 101–109 (2017).

153. Magalhães TP, Cravo S, Silva DDD *et al.* Quantification of methadone and main metabolites in nails. *J. Anal. Toxicol.* 42(3), 192–206 (2018).

154. Cobo-Golpe M, De-Castro-Ríos A, Cruz A, López-Rivadulla M, Lendoiro E. Determination and distribution of cannabinoids in nail and hair samples. *J. Anal. Toxicol.* (2020).

155. Ginsburg BC, Schulze DR, Hruba L, Mcmahon LR. JWH-018 and JWH-073: Δ9-tetrahydrocannabinol-like discriminative stimulus effects in monkeys. *J. Pharmacol. Exp. Ther.* 340(1), 37–45 (2012).

156. Chung H, Choi H, Heo S, Kim E, Lee J. Synthetic cannabinoids abused in South Korea: drug identifications by the National Forensic Service from 2009 to June 2013. *Forensic Toxicol.* 32(1), 82–88 (2014).

157. Kim J, In S, Park Y, Park M, Kim E, Lee S. Deposition of JWH-018, JWH-073 and their metabolites in hair and effect of hair pigmentation. *Anal. Bioanal. Chem.* 405(30), 9769–9778 (2013).

158. Park M, Yeon S, Lee J, In S. Determination of XLR-11 and its metabolites in hair by liquid chromatography–tandem mass spectrometry. *J. Pharm. Biomed. Anal.* 114, 184–189 (2015).

Bioanalysis

ISSN: (Print) (Online) Journal homepage: www.tandfonline.com/journals/ibio20

Biopharmaceutical Quality Control with Mass Spectrometry

Shulei Liu & Benjamin L Schulz

To cite this article: Shulei Liu & Benjamin L Schulz (2021) Biopharmaceutical Quality Control with Mass Spectrometry, Bioanalysis, 13:16, 1275-1291, DOI: 10.4155/bio-2021-0123

To link to this article: https://doi.org/10.4155/bio-2021-0123

Published online: 31 Aug 2021.

Review

For reprint orders, please contact: reprints@future-science.com

Bioanalysis

Biopharmaceutical quality control with mass spectrometry

Shulei Liu[1,2] & Benjamin L Schulz*[,1,2]

[1]School of Chemistry & Molecular Biosciences, The University of Queensland, St Lucia, QLD 4072, Australia

[2]Australian Research Council Industrial Transformation Training Centre for Biopharmaceutical Innovation, Australian Institute for Bioengineering & Nanotechnology, The University of Queensland, St Lucia, QLD 4072, Australia

*Author for correspondence: b.schulz@uq.edu.au

Mass spectrometry (MS) is a powerful technique for protein identification, quantification and characterization that is widely applied in biochemical studies, and which can provide data on the quantity, structural integrity and post-translational modifications of proteins. It is therefore a versatile and widely used analytic tool for quality control of biopharmaceuticals, especially in quantifying host-cell protein impurities, identifying post-translation modifications and structural characterization of biopharmaceutical proteins. Here, we summarize recent advances in MS-based analyses of these key quality attributes of the biopharmaceutical development and manufacturing processes.

Tweetable abstract: MS is powerful for biopharmaceutical quality control. We review the status and opportunities of data independent acquisition, glycoproteomics, top-down MS and hydrogen-deuterium exchange MS for measuring host-cell protein contamination, post-translational modifications and protein structure.

First draft submitted: 3 June 2021; Accepted for publication: 17 August 2021; Published online: 31 August 2021

Keywords: biopharmaceutical quality control • host-cell proteins • mass spectrometry • protein post-translational modifications • protein structure

Biopharmaceuticals

Biopharmaceuticals (also known as biologics) are a category of medical products composed of nucleic acids, proteins or living cells that are produced through biotechnology. Most commonly, recombinant DNA technology is used to heterologously express protein biopharmaceuticals from mammalian cell lines [1]. Today, they are broadly used to treat disease indications including cancer, inflammatory and infectious diseases, wound healing, fertility, supplementation of hormone or cytokine deficiencies, modulation of immune function and replacement of enzymes. The general categories of biopharmaceuticals with corresponding examples and estimated current market values are shown in Table 1.

Biopharmaceuticals are safe and effective high-molecular weight drugs with few side effects compared with small-molecule drugs [10]. The chemical structure of many small-molecule drugs cannot be found in the human body, while the structures of biopharmaceuticals are often very similar to native human compounds because they are derived from a biological source [11]. This high complexity and structural similarity give them high specificity with few side effects, as well as the potential capacity to cure diseases instead of just treating the symptoms. However, this structural diversity and complexity, along with their high molecular mass, makes the manufacture of biopharmaceuticals comparatively complex [12]. Thus, quality control is extremely important during the whole manufacturing process including production, purification and packaging. This quality control includes assessment of the identity, purity and potency of the product. To precisely control biopharmaceutical quality, MS is a front-line tool for protein identification and characterization.

newlands press

Table 1. Classification of biopharmaceuticals with examples and market values.

Types	Examples	Annual revenue (US$)	Ref.
Coagulation factors	Factor VIII and IX	8.5 billion in 2017	[2]
Thrombolytic agents	Tissue plasminogen activator	5 million in 2012	[3]
Hormones	Insulin, growth hormone and gonadotropins	8 billion in 2019	[4]
Growth factors	Erythropoietin and colony stimulating factors	6 million in 2019	[5]
Interferon	IFN-α, -β and -γ	9 billion in 2019	[6]
Interleukin-based products	IL-2	6 billion by 2026	[7]
Vaccines	Hepatitis B surface antigen, varicella and HPV	61 billion by 2020	[8]
Monoclonal antibodies	Herceptin, alemtuzumab and rituximab	115.2 billion in 2018	[9]
Additional products	Tumor necrosis factor and therapeutic enzymes	–	

HPV: Human papillomavirus.

Overview of current biopharmaceutical markets

The global biopharmaceutical market has grown continuously in recent decades with increasing demand from geriatric populations, and investment in related research as well as manufacturing processes has effectively expanded the market by providing customers greater choice and biopharmaceuticals with improved potency. At present, biopharmaceuticals occupy nearly a quarter of newly introduced drugs to the market, and demonstrate high competitiveness and large potential partly because of their ability to treat previously incurable diseases.

In 1990, the total annual revenue from biopharmaceuticals was only around US$4.4 billion, while it has significantly increased to over US$275 billion at present with a growth rate of 61.5%, and is expected to continue to maintain an annual increase rate around 12–13% [13]. The year 2019 was an outstanding year for global biopharmaceutical markets with 7.32% of compound annual growth rate, which is well positioned for further stable increases [14].

Biopharmaceutical manufacturing process

The key conceptual steps in the biopharmaceutical manufacturing process are cell-line development, upstream processes and downstream processes (Figure 1). Microbial systems (bacteria, yeast, filamentous fungi and unicellular algae) and mammalian systems (CHO, NS0 and HEK 293 cells) are both widely used as host cells to produce protein-based biopharmaceuticals. *Escherichia coli* is a common and inexpensive bacterial system with fast growth that is used to produce first-generation biopharmaceuticals like insulin and growth hormone [15]. However, not all biopharmaceuticals can be produced in bacterial systems as these are not natively able to modify proteins after translation, which can lead to production of misfolded or inactive proteins [16]. Most therapeutic protein drugs require complex post-translational modifications (PTMs) such as glycosylation, acetylation, disulfide bonds or phosphorylation for desired drug stability and efficacy [17]. Thus, mammalian cells are widely used to produce the protein products that must be modified, such as monoclonal antibodies (mAbs) [18].

Upstream process can be divided into cell culture optimization, fermentation process optimization and application in large-scale bioreactors. Batch, fed-batch and continuous perfusion fermentation are common types of fermentation processes, with batch fermentation currently the most common with a 90% usage rate in industry [19]. During the fermentation process, fermentation conditions involving temperature, pH and oxygen concentration need to be monitored and regulated to guarantee optimal yield and production efficiency [20]. Additionally, sterile techniques or antibiotics can be used to protect the bioreactor environment from contamination.

Downstream processes refer to the process from after cell culture to the final biopharmaceutical product, and involve clarification, purification, polishing and viral inactivation to collect biomolecules of interest and remove impurities such as host cell debris and endotoxin [21]. Purified proteins can then be optionally modified by enzymatic conversion [22] or other methods depending on the specific biopharmaceutical, followed by formulation and/or lyophilization. Before packaging, product quality is controlled through a series of analyses to ensure the identity, purity, and quantity of the biopharmaceutical. MS is one of the most powerful analytical techniques for these purposes.

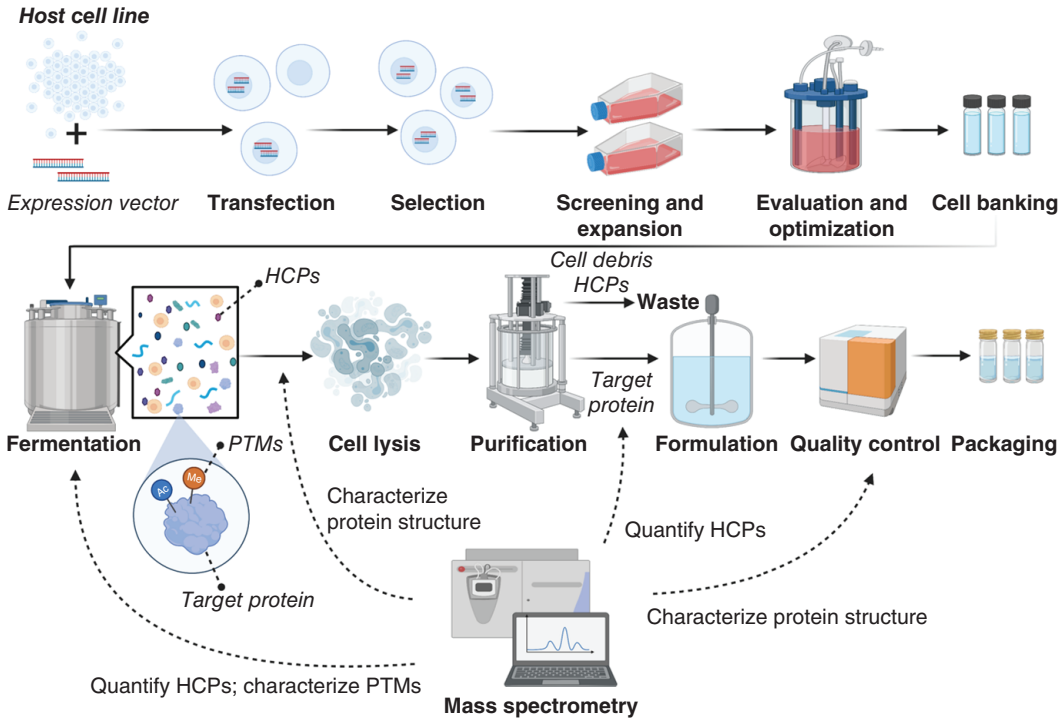

Figure 1. Biopharmaceutical manufacturing processes with MS applications. HCPs are contaminating proteins secreted from host cells along with the target protein. PTMs refer to the chemical modification of proteins through the removal or addition of functional groups that affect the structure and function of proteins. Created with BioRender.com.
HCP: Host-cell protein; PTM: Post-translational modification.

Mass spectrometry

MS is an indispensable analytical technique that is widely used in chemistry, biochemistry and pharmacy. It plays an essential role in the biopharmaceutical industry to identify, quantify and characterize proteins during production, purification and packaging processes to ensure the final biopharmaceutical products are pure, correctly folded and active proteins.

MS analysis of complex samples is commonly enabled by online or offline fractionation by various separation techniques. LC is particularly powerful and popular for this purpose. Separation of peptides or proteins typically uses reversed-phase LC. In addition to simplifying samples before MS analysis, LC of glycans or glycopeptides can separate different structures or isomers to improve identification [23]. Ion-exchange chromatography is suitable for fractionation and purification of charged compounds, including peptides and proteins [24]. Size-exclusion chromatography can separate biomolecules according to size, and can be combined with MS to characterize protein structural diversity or protein–protein interactions [25]. Hydrophobic interaction chromatography is a nondenaturing separation technique based on the hydrophobicity of the native analyte, and is becoming more popular to characterize the hydrophobicity, heterogeneity, sequence and structure of mAbs [26].

The three key components of an MS instrument are an ion source, a mass analyzer and a detector [27]. However, MS instruments can have many different and varied configurations. The basic theory of MS is to produce ions by one of the various ionization methods (depending on the characteristics of the sample), to separate these ions by virtue of their m/z, and to detect the ions to determine their m/z and abundance [28].

ESI and MALDI are the two most common methods used for analysis of proteins and peptides [29]. ESI ionizes analytes from a solution, and so is easily coupled to techniques that apply liquid-based separation such as LC. Integrated LC ESI–MS systems (LC–MS) are therefore commonly used to analyze complex samples. In contrast, MALDI uses laser pulses to sublimate and ionize molecules in samples from a dry crystalline matrix, and is usually used to analyze relatively simple peptide mixtures [30].

The mass analyzer is the central component of an MS instrument, and separates the ionized molecules based on their m/z ratios [31]. Mass analyzers are sensitive, high-resolution and capable of generating information-rich ion

mass spectra from proteins, peptides and their fragments. Quadrupole, TOF and Orbitrap are the most common types of analyzer, and these analyzers can be used singly or in combination to take advantage of the strengths of each [32].

MS/MS is a popular and powerful option in biomolecular analysis. In MS/MS, the ionized proteins or peptides are separated by the first mass analyzer (MS1) by their m/z ratio, and then ions of a certain m/z-ratio are selected to be further fragmented. After fragmentation, the smaller fragment ions are introduced into the second mass analyzer (MS2) which separates the fragments by their m/z ratio again and detects them [33]. As such, MS/MS can provide information on the composition or structure of complex molecules. Different fragmentation methods can provide complementary structural information, and are suitable for different types of biomolecules. For example, Collision Induced Dissociation (CID) or Higher Energy Collision Dissociation (HCD) are commonly used for analysis of peptides, as they result in efficient and predictable fragmentation at peptide bonds. Electron Transfer Dissociation (ETD) or Electron Capture Dissociation (ECD) provide complementary fragmentation patterns, and are particularly useful for assigning the site of modification in glycopeptides.

Other gas phase separation techniques can be combined with MS, including ion mobility spectrometry (IMS), which is increasing in popularity in modern MS instruments. The basic principle of IMS is that ionized molecules are separated through a cell filled with an inert 'drift gas' on a millisecond timescale according to their ion mobility, which is related to their mass, shape and charge [34]. IMS can be used between LC and MS as an additional intermediate fractionation technique for complex samples, and can also be used to obtain structural information by separating isomeric ions, revealing primary conformations and tracking dynamic changes in structure [35]. IM–MS can also be combined with complementary strategies such as fragmentation with ETD to obtain insights into protein conformation and modifications, or collision-induced unfolding to characterize protein dynamic structure and stability [36].

With the rapid development of MS instrumentation in recent years improving speed, accuracy, sensitivity and robustness, and offering diverse fragmentation options, this technology has become one of the most powerful analytical techniques for analysis and quantification in proteomics, glycoproteomics and detailed protein characterization. MS is therefore clearly a useful and versatile tool for many aspects of biopharmaceutical quality control which can quantify host-cell proteins (HCPs), identify PTMs and characterize the structure of biopharmaceutical proteins to guarantee the purity, safety and potency of biopharmaceuticals.

Recent advances

Quantification of HCPs

HCPs are contaminating proteins expressed and secreted from host cells that accompany the production of intended recombinant biopharmaceutical proteins [37]. The presence of HCPs is what necessitates additional purification steps to obtain pure biopharmaceutical protein product. HCPs must be removed during the purification process, as if some of them still remain as impurities in the final products they may result in reduction of biopharmaceutical efficacy or unintended immunogenic responses. The general guideline for acceptable levels of HCPs in biopharmaceutical products is less than 100 ng/ml (100 p.p.m.), and products with higher levels are generally not accepted by regulatory agencies [38]. Thus, quantification of residual HCPs in biopharmaceutical products is critical to ensure their adequate removal during the manufacturing process.

Traditionally, ELISA are commonly used to detect and measure HCPs during the biopharmaceutical manufacturing process [39]. ELISAs typically provide both high sensitivity and selectivity. However, ELISAs are only available for around 70% of all HCPs in typical samples [40], and development of new anti-HCP antibodies for use in ELISAs can be difficult and time consuming. In addition, HCPs may sometimes not be successfully detected even though the reagent contains the corresponding antibodies due to incompatible binding conditions or the accessibility of the relevant HCP epitopes [41].

As it is not possible for ELISA to identify all possible HCP contaminants, MS has emerged as an alternative technique for HCP analysis, as MS can monitor and identify multiple HCPs in a sample in one unbiased analysis. Moreover, even low quantities of HCPs are still able to be detected by MS; this is crucial for biopharmaceutical manufacture because even low levels of impurities can lead to adverse effects such as provoking immunogenicity.

HCP analysis requires both identification and quantification. MS can identify and quantify proteins, using either label-free or various chemical labeling strategies. In either approach, LC–MS/MS with rapid measuring speed as well as high sensitivity and selectivity has been widely applied to quantify HCPs in bottom-up proteomics workflows. In this method, proteins are digested with specific proteases, and the resulting peptides are desalted and analyzed

by LC–MS/MS. Proteins are identified by matching experimental MS/MS spectra to theoretical fragmentation patterns from predicted peptides. LC–MS/MS data can also be used for quantification of peptides and the proteins from which they originate. MS labeling strategies have been widely applied and demonstrate high accuracy. Such strategies include metabolic labeling such as stable isotope labeling with amino acids in culture [42] and chemical labeling of proteins such as 2D-difference fluorescence gel electrophoresis [43], or of peptides such as with isobaric tag for relative and absolute quantitation [44] or Tandem Mass Tag [45] systems. However, there are some drawbacks of labeling approaches, as they involve extra sample processing and are not possible for all sample types. In recent years, label-free quantification strategies have become an alternative popular and effective method used in MS proteomics [46–50]. Label-free quantification can use spectral counting or intensity-based measures. Spectral count is derived from identification from MS/MS spectra, or the total number of MS/MS spectra that correspond to a particular protein [51]. Generally, proteins with higher abundance in a sample will have more detectable peptides present after protease digestion and will therefore subsequently be represented by more MS/MS spectra [52]. Label-free quantification can also be based on peptide-ion intensity derived from LC–MS/MS data. Because the signal intensity of peptide ions is related to the peptide concentration, peptide abundance can be measured based on ion intensity through AUC or peak height. Data independent acquisition (DIA) LC–MS/MS workflows such as sequential window acquisition of all theoretical ions mass spectrometry (SWATH–MS) are powerful label-free approaches for deep, proteome-wide profiling with high-throughput and reproducible analysis [53]. Additionally, absolute quantification of proteins is an effective label-free strategy, in which stable isotopes are incorporated into synthetic peptides, imitating native peptides generated through proteolysis, and are added as internal standards to allow absolute quantification of targeted proteins [54,55].

A key challenge of HCP analysis is that the HCPs may be present at very low concentrations in the presence of a very high concentration of the biopharmaceutical product of interest. The analytical challenges posed by this difficulty can be overcome in several ways.

Sample preparation is key for all LC–MS/MS workflows, and can be used strategically to increase HCP detection. ProteoMiner technology has been used to increase detection of low abundance HCPs by reducing the dynamic range of peptides after proteolysis [56,57]. Depletion of the biopharmaceutical product before proteolysis has also been achieved with denatured HILIC fractionation [58]. The speed of sample preparation can be critical for the overall efficiency of HCP measurement. For example, sodium deoxycholate is a protein denaturant that does not need to be removed before trypsin digestion, and which can be easily removed by acidification after digestion to enable LC–MS/MS analysis [59].

After sample preparation, LC–MS/MS workflows can be tailored for HCP quantification. Targeted detection of known HCPs at very high sensitivity can be performed with multiple reaction monitoring [60,61]. However, multiple reaction monitoring relies on previous identification of HCPs which may be present. In contrast, DIA analysis can measure previously unpredicted proteins, and LC–MS/MS DIA–MS workflows also have excellent quantitative dynamic range and have been used for HCP quantification [62]. In a recent study that predicted yield and quality of the purified coagulation factor IX product through analysis of bioreactor supernatant, a set of LC–MS/MS DIA/SWATH workflows were established and used to quantify the factor IX product and HCPs, both during cell culture in bioreactors and after purification (Figure 2) [63]. In another study, a data independent liquid chromatography/mass spectrometry platform (2D-LC/MS^E) with Hi3 quantitation was used to measure HCPs in purified mAb samples to evaluate the impact of elution buffer choice for downstream purification, cell culture harvest time and additional downstream purification steps [64]. The high dynamic range of these DIA workflows allowed detection and quantification of low abundant HCPs in the presence of abundant biopharmaceutical product (Factor IX or mAb) without enrichment or depletion [65]. Another approach for increasing dynamic range, but using data-dependent acquisition (DDA), is the recently reported HCP-automated iterative MS workflow for identification and quantification of HCPs at extremely low levels (10 p.p.m.) without enrichment or pretreatment, in which samples were analyzed by LC–MS/MS multiple times, with precursor ions automatically excluded for selection for MS/MS in iterative replicates [66].

Recent years have seen the addition of IMS capabilities to MS instruments from several vendors. The additional online fractionation provided by IMS can allow deeper proteome profiling to increase the dynamic range of LC–MS/MS experiments. This is exemplified by the use of high-field asymmetric waveform ion mobility spectrometry on a Orbitrap Fusion Lumos Tribrid MS instrument, which increased the depth of HCP measurement [67].

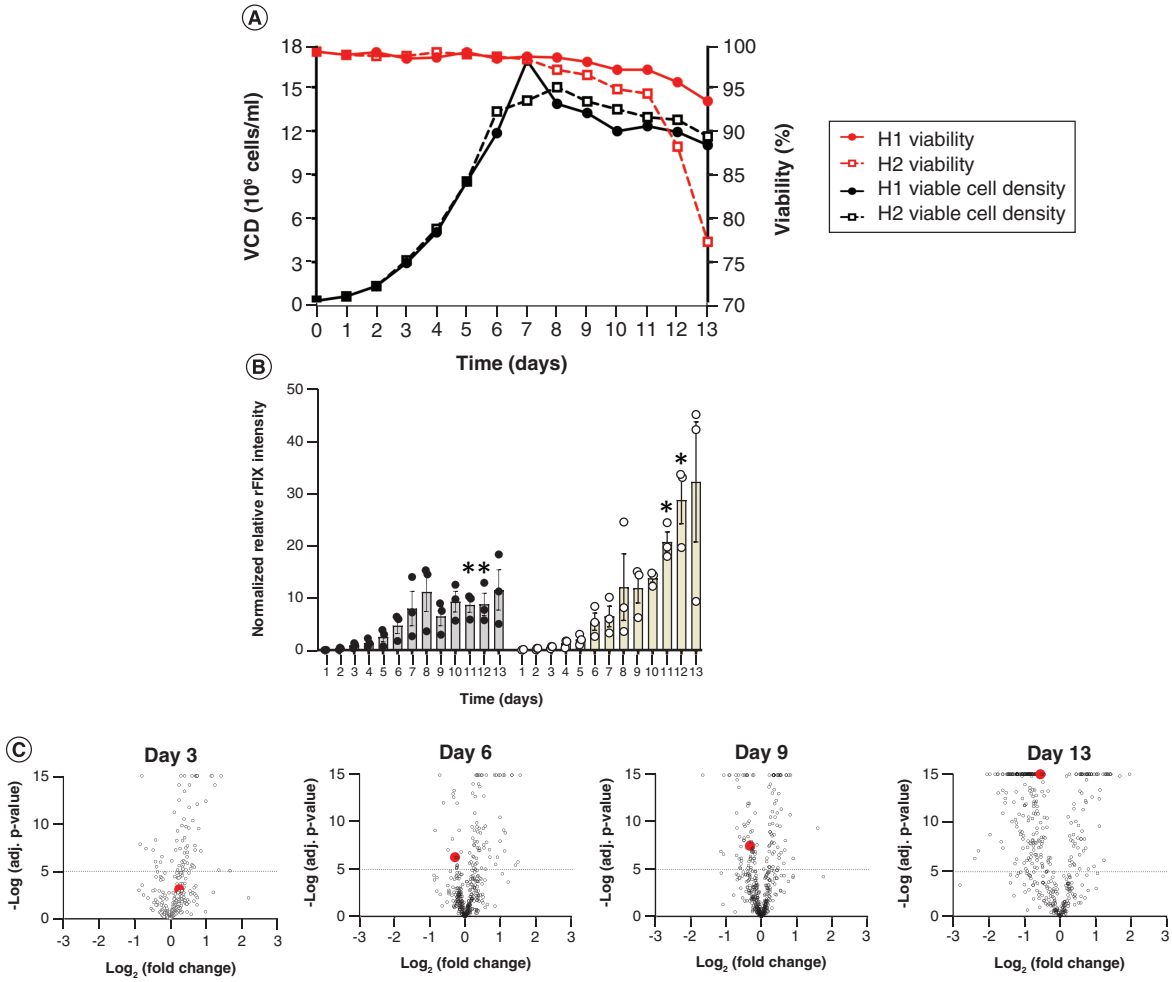

Figure 2. Viability, productivity and host cell protein profile of CHO cells expressing FIX in fed-batch conditions.
CHO cells co-expressing FIX and PACE/Furin were grown in fed-batch bioreactor mode with either EfficientyFeed A (H1) or EfficientFeed B (H2) as feeds. **(A)** Viability (red line) and (VCD; black line) in H1 (solid line, closed circle) and H2 (dotted line, open square); n = 1. **(B)** Relative FIX abundance (normalized to trypsin) in the bioreactor supernatants during operation (Mean ± SEM; multiple *t* test, n = 3 independent technical replicates; *p = 0.0072 and p = 0.0166 for day 11 and day 12 in H1 vs H2, respectively). Individual data points are indicated in black (H1 bioreactor, gray bars) or white circles (H2 bioreactor, yellow bars). **(C)** Volcano plots depicting log2 of the fold change in protein abundance versus -log10 of adjusted p-value for comparisons of culture media of bioreactor H1 versus H2 at days 3, 6, 9 and 13. The dotted horizontal line indicates the value above which the comparisons were significant (MSstats, $p < 10^{-5}$, n = 3 independent technical replicates). The red dots indicate rFIX at day 3 (adjusted p = 0.00078), day 6 (adjusted $p = 5.02 \times 10^{-7}$), day 9 (adjusted $p = 3.1 \times 10^{-8}$) and day 13 (adjusted p = 0) in H1 versus H2. Each open circle is a unique protein.
SEM: Standard error of the mean; VCD: Viable cell density.
Reproduced with permission from [63] © Zacchi *et al.* (2021).

The increased sensitivity and speed of modern MS instruments is enabling their use with rapid LC systems, while still maintaining deep proteome coverage. For instance, the Evosep ONE LC system can allow rapid robust online LC separation, for up to 60 samples per day [68].

HCPs are a major process-related impurity, and their sufficient removal (<100 p.p.m.) is crucial to obtain high-quality biopharmaceutical products. Thus, quantification of HCPs is necessary during and after purification. ELISA is an effective method for quantification of HCPs, but it has largely been replaced by LC–MS/MS due to the latter's rapid analysis time, high sensitivity and ability to measure all detectable HCPs in a sample in an unbiased manner. A variety of quantitative LC–MS/MS workflows are possible for this purpose, including labeled and label-free methods, depending on the precise experimental questions at hand.

Characterization of PTMs

Proteins can be modified with a highly diverse range of PTMs, including glycosylation, phosphorylation, proteolysis, acetylation, formylation, methylation, ubiquitination, carboxylation and many more. These PTMs increase the structural and functional diversity of proteomes [69]. Most PTMs are catalyzed by enzymes, allowing tight regulation of these functionally important features of proteins. As the correct presence and structure of PTMs are often critical for protein function, their detailed characterization is a necessary step in the quality control of biopharmaceuticals. For instance, antibodies, blood factors, erythropoietin, some IFNs and some hormones are glycosylated, which is important for their folding, stability, function, half-life and immunogenicity [70,71]. However, the diversity and structural complexity of PTMs on biopharmaceuticals can make their analysis complex and time-consuming.

Although PTMs are critical for biopharmaceutical quality, the measurement of various PTMs is challenging. Conventionally, Edman degradation, isotopic labelling, immunochemistry and amino acid analysis were commonly used techniques used to measure PTMs [72]. These approaches can be very sensitive, and are effective in single-site PTM detection, but their low-throughput makes them inappropriate for large-scale measurement of PTMs. This is a critical flaw, as many biopharmaceuticals are modified with multiple PTMs at many different sites. MS has emerged as the technique of choice for identifying and measuring PTMs. It has high sensitivity, and can identify specific-site PTMs, novel or unexpected PTMs, and PTMs in complex mixtures of proteins. None of the traditional methods has all of these abilities.

Generally, approaches for PTM identification by MS can be divided into bottom-up, middle-up and top-down strategies. Bottom-up analysis works at the peptide level, which means that the studied proteins are digested by proteases such as trypsin to produce peptides generally in the range of 500–3000 Da [73]. These proteolytically cleaved peptides tend to have few PTMs, which substantially simplifies their analysis. Bottom-up analyses are the most popular due to their high throughput and sensitivity, but they also have limitations. Specifically, not all proteolytic peptides resulting from digest with a given protease are normally able to be detected by MS, because some will be too large or too small [74]. This deficiency can be overcome, at least in part, by the use of independent treatment with different protease enzymes with complementary specificities. However, bottom-up analyses also lose any connectivity between sites of PTMs on the same protein molecule. To overcome these limitations, top-down approaches can be performed. In this approach, intact proteins are directly analyzed by LC–MS/MS without prior proteolytic digestion. This strategy is especially effective for characterization of essentially pure samples of small proteins without extensive or overly heterogeneous PTMs [75], and is inappropriate for high-throughput analyses owing to its low sensitivity and time-consuming data evaluation and interpretation [76]. Middle-down analyses, with restricted or limited proteolytic digestion, combine some of the benefits of top-down and bottom-up proteomics. These approaches aim to analyze protein fragments around 5–20 kDa in size, with intermediate PTM diversity [77].

Coagulation factor IX (FIX) is a biopharmaceutical with a very high number and diversity of PTMs, many of which are critical to its function. In particular, FIX is modified with many glycosylation events and γ-carboxylation of its N-terminal GLA domain. γ-carboxylation is a PTM mediated by γ-glutamyl carboxylase during protein biosynthesis, and complete γ-carboxylation is a key quality determinant of recombinant FIX [78]. The study mentioned above developed DIA LC–ESI–MS/MS methods to measure site-specific PTMs across FIX during bioreactor operation and after purification [63]. It was found that it is difficult to detect and identify fully γ-carboxylated GLA peptides in positive ion mode LC–ESI–MS/MS owing to the negative charge of the γ-carboxyl groups, and neutral loss of CO_2 upon CID fragmentation. However, standard bottom-up DIA LC–ESI–MS/MS could detect uncarboxylated or partially γ-carboxylated GLA peptides in positive ion mode, and could be used to infer the extent of site-specific γ-carboxylation. Derivatization of γ-carboxyl groups also allowed measurement of fully modified peptides, although this increased the complexity of the procedure [79]. These DIA–MS methods were used to monitor γ-carboxylation throughout bioreactor operation and compare differences in the extent of modification in the finished product with varied bioreactor operation. FIX is also modified by other heterogeneous PTMs such as proteolysis, *N*- and *O*-glycosylation, sulfation, phosphorylation, β-hydroxylation and disulfide bonds. To test the occupancy and structure of these PTMs, in-depth DDA–MS analysis was performed to identify and characterize PTMs, which was then used as the basis for DIA–MS quantification. The majority of the known PTMs on rFIX and several new PTMs (Figure 3) were observed and monitored in this study, highlighting the benefits of DIA–MS for PTM profiling of biopharmaceuticals.

Glycosylation is one of the most widespread, important and analytically challenging PTMs present on biopharmaceutical products. Glycoproteomic workflows are powerful and commonly used approaches for profiling the

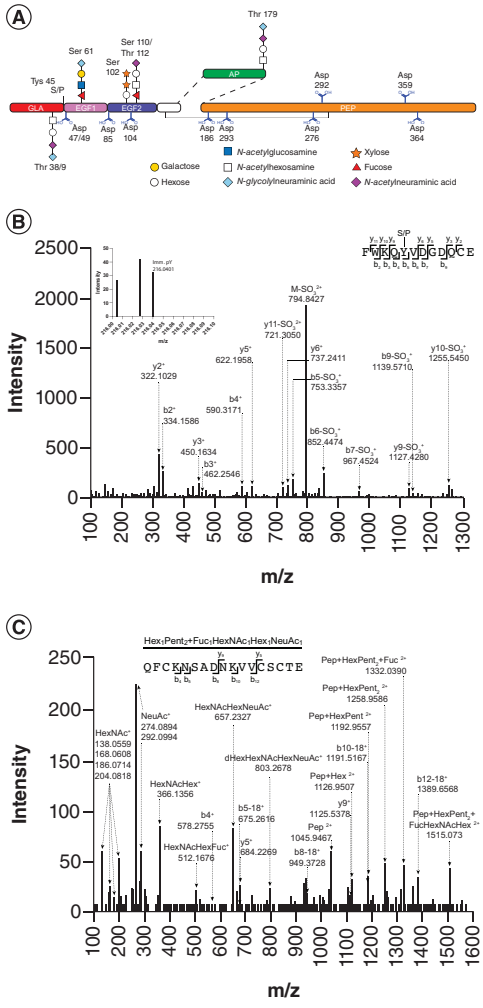

Figure 3. New post-translational modifications identified by DDA LC–MS/MS on recombinant Factor IX. (A) Schematics of FIX containing the new PTMs identified on rFIX. **(a, b)** CID fragmentation of select GluC FIX peptides. **(B)** F^{41}WKQYVDGDQCE^{54} peptide with sulfation/phosphorylation (S/P) at Y^{45} (observed precursor m/z 834.8189^{2+}, Δ2.4 p.p.m.). The inset shows the phosphotyrosine immonium ion (pY, 216.0401 m/z, Δ2.9 p.p.m.). **(C)** Q^{97}FCKN(+1)SADN(+1)KVVCSCTE^{113} glycopeptide with Hex_1Xyl_2 and $Fuc_1HexNAc_1Hex_1NeuAc_1$ *O*-glycans attached to $S^{102/110}$ and T^{112} (observed precursor m/z 1107.1067^{3+}, Δ7.56 p.p.m.). Pep, peptide.
CID: Collision-induced dissociation; PTM: Post-translational modification.
Reproduced with permission from [63] © Zacchi *et al.* (2021).

site-specific glycosylation of biopharmaceuticals, as they use relatively standard proteomic bottom-up LC–MS/MS techniques [80–82]. CID or HCD fragmentation can provide substantial information on the peptide identity and glycan monosaccharide composition of glycopeptides [83], while ETD or ETD with HCD supplemental activation (EThcD) fragmentation is typically required for unambiguous localization of the site of modification, especially for *O*-glycans [84]. Data analysis pipelines must consider the additional structural complexity of glycopeptides compared with peptides, and many informatics solutions are currently available and under further development [85]. Glycoproteomic workflows can also be complemented with identification of the sites of *N*-glycosylation by deglycosylating biopharmaceuticals with enzymes such as peptide-N-glycosidase F (PNGase F), which leave a 'chemical scar' of deamidation of asparagine to aspartate at previous sites of glycosylation, prior to LC–MS/MS analysis [86,87]. Enzymatically released glycans can also be analyzed using glycomics workflows, which can provide detailed structural information about the glycans which can be difficult to obtain with glycoproteomic LC–MS/MS workflows alone [88]. Analysis of both released glycans and intact glycopeptides can also benefit from complementary separation methods such as LC, capillary electrophoresis and IMS [23,89], which can allow separation of glycan structural isomers [90].

A recent study characterizing the SARS-CoV-2 glycan shield demonstrated the power of mass spectrometric glycoproteomics to reveal the site-specific glycosylation of a recombinant SARS-CoV-2 S immunogen, including site-specific *N*-linked glycan composition and occupancy [91]. To maximize the coverage of the many *N*-glycosylation sites present on the S glycoprotein, three different proteases were used – trypsin, chymotrypsin and alpha-lytic protease. LC–MS/MS with high-energy HCD fragmentation was then used to analyze the glycopeptide pools and determine the glycan composition. Different glycosylation sites were found to vary in their site-specific *N*-glycosylation profiles (Figure 4). More specifically, three sites, N234, N709 and N801, were mainly oligomannose-type glycosylation; several sites, especially N657, possessed diverse hybrid-type glycans; and sites N61, N122, N165, N603, N657 and N1074 were occupied by a mixture of oligomannose- and complex-type glycans. The high confidence characterization of site-specific *N*-glycosylation structures and occupancy across the many modified sites of the S protein achieved by this analytical approach demonstrates its utility for glycoprotein biopharmaceutical quality control.

The previous examples highlight the power of bottom-up analysis for PTM identification and quantification at the peptide level. However, the peptide-centric focus of this approach means that most analyzed peptides have single PTMs, which hinders overall profiling of the entire protein. A recent study used an integrated strategy combining high-resolution native MS and middle-down proteomics to characterize co-occurring PTMs of human erythropoietin and human plasma properdin, enabling profiling of the structural micro-heterogeneity that often affects the functionality of biopharmaceuticals [92]. Native MS could measure the relative abundance and overall PTM composition of different proteoforms that could be distinguished by mass [93]. Middle-down analyses were then applied to characterize the site-specificity of these PTMs. The data from both approaches were then combined and compared to assess the completeness and reliability of PTM assignments. This combined integrated MS strategy provided a very complete profile of the measured glycoproteins and also discovered unexpected heterogeneity in three C-glycosylation sites on properdin. In theory, this integrative workflow could be used to quantitatively profile the site-specific molecular heterogeneity of PTMs on any protein, only limited by the resolution of the MS and the PTM heterogeneity of the protein.

Most biopharmaceuticals are proteins with diverse and complex PTMs that play important roles in their stability, function, half-life or immunogenicity. Detailed characterization of PTMs is therefore critical to guarantee high quality and effective potency of biopharmaceuticals. LC–MS/MS is a powerful technique for identifying and quantifying site-specific PTM structure and occupancy, particularly with a combination of bottom-up, middle-up, top-down or integrated analytical strategies.

Structural characterization of proteins

Protein function depends on correct folding and structure. Unfolding or misfolding can lead to unstable proteins with partial or total loss of function. Additionally, and of particular importance for biopharmaceuticals, disordered or misfolded proteins may aggregate, decreasing the effectiveness of the biopharmaceutical products and leading to other risks such as increased immunogenicity [94]. As correct protein structure is crucial for therapeutic proteins, the structural characterization of biopharmaceuticals is therefore necessary to ensure product quality by avoiding unfolded, misfolded or aggregated proteins.

X-ray crystallography and NMR are both classical tools for protein structural analysis, while hydrogen-deuterium exchange mass spectrometry (HDX–MS) has emerged as a highly complementary technique for mapping protein folding, protein–protein and protein–ligand interactions, and dynamic conformational changes in proteins. Additionally, HDX–MS is versatile and can be used to explore other systems including highly dynamic proteins, large biomolecular complexes and membrane-associated species [95]. In a typical HDX–MS analysis, proteins in H_2O-based solvent are diluted into D_2O-based solvent, which induces the liable hydrogens on the protein to exchange with deuterium in the solvents, with the exchange rate largely determined by surface accessibility, protein structure and dynamics, as limited solvent access and hydrogen bonding can protect hydrogens from exchange. Data on the extent of exchange are typically collected at several intervals, providing a profile of deuterium exchange versus time which reflects protein conformation and dynamics [96].

Bottom-up and top-down workflows are both available for HDX–MS analysis, with the former more common as it can be used for any protein without limitations on protein size. In this approach, proteins are rapidly digested with pepsin and LC–MS/MS data are collected, which can measure the extent of HDX at a peptide- or even amino acid-level. However, approximately 10–50% deuterium label loss can occur in this approach during enzymatic digestion and HPLC separation of the peptides [97]. In contrast, in top-down workflows, intact protein is directly analyzed

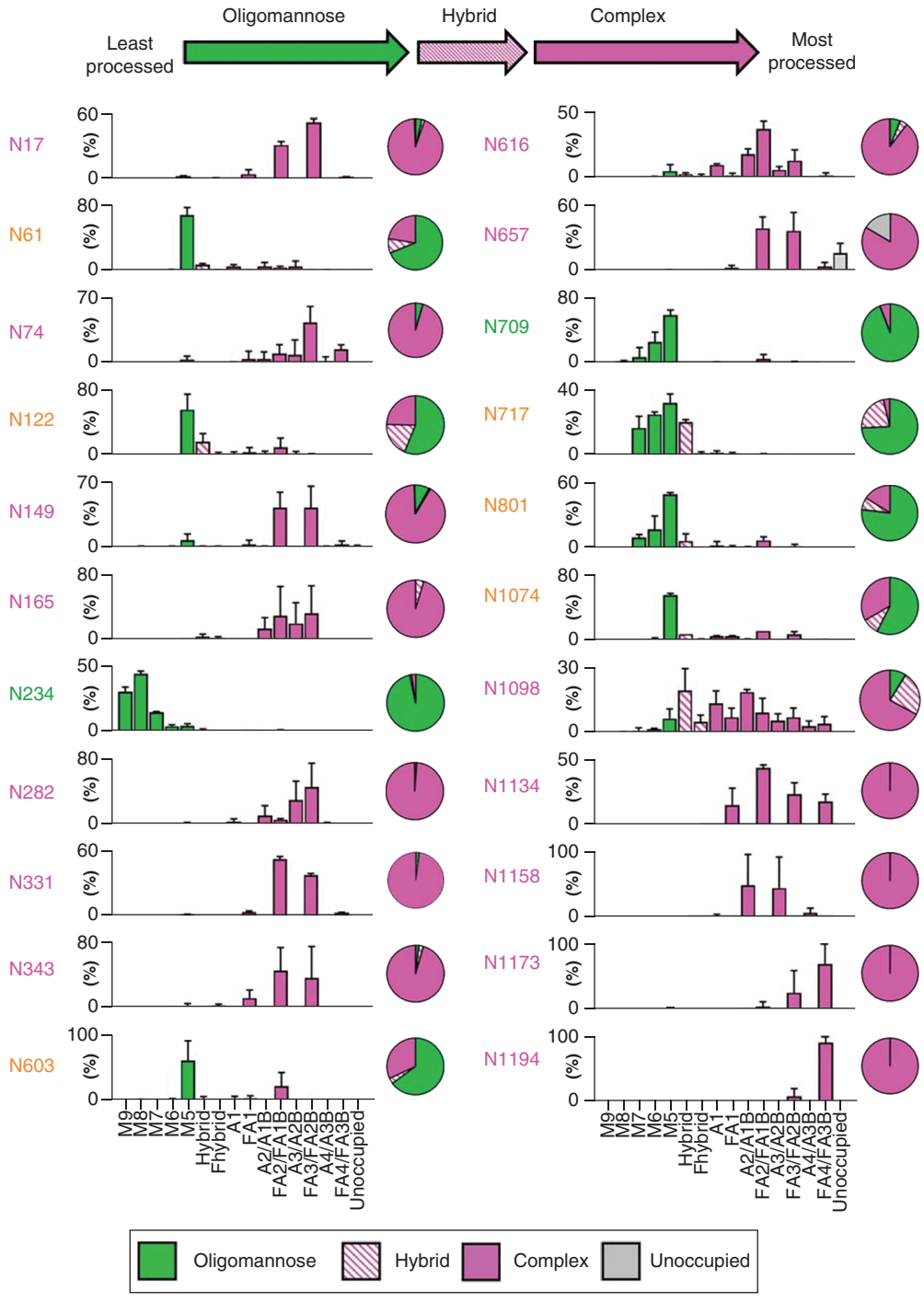

Figure 4. Site-specific *N*-linked glycosylation of the SARS-CoV-2 S glycoprotein. The schematic illustrates the color code for the principal glycan types that can arise along the maturation pathway from oligomannose- to hybrid- to complex-type glycans. The graphs summarize quantitative mass spectrometric analysis of the glycan population present at individual *N*-linked glycosylation sites simplified into categories of glycans. The oligomannose-type glycan series (M9 to M5; Man9GlcNAc2 to Man5GlcNAc2) is colored green, afucosylated and fucosylated hybrid-type glycans (hybrid and F hybrid) are dashed pink, and complex glycans are grouped according to the number of antennae and presence of core fucosylation (A1 to FA4) and are colored pink. Unoccupancy of an *N*-linked glycan site is represented in gray. The pie charts summarize the quantification of these glycans. Glycan sites are colored according to oligomannose-type glycan content, with the glycan sites labeled in green (80–100%), orange (30–79%) and pink (0–29%). The bar graphs represent the mean quantities of three biological replicates, with error bars representing the standard error of the mean.
Reproduced with permission from [91] © Watanabe *et al.* (2020).

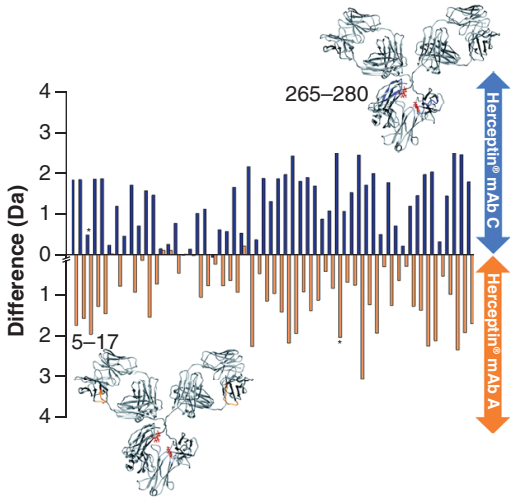

Figure 5. Deuterium uptake difference plots for heavy chain intact versus endoS2 treated Herceptin®; endoS2–intact. Each bar represents a different peptide (HC sequence coverage = 70.2%, 55 peptides). Blue bars represent the deuterium uptake differences for Herceptin lot C; orange bars represent deuterium uptake differences for Herceptin lot A. Labeled peptides 5–17 (VESGGGLVQPGGS) and 265–280 (VVVDVSHEDPEVKFNW) are those with significant uptake differences between the two Herceptin lots, i.e., a difference of >1 Da. The peptide locations for the two peptides with uptake differences >1 Da are highlighted on the mAb structures in blue and orange for lot C and lot A, respectively (PDB: 1IGY). A representation of endoS2 treated glycans are shown in red. Subtraction of intact mAb data from enzyme treated mAb data for individual lots, means that the intact data serves as a control to counteract any day-to-day variations in the HDX setup.
*Corresponds to the equivalent peptide in the other sample.
HC: Heavy chain; HDX: Hydrogen-deuterium exchange; mAb: Monoclonal antibody; PDB: Protein data bank.
Reproduced with permission from [111] © The Royal Society of Chemistry (2019).

by LC–MS/MS, involving ionization and fragmentation. This minimizes loss of deuterium and potentially allows true site-specific HDX measurement [98]. However, the success of this method decreases with increasing protein size, and is only currently feasible with proteins less than 30 kDa [99,100]. Additionally, deuterium scrambling can occur during MS/MS fragmentation, where hydrogen or deuterium migrate along the peptide backbone leading to distortion or loss of the original labeling pattern [96].

A recent study combined the complementary approaches of bottom-up and top-down HDX-MS to characterize and compare the higher-order structure of an originator antibody drug and two batches of biosimilars [101]. Although the same samples were used in the two approaches, it is somewhat difficult to directly compare the results due to the different back-exchange rates and spatial resolution achieved with the two methods. Nonetheless, the structural data from the two approaches were consistent and complementary, with both approaches finding no structural differences between the three drug samples. Moreover, the sequence coverage for heavy chain and light chain was 87 and 74%, respectively with bottom-up analysis, and 50 and 100% with the top-down approach. This highlights the consistency and complementarity of the two methods. Overall, the combination of both methods provided high-quality complete structural information for the whole antibody without any missed regions or residues. HDX–MS is an effective technique to rapidly map binding epitopes in the early stage of biosimilar development, providing data to assess similarity [102–104]. Compared with more traditional HDX–MS, time-resolved ESI hydrogen-deuterium exchange MS (TRESI–HDX–MS) with ms time-scale deuterium labeling can detect more subtle changes in protein conformation and interactions [105–109]. This powerful tool was used in a recent study to compare the interactions of a commercial Avastin and its biosimilar ApoBev with their biological target, VEGF-A. Clear epitope mapping was obtained through TRESI–HDX–MS, which showed that the binding epitopes of Avastin and ApoBev for VEGF-A are very similar, but with subtle differences in VEGF dynamics [110]. Combinations of techniques can provide particularly informative descriptions of protein structure and dynamics. For instance, HDX–MS has been used together with IM–MS to identify batch-to-batch signatures of the mAb Herceptin that correspond with the impact of *N*-glycosylation on protein structure and dynamics (Figure 5) [111]. IM–MS can be particularly informative in combination with collision-induced unfolding, to characterize the structure, dynamics and interactions of proteins [36,112,113].

The potency of biopharmaceuticals depends on them having correct structures, so correct folding is a key quality requirement. HDX–MS can be applied as a rapid and unbiased technique to monitor the folding or aggregation status of diverse proteins, with bottom-up, top-down or integrated analytical workflows, while TRESI–HDX–MS is capable to achieve faster and more unambiguous detection. IM–MS also shows exciting potential for rapid and informative structural profiling of biopharmaceuticals.

Conclusion

MS is a mature and powerful technique that is applicable to many aspects of biopharmaceutical quality control. In particular, it is useful for identification and quantification of HCP contaminants, characterisation of complex PTMs and monitoring the structural integrity of biopharmaceutical products. Diverse MS workflows enable this wide range of applications, including DIA LC-MS/MS, DDA LC-MS/MS with diverse fragmentation techniques, IM-MS, HDX-MS and native MS. Future developments in sample preparation, instrumentation and data analysis will undoubtedly further extend the capabilities and utility of MS analyses in biopharmaceutical quality control.

Future perspective

LC–MS/MS technology and applications are expected to rapidly progress in coming years, with wider and more frequent application in biopharmaceutical process and product quality control. Modern MS instruments have incredible performance in sensitivity and resolution, and the amount of biopharmaceutical product required for analysis is not generally limiting. Instead, it is analytical through-put which limits the usefulness of MS for many applications. Current MS workflows including sample preparation, analysis, and data processing typically take 1–2 days, limiting their utility in time-sensitive applications such as process monitoring. We therefore see improvements in the speed, through-put, automation and robustness of LC–MS/MS analytic workflows as a critical opportunity, with rapid automated digestion and sample preparation for bottom-up strategies, or improved technology for top-down strategies. For instance, with such improvements it may prove feasible to use LC–MS/MS during fermentation to monitor desired or unwanted product PTMs, or to monitor the purification process for residual HCP impurities in real-time, increasing product quality and purification efficiency of target biopharmaceutical proteins.

Executive summary

- MS has become one of the key methods used in the characterization and quantitation of proteins in biopharmaceutical quality control during the past two decades owing to improvements in instrument sensitivity, resolution, specificity and selectivity.
- Detailed information is needed for quality control of biopharmaceuticals, including residual host-cell proteins (HCPs), site-specific post-translational modifications (PTMs) and protein folding status.
- LC–MS/MS can identify and quantify HCPs with high selectivity and sensitivity, as even low quantities of HCPs are detectable by MS, and many HCPs can be identified in one analysis.
- For characterization of PTMs, MS strategies include bottom-up, top-down and middle-down. Bottom-up analyses are the most common, providing high sensitivity and high-throughput peptide level measurements, but can be limited by incomplete coverage of a protein's sequence. Top-down analyses are suitable for analysis of small proteins with modest PTM heterogeneity, although data interpretation can be time-consuming. Middle-down approaches, or an integrated combination of all three strategies, have emerged as an effective approach for detailed global, site-specific PTM analysis.
- Hydrogen-deuterium exchange MS allows structural characterization of the folding and aggregation status of proteins with bottom-up or top-down analyses, with bottom-up approaches being applicable for proteins of all sizes.
- Improvements in the speed, automation and throughput of bottom-up LC–MS/MS, and of the resolution and data analysis workflows of top-down LC–MS/MS are expected to allow these techniques to be useful for real-time monitoring of product quality during fermentation, or of HCP impurities during purification, improving process efficiency and product quality.

Financial & competing interests disclosure

This work was funded by an Australian Research Council Industrial Transformation Training Centre IC160100027 to BL Schulz. The authors have no other relevant affiliations or financial involvement with any organization or entity with a financial interest in or financial conflict with the subject matter or materials discussed in the manuscript apart from those disclosed.

No writing assistance was utilized in the production of this manuscript.

References

Papers of special note have been highlighted as: • of interest; •• of considerable interest

1. Introductory chapter: biopharmaceuticals. In: *Biopharmaceuticals* Chen YC, Yeh MK (Eds). IntechOpen, London, UK (2018).
2. Top O, Geisen U, Decker EL, Reski R. Critical evaluation of strategies for the production of blood coagulation factors in plant-based systems. *Front. Plant Sci.* 10, 261 (2019).

3. Adivitiya Khasa YP. The evolution of recombinant thrombolytics: current status and future directions. *Bioengineered* 8(4), 331–358 (2017).
4. Grand View Research. Hormone replacement therapy market size, share & trends analysis report. https://www.grandviewresearch.com/industry-analysis/hormone-replacement-therapy-market
5. Global market study on growth factors - 'reinforcing' the life sciences research. https://www.persistencemarketresearch.com/market-research/growth-factors-market.asp
6. Interferons global market report. https://www.thebusinessresearchcompany.com/report/interferons-market-global-report-2020-2030-covid-19-implications-and-growth
7. Interleukin inhibitors market. https://www.bloomberg.com/press-releases/2019-09-11/interleukin-inhibitors-market-worth-74-6-billion-by-2026-cagr-17-4-grand-view-research-inc
8. Big pharma and big profits: the multibillion dollar vaccine market. https://www.globalresearch.ca/big-pharma-and-big-profits-the-multibillion-dollar-vaccine-market/5503945
9. Global Monoclonal Antibody Industry 2019–2025. https://apnews.com/press-release/pr-businesswire/af15cf4cf54e4698a93689afb4a906e8
10. Takahashi H, Letourneur D, Grainger DW. Delivery of large biopharmaceuticals from cardiovascular stents: a review. *Biomacromolecules* 8(11), 3281–3293 (2007).
11. Craik DJ, Fairlie DP, Liras S, Price D. The future of peptide-based drugs. *Chem. Biol. Drug Des.* 81(1), 136–147 (2013).
12. Kesik-Brodacka M. Progress in biopharmaceutical development. *Biotechnol. Appl. Biochem.* 65(3), 306–322 (2018).
13. Rader RA. Langer ES. Biopharma market: an inside look. https://www.pharmamanufacturing.com/articles/2018/biopharma-market-an-inside-look/
14. Mordor Intelligence LLP. Biopharmaceuticals market-growth, trends, and forecast. https://www.reportlinker.com/p05815028/Biopharmaceuticals-Market-Growth-Trends-and-Forecast.html
15. Baeshen NA, Baeshen MN, Sheikh A *et al.* Cell factories for insulin production. *Microb. Cell. Fact.* 13(1), 141 (2014).
16. Tripathi NK, Shrivastava A. Recent developments in bioprocessing of recombinant proteins: expression hosts and process development. *Front. Bioeng. Biotechnol.* 7, 420 (2019).
17. Jenkins N. Modifications of therapeutic proteins: challenges and prospects. *Cytotechnology* 53(1–3), 121–125 (2007).
18. Li F, Shen A, Amanullah A. Cell culture processes in monoclonal antibody production. In: *Pharmaceutical Sciences Encyclopedia: Drug Discovery, Development, and Manufacturing.* Gad SC (Ed.). John Wiley & Sons, NJ, USA (2010).
19. Molowa DT, Mazanet R. The state of biopharmaceutical manufacturing. *Biotechnol. Annu. Rev.* 9, 285–302 (2003).
20. Patel PK, King CR, Feldman SR. Biologics and biosimilars. *J. Dermatolog. Treat.* 26(4), 299–302 (2015).
21. Jozala AF, Geraldes DC, Tundisi LL *et al.* Biopharmaceuticals from microorganisms: from production to purification. *Braz. J. Microbiol.* 47, 51–63 (2016).
22. Braun AC, Gutmann M, Lühmann T, Meinel L. Bioorthogonal strategies for site-directed decoration of biomaterials with therapeutic proteins. *J. Control. Release.* 273, 68–85 (2018).
23. Pallister EG, Choo MS, Walsh I *et al.* Utility of ion-mobility spectrometry for deducing branching of multiply charged glycans and glycopeptides in a high-throughput positive ion LC-FLR-IMS-MS workflow. *Anal. Chem.* 92(23), 15323–15335 (2020).
24. Alia KB, Nadeem H, Rasul I *et al.* Separation and purification of amino acids. In: *Applications of Ion Exchange Materials in Biomedical Industries.* Inamuddin (Ed.). Springer, NY, USA, 1–11 (2019).
25. Ehkirch A, Hernandez-Alba O, Colas O, Beck A, Guillarme D, Cianférani S. Hyphenation of size exclusion chromatography to native ion mobility mass spectrometry for the analytical characterization of therapeutic antibodies and related products. *J. Chromatogr. B* 1086, 176–183 (2018).
26. Chen B, Lin Z, Alpert AJ *et al.* Online hydrophobic interaction chromatography–mass spectrometry for the analysis of intact monoclonal antibodies. *Anal. Chem.* 90(12), 7135–7138 (2018).
27. Parker C, Warren M, Mocanu V. Mass spectrometry for proteomics. In: *Neuroproteomics.* Alzate O (Ed.). CRC Press, FL, USA, 71–92 (2010).
28. Field ionization and field desorption. In: *Mass Spectrometry: A Text Book.* Gross JH (Ed.). Springer, NY, USA, 518 (2004).
29. Zhang Y, Wang J, Liu JA *et al.* Combination of ESI and MALDI mass spectrometry for qualitative, semi-quantitative and *in situ* analysis of gangliosides in brain. *Sci. Rep.* 6, 25289 (2016).
30. Clark AE, Kaleta EJ, Arora A, Wolk DM. Matrix-assisted laser desorption ionization–time of flight mass spectrometry: a fundamental shift in the routine practice of clinical microbiology. *Clin. Microbiol. Rev.* 26(3), 547–603 (2013).
31. Yates JR III. Mass spectrometry: from genomics to proteomics. *Trends Genet.* 16(1), 5–8 (2000).

32. Abushareeda W, Tienstra M, Lommen A *et al.* Comparison of gas chromatography/quadrupole time-of-flight and quadrupole Orbitrap mass spectrometry in anti-doping analysis: i. Detection of anabolic-androgenic steroids. *Rapid Commun. Mass Spectrom.* 32(23), 2055–2064 (2018).
33. Nesvizhskii AI, Keller A, Kolker E, Aebersold R. A statistical model for identifying proteins by tandem mass spectrometry. *Anal. Chem.* 75(17), 4646–4658 (2003).
34. D'atri V, Causon T, Hernandez-Alba O *et al.* Adding a new separation dimension to MS and LC–MS: what is the utility of ion mobility spectrometry? *J. Sep. Sci.* 41(1), 20–67 (2018).
35. Mu Y, Schulz BL, Ferro V. Applications of ion mobility-mass spectrometry in carbohydrate chemistry and glycobiology. *Molecules* 23(10), 2557 (2018).
36. Botzanowski T, Hernandez-Alba O, Malissard M *et al.* Middle level IM–MS and CIU experiments for improved therapeutic immunoglobulin subclass fingerprinting. *Anal. Chem.* 92(13), 8827–8835 (2020).
37. Wang X, Hunter AK, Mozier NM. Host cell proteins in biologics development: identification, quantitation and risk assessment. *Biotechnol. Bioeng.* 103(3), 446–458 (2009).
38. Chon JH, Zarbis-Papastoitsis G. Advances in the production and downstream processing of antibodies. *N. Biotechnol.* 28(5), 458–463 (2011).
39. Hogwood CE, Bracewell DG, Smales CM. Measurement and control of host cell proteins (HCPs) in CHO cell bioprocesses. *Curr. Opin. Biotechnol.* 30, 153–160 (2014).
40. Thompson JH, Chung WK, Zhu M *et al.* Improved detection of host cell proteins (HCPs) in a mammalian cell-derived antibody drug using liquid chromatography/mass spectrometry in conjunction with an HCP-enrichment strategy. *Rapid Commun. Mass Spectrom.* 28(8), 855–860 (2014).
41. Zhu-Shimoni J, Yu C, Nishihara J *et al.* Host cell protein testing by ELISAs and the use of orthogonal methods. *Biotechnol. Bioeng.* 111(12), 2367–2379 (2014).
42. Ma W, Jia J, Huang X *et al.* Stable isotope labelling by amino acids in cell culture (SILAC) applied to quantitative proteomics of Edwardsiella tarda ATCC 15947 under prolonged cold stress. *Microb. Pathog.* 125, 12–19 (2018).
43. Pasquali M, Serchi T, Planchon S, Renaut J. 2D-DIGE in proteomics. In: *Functional Genomics* Kaufman M, Klinger C, Savelsbergh A (Eds). Springer, NY, USA, 245–254 (2017).
44. Ding W, Qiu B, Cram DS *et al.* Isobaric tag for relative and absolute quantitation based quantitative proteomics reveals unique urinary protein profiles in patients with preeclampsia. *J. Cell. Mol. Med.* 23(8), 5822–5826 (2019).
45. Bo C, Geng X, Zhang J *et al.* Comparative proteomic analysis of silica-induced pulmonary fibrosis in rats based on tandem mass tag (TMT) quantitation technology. *PLoS ONE* 15(10), e0241310 (2020).
46. Ryu S, Gallis B, Goo YA, Shaffer SA, Radulovic D, Goodlett DR. Comparison of a label-free quantitative proteomic method based on peptide ion current area to the isotope coded affinity tag method. *Cancer Inform.* 6, doi: 10.4137/cin.s385 (2008) (Epub ahead of print).
47. Couto N, Al-Majdoub ZM, Achour B, Wright PC, Rostami-Hodjegan A, Barber J. Quantification of proteins involved in drug metabolism and disposition in the human liver using label-free global proteomics. *Mol. Pharm.* 16(2), 632–647 (2019).
48. Distler U, Kuharev J, Navarro P, Tenzer S. Label-free quantification in ion mobility–enhanced data-independent acquisition proteomics. *Nat. Protoc.* 11(4), 795–812 (2016).
49. Arike L, Peil L. Spectral counting label-free proteomics. In: *Shotgun Proteomics.* Martins-de-Souza D (Ed.). Humana Press, NY, USA, 213–222 (2014).
50. He B, Shi J, Wang X, Jiang H, Zhu H-J. Label-free absolute protein quantification with data-independent acquisition. *J. Proteomics* 200, 51–59 (2019).
51. Milac TI, Randolph TW, Wang P. Analyzing LC-MS/MS data by spectral count and ion abundance: two case studies. *Stat. Interface.* 5(1), 75 (2012).
52. Washburn MP, Wolters D, Yates JR. Large-scale analysis of the yeast proteome by multidimensional protein identification technology. *Nat. Biotechnol.* 19(3), 242–247 (2001).
53. Gupta S, Rost H. Automated workflow for peptide-level quantitation from DIA/SWATH-MS data. In: *Quantitative Methods for Proteomics.* Marcus K, Eisenacher M, Sitek B (Eds). Humana Press, NY, USA (2021).
54. Gerber SA, Rush J, Stemman O, Kirschner MW, Gygi SP. Absolute quantification of proteins and phosphoproteins from cell lysates by tandem MS. *Proc. Natl Acad. Sci. USA* 100(12), 6940–6945 (2003).
55. Szymkowicz L, Wilson DJ, James DA. Development of a targeted nanoLC-MS/MS method for quantitation of residual toxins from Bordetella pertussis. *J. Pharm. Biomed. Anal.* 188, 113395 (2020).
56. Chen I-H, Xiao H, Li N. Improved host cell protein analysis in monoclonal antibody products through ProteoMiner. *Anal. Biochem.* 610, 113972 (2020).
57. Mörtstedt H, Makower Å, Edlund P-O, Sjöberg K, Tjernberg A. Improved identification of host cell proteins in a protein biopharmaceutical by LC–MS/MS using the ProteoMiner™ Enrichment Kit. *J. Pharm. Biomed. Anal.* 185, 113256 (2020).

58. Wang Q, Slaney TR, Wu W, Ludwig R, Tao L, Leone A. Enhancing host-cell protein detection in protein therapeutics using HILIC enrichment and proteomic analysis. *Anal. Chem.* 92(15), 10327–10335 (2020).

59. Li D, Farchone A, Zhu Q *et al.* Fast, robust, and sensitive identification of residual host cell proteins in recombinant monoclonal antibodies using sodium deoxycholate assisted digestion. *Anal. Chem.* 92(17), 11888–11894 (2020).

60. Gao X, Rawal B, Wang Y *et al.* Targeted host cell protein quantification by LC–MRM enables biologics processing and product characterization. *Anal. Chem.* 92(1), 1007–1015 (2019).

61. Chen I-H, Xiao H, Daly T, Li N. Improved host cell protein analysis in monoclonal antibody products through molecular weight cutoff enrichment. *Anal. Chem.* 92(5), 3751–3757 (2020).

62. Pythoud N, Bons J, Mijola G, Beck A, Cianférani S, Carapito C. Optimized sample preparation and data processing of data-independent acquisition methods for the robust quantification of trace-level host cell protein impurities in antibody drug products. *J. Proteome Res.* 20(1), 923–931 (2020).

63. Zacchi LF, Roche-Recinos D, Pegg CL *et al.* Coagulation factor IX analysis in bioreactor cell culture supernatant predicts quality of the purified product. *Commun. Biol.* 4(1), 1–19 (2021).

•• **LC–MS/MS data independent acquisition workflow was performed to quantify host-cell proteins (HCPs) and measure post-translational modifications both during cell culture process in bioreactors and after purification.**

64. Farrell A, Mittermayr S, Morrissey B *et al.* Quantitative host cell protein analysis using two dimensional data independent LC–MSE. *Anal. Chem.* 87(18), 9186–9193 (2015).

65. Levin Y, Hradetzky E, Bahn S. Quantification of proteins using data-independent analysis (MSE) in simple and complex samples: a systematic evaluation. *Proteomics* 11(16), 3273–3287 (2011).

66. Huang Y, Molden R, Hu M, Qiu H, Li N. Toward unbiased identification and comparative quantification of host cell protein impurities by automated iterative LC–MS/MS (HCP-AIMS) for therapeutic protein development. *J. Phar. Biomed. Anal.* 200, 114069 (2021).

• **HCP–automated iterative MS workflow was applied for HCP identification and quantification.**

67. Johnson ROB, Greer T, Cejkov M, Zheng X, Li N. Combination of FAIMS, protein a depletion, and native digest conditions enables deep proteomic profiling of host cell proteins in monoclonal antibodies. *Anal. Chem.* 92(15), 10478–10484 (2020).

68. Ma J, Kilby GW. Sensitive, rapid, robust, and reproducible workflow for host cell protein profiling in biopharmaceutical process development. *J. Proteome Res.* 19(8), 3396–3404 (2020).

69. Parker CE, Mocanu V, Mocanu M, Dicheva N, Warren MR. Mass spectrometry for post-translational modifications. *Neuroproteomics* Chapter 5, 2010 (2010).

70. Jefferis R. Posttranslational modifications and the immunogenicity of biotherapeutics. *J Immunol. Res.* 2016, 5358272 (2016).

71. Jenkins N, Murphy L, Tyther R. Post-translational modifications of recombinant proteins: significance for biopharmaceuticals. *Mol. Biotechnol.* 39(2), 113–118 (2008).

72. Larsen MR, Trelle MB, Thingholm TE, Jensen ON. Analysis of posttranslational modifications of proteins by tandem mass spectrometry: mass spectrometry for proteomics analysis. *BioTechniques* 40(6), 790–798 (2006).

73. Wolters DA, Washburn MP, Yates JR. An automated multidimensional protein identification technology for shotgun proteomics. *Anal. Chem.* 73(23), 5683–5690 (2001).

74. Moradian A, Kalli A, Sweredoski MJ, Hess S. The top-down, middle-down, and bottom-up mass spectrometry approaches for characterization of histone variants and their post-translational modifications. *Proteomics* 14(4–5), 489–497 (2014).

75. Tran JC, Zamdborg L, Ahlf DR *et al.* Mapping intact protein isoforms in discovery mode using top-down proteomics. *Nature* 480(7376), 254–258 (2011).

76. Durbin KR, Fornelli L, Fellers RT, Doubleday PF, Narita M, Kelleher NL. Quantitation and identification of thousands of human proteoforms below 30 kDa. *J. Proteome Res.* 15(3), 976–982 (2016).

77. Zhang Y, Fonslow BR, Shan B, Baek M-C, Yates JR III. Protein analysis by shotgun/bottom-up proteomics. *Chem. Rev.* 113(4), 2343–2394 (2013).

78. Lindberg I, Peinado J. Posttranslational modifications: key players in health and disease. *Encyclopedia Cell Biol.* 1, 84–90 (2015).

79. Hallgren K, Zhang D, Kinter M, Willard B, Berkner K. Methylation of γ-carboxylated Glu (Gla) allows detection by liquid chromatography–mass spectrometry and the identification of gla residues in the γ-glutamyl carboxylase. *J. Proteome Res.* 12(6), 2365–2374 (2013).

80. Thaysen-Andersen M, Packer NH, Schulz BL. Maturing glycoproteomics technologies provide unique structural insights into the N-glycoproteome and its regulation in health and disease. *Mol. Cell. Proteomics* 15(6), 1773–1790 (2016).

81. Chang D, Zaia J. Methods to improve quantitative glycoprotein coverage from bottom-up LC-MS data. *Mass Spectrom. Rev.* (2021) doi: 10.1002/mas.21692 (Epub ahead of print).

82. Ye Z, Vakhrushev SY. The role of data-independent acquisition for glycoproteomics. *Mol. Cell. Proteomics* 20, 100042 (2021).

83. Nilsson J. Liquid chromatography-tandem mass spectrometry-based fragmentation analysis of glycopeptides. *Glycoconj. J.* 33(3), 261–272 (2016).

84. Riley NM, Malaker SA, Driessen MD, Bertozzi CR. Optimal dissociation methods differ for N-and O-glycopeptides. *J. Proteome Res.* 19(8), 3286–3301 (2020).

85. Kawahara R, Alagesan K, Bern M *et al.* Community evaluation of glycoproteomics informatics solutions reveals high-performance search strategies of glycopeptide data. *bioRxiv* (2021). https://doi.org/10.1101/2021.03.14.435332

86. Bodnar J, Szekrenyes A, Szigeti M *et al.* Enzymatic removal of N-glycans by PNGase F coated magnetic microparticles. *Electrophoresis* 37(10), 1264–1269 (2016).

87. Xu Y, Bailey UM, Schulz BL. Automated measurement of site-specific N-glycosylation occupancy with SWATH-MS. *Proteomics* 15(13), 2177–2186 (2015).

88. West CM, Malzl D, Hykollari A, Wilson IB. Glycomics, glycoproteomics and glycogenomics: an inter-taxa evolutionary perspective. *Mol. Cell. Proteomics* 100024 (2021).

89. Quaranta A, Spasova M, Passarini E *et al.* N-Glycosylation profiling of intact target proteins by high-resolution mass spectrometry (MS) and glycan analysis using ion mobility-MS/MS. *Analyst* 145(5), 1737–1748 (2020).

90. Peng W, Reyes CDG, Gautam S *et al.* MS-based glycomics and glycoproteomics methods enabling isomeric characterization. *Mass Spectrom. Rev.* 10982787 (2021). doi: 10.1002/mas.21713

91. Watanabe Y, Allen JD, Wrapp D, McLellan JS, Crispin M. Site-specific glycan analysis of the SARS-CoV-2 spike. *Science* 369(6501), 330–333 (2020).

- **Bottom-up LC–MS used in characterization of glycosylation on SARS-CoV-2 spike protein.**

92. Yang Y, Liu F, Franc V, Halim LA, Schellekens H, Heck AJ. Hybrid mass spectrometry approaches in glycoprotein analysis and their usage in scoring biosimilarity. *Nat. Commun.* 7(1), 1–10 (2016).

93. Rosati S, Rose RJ, Thompson NJ *et al.* Exploring an orbitrap analyzer for the characterization of intact antibodies by native mass spectrometry. *Angew. Chem. Int. Ed.* 51(52), 12992–12996 (2012).

94. Zidar M, Kuzman D, Ravnik M. Characterisation of protein aggregation with the Smoluchowski coagulation approach for use in biopharmaceuticals. *Soft matter* 14(29), 6001–6012 (2018).

95. Trabjerg E, Nazari ZE, Rand KD. Conformational analysis of complex protein states by hydrogen/deuterium exchange mass spectrometry (HDX-MS): challenges and emerging solutions. *TrAC, Trends Anal. Chem.* 106, 125–138 (2018).

96. Narang D, Lento C, Wilson DJ. HDX-MS: an analytical tool to capture protein motion in action. *Biomedicines* 8(7), 224 (2020).

97. Kaltashov IA, Bobst CE, Abzalimov RR. H/D exchange and mass spectrometry in the studies of protein conformation and dynamics: is there a need for a top-down approach? *Anal. Chem.* 81(19), 7892–7899 (2009).

98. Zehl M, Rand KD, Jensen ON, Jørgensen TJ. Electron transfer dissociation facilitates the measurement of deuterium incorporation into selectively labeled peptides with single residue resolution. *J. Am. Chem. Soc.* 130(51), 17453–17459 (2008).

99. Wang G, Kaltashov IA. Approach to characterization of the higher order structure of disulfide-containing proteins using hydrogen/deuterium exchange and top-down mass spectrometry. *Anal. Chem.* 86(15), 7293–7298 (2014).

100. Pan J, Zhang S, Parker CE, Borchers CH. Subzero temperature chromatography and top-down mass spectrometry for protein higher-order structure characterization: method validation and application to therapeutic antibodies. *J. Am. Chem. Soc.* 136(37), 13065–13071 (2014).

101. Pan J, Zhang S, Borchers CH. Comparative higher-order structure analysis of antibody biosimilars using combined bottom-up and top-down hydrogen-deuterium exchange mass spectrometry. *Biochim. Biophys. Acta Proteins. Proteom.* 1864(12), 1801–1808 (2016).

102. Prądzińska M, Behrendt I, Astorga-Wells J *et al.* Application of amide hydrogen/deuterium exchange mass spectrometry for epitope mapping in human cystatin C. *Amino Acids* 48(12), 2809–2820 (2016).

103. Opuni KF, Al-Majdoub M, Yefremova Y, El-Kased RF, Koy C, Glocker MO. Mass spectrometric epitope mapping. *Mass Spectrom. Rev.* 37(2), 229–241 (2018).

104. Comamala G, Wagner C, De La Torre PS *et al.* Hydrogen/deuterium exchange mass spectrometry with improved electrochemical reduction enables comprehensive epitope mapping of a therapeutic antibody to the cysteine-knot containing vascular endothelial growth factor. *Anal. Chim. Acta* 1115, 41–51 (2020).

105. Rob T, Wilson DJ. A versatile microfluidic chip for millisecond time-scale kinetic studies by electrospray mass spectrometry. *J. Am. Soc. Mass Spectrom.* 20(1), 124–130 (2009).

106. Rob T, Gill PK, Golemi-Kotra D, Wilson DJ. An electrospray ms-coupled microfluidic device for sub-second hydrogen/deuterium exchange pulse-labelling reveals allosteric effects in enzyme inhibition. *Lab Chip* 13(13), 2528–2532 (2013).

107. Deng B, Zhu S, Macklin AM *et al.* Suppressing allostery in epitope mapping experiments using millisecond hydrogen/deuterium exchange mass spectrometry. *MAbs* 9(8), 1327–1336 (2017).

108. Resetca D, Wilson DJ. Characterizing rapid, activity-linked conformational transitions in proteins via sub-second hydrogen deuterium exchange mass spectrometry. *FEBS J.* 280(22), 5616–5625 (2013).

109. Resetca D, Haftchenary S, Gunning PT, Wilson DJ. Changes in signal transducer and activator of transcription 3 (STAT3) dynamics induced by complexation with pharmacological inhibitors of Src homology 2 (SH2) domain dimerization. *J. Biol. Chem.* 289(47), 32538–32547 (2014).

110. Brown KA, Lento C, Rajendran S, Dowd J, Wilson DJ. Epitope mapping for a preclinical bevacizumab (Avastin) biosimilar on an extended construct of vascular endothelial growth factor a using millisecond hydrogen–deuterium exchange mass spectrometry. *Biochemistry* 59(30), 2776–2781 (2020).

•• **Time-resolved ESI hydrogen-deuterium exchange MS workflow was used to compare epitopes between commercial Avastin and its biosimilar.**

111. Upton R, Migas LG, Pacholarz KJ *et al.* Hybrid mass spectrometry methods reveal lot-to-lot differences and delineate the effects of glycosylation on the tertiary structure of Herceptin®. *Chem. Sci.* 10(9), 2811–2820 (2019).

• **Combination of hydrogen-deuterium exchange MS and IM–MS workflow was used to characterize protein structure and dynamics.**

112. Dixit SM, Polasky DA, Ruotolo BT. Collision induced unfolding of isolated proteins in the gas phase: past, present, and future. *Curr. Opin. Chem. Biol.* 42, 93–100 (2018).

113. Zheng X, Kurulugama RT, Laganowsky A, Russell DH. Collision-induced unfolding studies of proteins and protein complexes using drift tube ion mobility-mass spectrometer. *Anal. Chem.* 92(10), 7218–7225 (2020).

Bioanalysis ZONE

Contact us

Editorial Department

editor@bioanalysis-zone.com

Business Development & Support

hub.advertising@tandf.co.uk

This supplement is brought to you by Bioanalysis Zone in association with

SCIEX

The Power of Precision